Aus dem Charité Comprehensive Cancer Center
der Medizinischen Fakultät Charité – Universitätsmedizin Berlin

DISSERTATION

Die Rolle von Antikörperabhängiger zellulärer Zytotoxizität für die Behandlung des metastatischen kolorektalen Karzinoms mit IgG1 monoklonalen Antikörpern

The role of antibody-dependent cellular cytotoxicity for IgG1 monoclonal antibody therapy of metastatic colorectal cancer

zur Erlangung des akademischen Grades
Doctor medicinae (Dr. med.)

vorgelegt der Medizinischen Fakultät
Charité – Universitätsmedizin Berlin

von

Stefan Kolling

Datum der Promotion: 30.11.2023

Contents

List of Figures

List of Tables

List of Abbreviations

ADCC	antibody-dependent cell-mediated cytotoxicity
APC	antigen-presenting cell
B3GNT3	β-1,3-N-acetylglucosaminyl transferase
BOR	best overall response
BSA	bovine serum albumin
CAPOX	Chemotherapy regimen for treatment of colorectal cancer, consisting of capecitabin and oxaliplatin
CRC	colorectal cancer
CTLA4	cytotoxic t-lymphocyte-associated protein 4
DC	dendritic cell
DCR	disease control rate
ECOG	Eastern Cooperative Oncology Group
EGFR	epidermal growth factor receptor
EMT	epithelial-to-mesenchymal transition
EpCam	Epithelial cell adhesion molecule
ETT ratio	effector-to-target ratio
Fab	fragment antigen binding
FACS	fluorescence-activated cell sorting; synonym for flow cytometry

FBS	Fetal bovine serum
Fc	fragment crystallisable
FcgR	Fc gamma receptor
FOLFIRI	Chemotherapy regimen for treatment of colorectal cancer, consisting of folinic acid, fluorouracil and irinotecan
FOLFOX	Chemotherapy regimen for treatment of colorectal cancer, consisting of folinic acid, fluorouracil and oxaliplatin
FOLFOXIRI	Chemotherapy regimen for treatment of colorectal cancer, consisting of folinic acid, 5-fluorouracil, oxaliplatin and irinotecan
ICI	immune checkpoint inhibitor
Ig	immunoglobulin
KIR	killer immunoglobulin-like receptor
LDA	linear discriminant analysis
LDH	lactate dehydrogenase
mAb	monoclonal antibody
mCRC	metastatic colorectal cancer
MDSC	myeloid-derived suppressor cell
MFI	median fluorescence intenstiy
MHC	major histocompatibility complex
MICA/B	MHC class I chain-related protein A and B
MSI	microsatellite instability
NK cell	Natural killer cells
NKG2D	natural-killer group 2, member D receptor

ORR	objective response rate
OS	overall survival
P/S	Penicillin-Streptomycin
PBMC	peripheral blood mononuclear cell
PBS	phosphate buffered saline
PD1	programmed cell death 1
PFS	progression-free survival
REML	restricted maximum likelihood
REML	restricted maximum likelihood
ROC	receiver operating characteristic
S/N ratio	signal-to-noise ratio
SEM	standard error of mean
SNP	single nucleotide polymorphism
TAM	tumour-associated macrophage
TKI	tyrosine kinase inhibitor
TMB	tumour mutational burden
TNF	tumour necrosis factor
Treg	regulatory T cell
VEGF	vascular endothelial growth factor
VIF	variance inflation factor

Zusammenfassung

Natürliche Killerzellen (NK Zellen) können direkte Zelllyse mittels des Mechanismus der antikörperabhängigen zellvermittelten Zytotoxizität (engl. ADCC) betreiben, indem sie mit ihren Fcg-Rezeptoren (FcgR) an IgG1 monoklonale Antikörper (mAk) binden, die gegen exprimierte Antigene auf der Oberfläche der Tumorzellen gerichtet sind. Polymorphismen des FcgRIIIa, der sich hauptsächlich auf NK Zellen findet, beeinflussen die Bindungsaffinität für IgG1 mAk und damit das ADCC Potenzial. Unter diesen stellt der FcgRIIIa-158 V/F Einzelnukleotid-Polymorphismus den wissenschaftlich am besten untersuchten dar. Um die Rolle von ADCC und FcgRIIIa-158 Phänotyp für IgG1 mAk-basierte Therapien zu klären, wurde ein experimentelles Setup entwickelt, das aus (1) einem FcgRIIIa Durchflusszytometrie-Assay und (2) einem Modell zur in vitro Quantifizierung der ADCC-Aktivität und Aktivierung von Immunzellpopulationen besteht.

Der FcgRIIIa Assay basiert vorrangig auf einem anti-FcgRIIIa Klon (MEM-154), der ausschließlich das FcgRIIIa-158 V Allel erkennt, unter gleichzeitiger Verwendung eines zweiten Klons (LNK16), der beide FcgRIIIa-158 Allele bindet. Aus diesen Messdaten wurde mit Hilfe eines Trainings-Set (n = 39) ein Vorhersagemodell berechnet und anschließend mit einer Genauigkeit von $> 90\%$ für ein Test-Set (n = 52) validiert. Dabei gelang die klinisch relevanteste Unterscheidung des FF Phänotyps mit niedriger Bindungsaffinität von den VF und VV Phänotypen mit hoher Bindungsaffinität zweifelsfrei in allen Fällen. Fehlklassifikationen traten ausnahmslos zwischen den Phänotypen VF und VV auf. Die Vorteile des entwickelten FcgRIIIa Assay gegenüber alternativen Methoden bestehen aus einer breiten Anwendbarkeit, kurzer Umlaufzeit und geringen Kosten.

Eine zuverlässige Detektion von in vitro ADCC-Aktivität und Aktivierung von NK Zellen konnte durch ein Kokultur-Modell von mononukleären Zellen des peripheren Blutes (engl. PBMCs) mit kolorektalen Krebszelllinien unter Zugabe eines anti-EGFR (Cetuximab) und anti-PDL1 (Avelumab) IgG1 mAk erreicht werden. Experimentelle Werte wurden mittels der Messung von Laktatdehydrogenase-Freisetzung und einem Durchflusszytometrie-Assay quantifiziert. Im Einklang mit der Literatur wurde eine Korrelation zwischen der Stärke der ADCC-Aktivität und der Expression (EGFR, PDL1, MICA/B, CD137L) bzw. des Fehlens (HLA-A/B/C) von Oberflächenmarkern auf den Krebszellen gefunden.

Im Rahmen der multizentrischen Phase II FIRE6 Studie wurden die entwickelten Methoden an PBMCs von 55 Patienten mit RAS und BRAF Wildtyp metastatischem kolorektalen Karzinom unter Chemotherapie und Kombinationstherapie von Cetuximab und Avelumab getestet. Obwohl der FcgRIIIa-158 Phänotyp und die Aktivierung von NK Zellen mit der gemessenen in vitro ADCC-Aktivität korrelierten, wurde keine prognostische Relevanz dieser Parameter in Hinblick auf die klinischen Ergebnisgrößen des Therapieansprechens und progressionsfreien Überlebens festgestellt.

Abstract

In the context of cancer therapy, natural killer cells (NK cells) may mediate direct tumour lysis upon binding of their Fcg receptors (FcgR) to IgG1 monoclonal antibodies (mAb) targeted at tumour-expressed surface antigens in a process termed antibody-dependent cellular cytotoxicity (ADCC). Polymorphisms in the FcgRIIIa predominantly expressed by NK cells influence the binding affinity of IgG1 mAbs and in turn their ADCC potential, with the FcgRIIIa-158 V/F single-nucleotide polymorphism being the most extensively studied. In order to elucidate the role of ADCC and FcgRIIIa-158 phenotype in the context of IgG1 mAb therapy, we successfully established a novel setup comprising (1) a flow cytometric FcgRIIIa panel to swiftly determine an individual's FcgRIIIa-158 phenotype and (2) an experimental model to quantify ADCC activity and immune cell activation in vitro.

The FcgRIIIa panel employs an anti-FcgRIIIa clone that only recognises the FcgRIIIa-158 V allele (MEM-154) in combination with a clone that detects both FcgRIIIa-158 alleles (LNK16). Using the results from melting curve analysis as ground truth, a supervised machine-learning based prediction model computed on the flow cytometry measurements of a training set (n = 39) could be validated with a prediction accuracy $> 90\%$ on a test set (n = 52). Importantly, the clinically most relevant distinction between the low-affinity FF phenotype and the high-affinity VF/VV phenotypes was flawless, with the few misclassifications exclusively occurring between the VF and VV phenotypes. Advantages of the FcgRIIIa panel over alternative techniques include its wide applicability, quick turnaround time and low cost.

The experimental model based on a 24h co-culture of peripheral blood mononuclear cells (PBMCs) with a range of colorectal cancer cell lines treated with two IgG1 mAbs, namely anti-EGFR cetuximab and/or anti-PDL1 avelumab, could be shown to reliably detect both in vitro ADCC activity and NK cell activation. Experimental readouts were generated using a lactate dehydrogenase release assay together with a flow cytometry panel. In line with the literature, the strength of ADCC activity correlated with the expression (EGFR, PDL1, MICA/B, CD137L) or absence (HLA-A/B/C) of surface markers on tumour cells.

These methods were applied to PBMCs derived from 55 patients with RAS and BRAF wild-type metastatic colorectal cancer receiving chemotherapy with cetuximab and avelumab combination therapy within the context of the single-arm multi-centre phase-II FIRE6 clinical trial. While FcgRIIIa-158 phenotype and NK cell activation strongly correlated with in vitro ADCC activity, no benefit could be observed for either of these parameters with respect to clinical outcome measures such as response to treatment or progression-free survival.

1 Background

1.1 Targeted cancer therapy with monoclonal antibodies

Currently, two out of three Europeans will be diagnosed with cancer at some point of their lives. Despite a continuous improvement of therapy options and a consequential decline in lethality, yet about 48% of these patients are estimated to die of cancer-related causes, making cancer the second-leading cause of death worldwide behind cardiovascular disease, which it has already overtaken in high-income countries[1]. Throughout much of its history, the arsenal of cancer therapy has been based around two inherent vulnerabilities of cancer, namely (1) locally restricted tumour growth in its initial stages, exploited by surgery and radiation therapy, and (2) rapid cell division at a rate drastically faster than that of normal cells, exploited by chemotherapy. However, pushing the boundaries of these approaches in an attempt to cure more patients with ever more radical surgery or more radical chemotherapy quickly hit biological ceilings and fell short of improving patient outcome. It was not until the 1980s, when a better understanding of carcinogenesis after decades of research led to the emerging discovery that cancer may be seen as a distorted version of normal self, driven by the accumulation of mutations in DNA of initially normal human cells. The discovery of this paradigm-shifting third and new Achilles' heel was the starting point for the era of modern targeted cancer therapy, of which the development of monoclonal-antibody based treatments is a shining example.

1.1.1 Definition and overview

In the early 1900s, German immunologist Paul Ehrlich was the first to propose the idea of a magic bullet (*Zauberkugel* in German), a substance to kill specific disease-causing agents without harming the body itself as a bystander - similar to a bullet fired from

a well-aimed gun to hit a specific target [2]. He went on to discover antibodies as the envisioned magic bullet and their enormous potential, in the form of specifically engineered monoclonal antibodies (mAb) binding to the very same epitope (the part of an antigen that is recognised by the antibody), to target and eliminate abnormal cancer cells and thereby induce an immune response against the tumour was swiftly realised. The particular structure of mAbs provides them with various properties chiefly responsible for their anti-tumour activity (Fig. 1.1). Antibodies are large Y-shaped proteins arranged in three globular regions that consist of two *heavy chains* and two *light chains* joined and held together by disulfide bonds [3]. The antigen-binding specificity of each antibody is defined by the variable regions of these heavy and light chains which together form the *fragment antigen binding* (Fab), binding of which to the recognised epitope on the target cell results in blocking (antagonistic antibodies) or stimulation (agonistic antibodies) of downstream signal transduction pathways. Unlike the virtually unlimited repertoire of highly variable Fab fragments, the *fragment crystallisable* (Fc) is comprised of a restricted number of constant regions of the heavy chains that allow the classification of antibodies into five distinct groups of immunoglobulin isotypes (IgA, IgD, IgE, IgG, IgM)[4]. Of these groups, IgGs are a major component of humoral immunity, making up approximately 75% of serum antibodies in humans, and may be further divided into four subgroups (γ1-4) based on subtle differences in the Fc fragment of their heavy chains. Their widespread abundance in serum has made them a primary research target and, not surprisingly, all clinically approved monoclonal antibodies to date are of the IgG isotype [5].

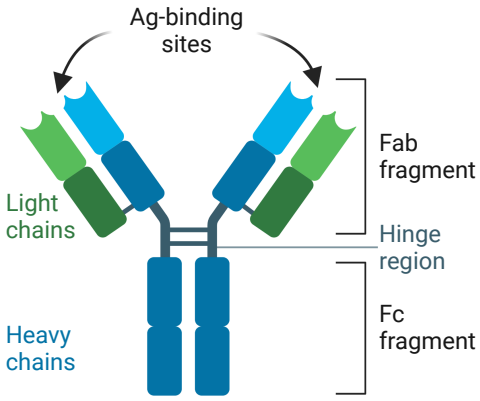

Figure 1.1: Basic antibody structure comprising the antigen-binding Fab fragment and the constant Fc fragment.

1.1.2 Role of ADCC and FcgRIIIa polymorphisms

Among the vast repertoire of protective IgG-mediated mechanisms, interactions of the Fc portion of IgGs with Fcg receptors (FcgR) predominantly expressed on the surface of innate immune cells are crucial for triggering the activation or inhibition of the latter as well as for the antibody-mediated crosslinking of the bound target antigen. As

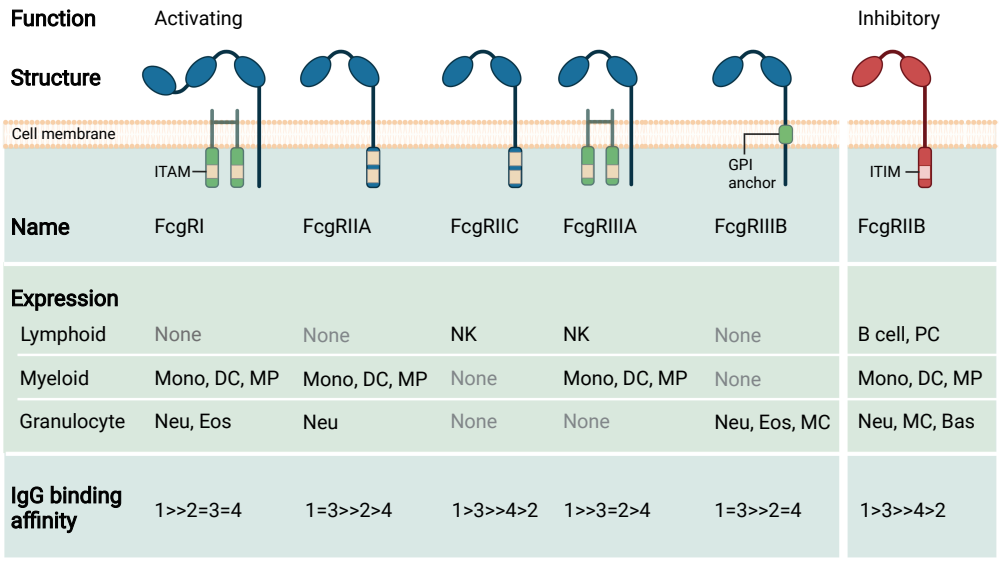

(a) Overview of FcgR types

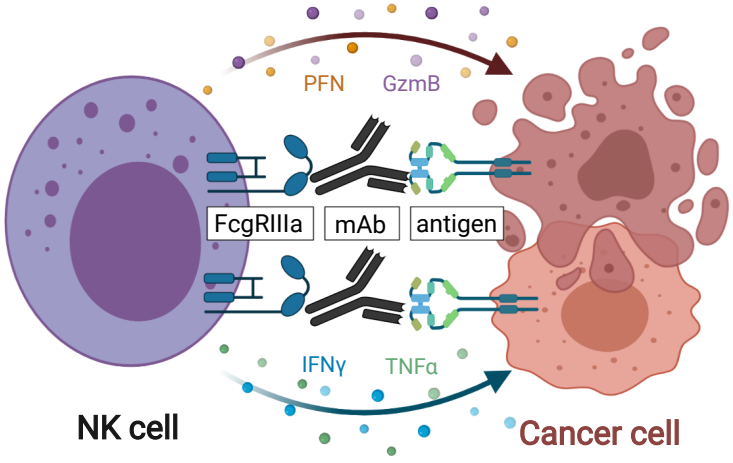

(b) ADCC mechanism

Figure 1.2: Role of IgG isotype and FcgR types in NK-cell mediated ADCC. (a) Cell-type specific expression and IgG binding affinity of the different FcgR [6–8]. IgG1 antibodies have the highest binding affinity to the FcgRIIIa expressed on the surface of NK cells. (b) ADCC is triggered via engagement of FcgRIIIa on NK cells with mAbs bound to their target antigen on the surface of tumour cells, inducing cell lysis via the release of perforin and granzyme B. Abbreviations: DC = dendritic cell; MP = macrophage; Mono = monocyte; Neu = neutrophil; Eos = eosinophil; Bas = basophil; PC = plasma cell; MC = mast cell.

shown in Fig. 1.2(a), the binding affinity to the different types of FcgR varies with IgG subgroup and, thus, the choice of a specific isotype strongly influences the effector functions induced by a monoclonal antibody. With regards to antibody-based targeted cancer therapy, antibody-dependent cellular cytotoxicity (ADCC) is considered an important example of such immune-cell mediated effector functions (Fig. 1.2(b)). The typical ADCC involves activation of natural killer cells (NK cells) through the recognition and binding of their FcgRIIIa (also called CD16) to the reciprocal Fc fragment of an IgG antibody bound to the surface of the target cell. Once activated, NK cells release a battery of cytotoxic molecules, such as perforin and granzyme B, which eventually cause the target cell to be destroyed. Of all four subgroups, IgG1 mAbs exhibit the highest binding affinity for the FcgRIIIa receptor and, in turn, have been shown to induce the strongest NK-cell mediated anti-tumour activity both in vitro and in vivo [9, 10]. Yet, the binding affinity is also influenced by polymorphisms in the FcgRIIIa-encoding gene. The most well-studied of these in the context of NK cells is the FcgRIIIa-V158F polymorphism that has a single nucleotide missense mutation (thymine to guanine), resulting in a change from a valine (V) to a phenylalanine (F) residue at amino acid position 158. Since the substitution occurs in the ligand-binding domain of the receptor, it is not surprising that it entails functional differences, with the V isoform of FcgRIIIa having a stronger binding affinity to IgG1 than the F isoform [11]. In turn, individuals homozygous for the high-affinity V allele are reported to mount a significantly stronger NK-cell mediated ADCC than FF homozygotes [12–14] and, hence, the FcgRIIIa-158 polymorphism has been implicated with disease progression and responsiveness to treatments based on mAbs in the literature. For example, Weng et al. found a higher response rate and longer progression-free survival for VV homozygous patients with follicular lymphoma treated with the IgG1 mAb rituximab as first-line therapy [15]. Similarly, Musolino et al. observed that the VV phenotype was correlated with a better response rate and progression-free survival in patients with HER2+ metastatic breast cancer treated with the IgG1 mAb trastuzumab [16]. Taken together, these observations underline how the combination of both patient-specific characteristics (FcgRIIIa polymorphism) and antibody-specific properties (IgG isotype) may have important clinical implications on the treatment of cancer patients.

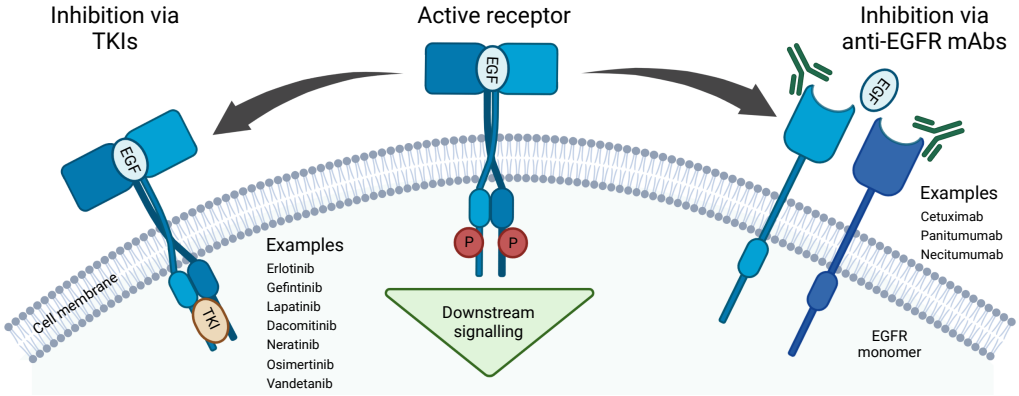

Figure 1.3: EGFR signalling triggers cell proliferation, survival and angiogenesis. Two main strategies are exploited clinically to inhibit downstream EGFR signalling, namely (1) blocking its tyrosine kinase activity by TKIs or (2) preventing the interaction with EGF and subsequent receptor dimerisation by EGFR-specific blocking mAbs. Figure adapted from Schiele et al. [22].

1.1.3 Targeting EGFR

Among the different families of growth factors and respective growth factor receptors involved in the autonomous growth of cancer cells, the epidermal growth factor receptor (EGFR) plays a pivotal role in the pathogenesis and progression of several carcinoma types [17, 18]. The 170 kDa transmembrane EGFR protein is one of four distinct members of the ErbB receptor family, all of which consist of (1) an extracellular ligand-binding domain, (2) a single hydrophobic transmembrane α helix and (3) a cytoplasmic tyrosine-kinase-containing domain [19]. Upon binding of the cognate ligand to the extracellular domain of EGFR, receptor dimerisation leads to activation of the intracellular tyrosine kinase domain. Subsequently autophosphorylated specific tyrosine residues within its cytoplasmic tail serve as docking sites for the recruitment of intracellular proteins that sit at the top of cellular signalling pathways in control of cell proliferation, differentiation, migration, apoptosis and angiogenesis [20, 21].

Natively expressed on healthy cells of the human epithelium, the EGFR forms a coordinating hub in charge of proper development of epithelial structures of the gastrointestinal tract, lung, central nervous system and skin by directing cell growth, differentiation and repair [23–28]. However, the flipside of its importance in these fundamental processes of normal human development becomes evident when these signalling pathways are constitutively activated due to two types of pathological alterations, namely kinase-activating mutations in EGFR or membrane overexpression of the EGFR, both of which may in

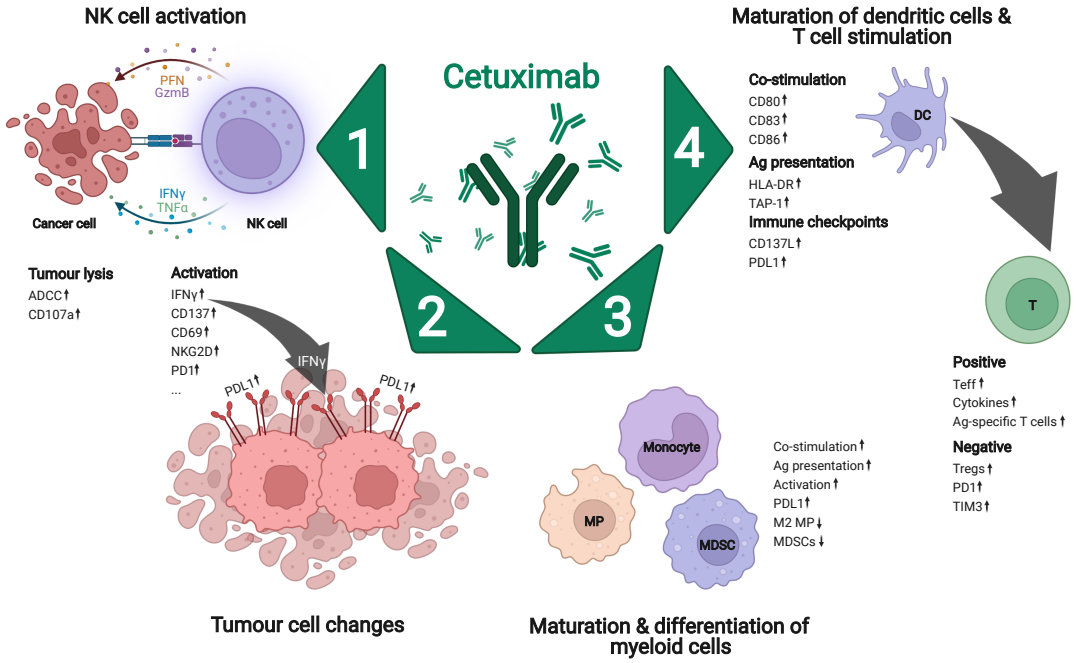

Figure 1.4: Clinically relevant effector mechanisms of the IgG1 mAb cetuximab. (1) The interaction of cetuximab with FcgRIIIa on NK cells induces ADCC against tumour cells, cytokine production as well as upregulation of activation markers and checkpoint molecules. (2) Cytokine release by immune cells (e.g. IFNγ) and tumour lysis trigger surface expression of inhibiting receptors (e.g. PDL1). (3) Cetuximab-mediated changes in cytokine secretion and interactions with FcgR lead to activation, differentiation and maturation of myeloid cells. (4) ADCC-dependent release of tumour neoantigens promotes maturation of antigen-presenting cells, contributing to co-stimulation and better anti-tumour activity of T cells. Figure adapted from Schiele et al. [22], based on references [32–36].
Abbreviations: MP = macrophage; DC = dendritic cell; MDSC = myeloid-derived suppressor cell; Teff = effector T cell; Treg = regulatory T cell; Ag = antigen; PFN = perforin; GzmB = granzyme B.

turn give rise to a wide variety of tumours of epithelial origin (e.g. lung, colon, head and neck, mammary gland or pancreas). Equipped with a comparative survival advantage given by this boost, EGFR-positive cancers become largely refractory to standard cytotoxic chemotherapy and, thus, targeting the EGFR in order to block these downstream signalling pathways presents an appealing treatment strategy [29–31].

To exploit the vulnerability of EGFR addiction, the two commonly employed approaches are centered around either (1) inactivating the kinase activity of the intracellular domain with specific tyrosine kinase inhibitors (TKI) or (2) preventing receptor dimerisation by anti-EGFR mAbs targeted at the ligand-binding site of the extracellular domain (Fig. 1.3). Several TKIs and mAbs have already shown clinical benefits and are currently approved for select EGFR-dependent tumour entities, primarily for small cell lung cancer (NSCLC),

breast cancer, head and neck squamous cell carcinoma (HNSCC) and colorectal cancer (CRC). This notwithstanding, the majority of patients experience either primary (intrinsic) resistance or acquired resistance following an initial response to EGFR-targeted therapy due to specific mutations of the EGFR (or downstream molecules) or the activation of alternative escape signalling pathways [37, 38]. The diverse mechanisms of resistance make the identification of those patients who will eventually benefit from EGFR targeting rather complex and it is often necessary to limit the use of anti-EGFR therapy to responsive subcohorts of patients with known mutations (more commonly, the absence thereof), develop new drugs against specific mutations or administer combination treatments to overcome resistance. In this regard, there is a general consensus that blocking of EGFR alone is likely not sufficient for longterm tumour control and should ideally be combined with a concurrent induction of a durable immune response against the tumour. A promising leverage point to link EGFR blockade and immune activation is the described interaction of anti-EGFR mAbs with FcgR on immune cells (Section 1.1.2) and, among the therapeutic armamentarium currently at hand, IgG1 mAbs are predestined for this purpose, having the highest binding affinity to FcgR. In clinical studies of CRC and HNSCC patients receiving anti-EGFR therapy, the IgG1 mAb cetuximab showed a clinical benefit over the IgG2 mAb panitumumab as well as the treatment with TKIs, underpinning the hypothesis of additional immune effector functions mediated by cetuximab (Fig. 1.4) [39, 40].

1.1.4 Targeting immune checkpoints

Immune evasion is one of the hallmarks of cancer and presents a considerable hindrance to designing effective therapeutic anticancer strategies. Hence, suitable measures to counteract tumour escape from immune destruction are of great interest in cancer research and in this context immune checkpoint molecules have played a central role in recent years, with the Nobel Prize in Physiology or Medicine being awarded to their discoverers in 2018 [48]. In normal human physiology, these immune checkpoints are in charge of regulating the immune response in order to maintain self-tolerance and limit its extent and duration, thereby preventing excessive tissue damage and reducing the likelihood of autoimmune disease [49–51]. However, the very same mechanisms are prone to being hijacked and

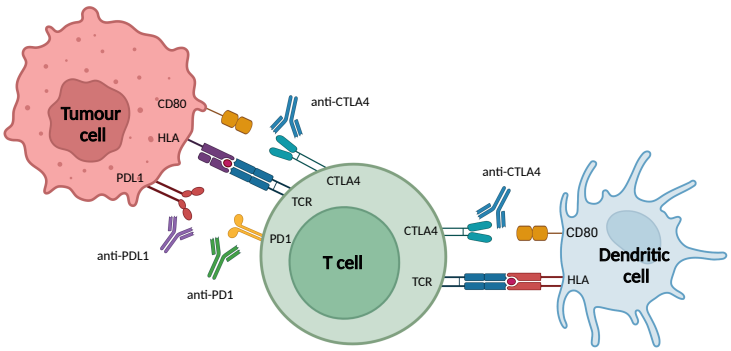

Figure 1.5: Immune checkpoints on T cells. Binding of the two immune checkpoints CTLA4 and PD1 on T cells to their respective ligands CD80/CD86 and PDL1 upregulated on the surface of tumour cells results in inhibition of tumour-infiltrating T cells. Therapy with mAbs directed at the checkpoint molecules aims to block these interactions and restore anti-tumour activity. Figure based on references [41–47].
Abbreviations: CTLA4 = cytotoxic t-lmyphocyte-associated protein 4; PD1 = programmed cell death 1; PDL1 = PD1 ligand; TCR = T cell receptor; HLA = human leukocyte antigen.

misused by cancer cells to escape immune surveillance and suppress an immune-mediated anti-tumour response. Interruption of tumour signalling via immune checkpoint pathways is an appealing strategy and the development of the first two checkpoint-inhibiting mAbs ipilimumab and nivolumab that target the two major immune checkpoints *cytotoxic t-lmyphocyte-associated protein 4* (CTLA4) and *programmed cell death 1* (PD1), respectively, has been a breakthrough in cancer therapy [52–54]. Albeit initially used for the treatment of metastatic melanoma, checkpoint inhibitors do not target a specific tumour-associated antigen (unlike e.g. anti-EGFR therapy) but rather act on immune cell populations to unleash their anti-tumour effector functions, leading to them being utilised for the treatment of a constantly growing spectrum of tumour entities. CTLA4 is a member of the CD28:B27 protein family that is constitutively expressed on regulatory T cells (Tregs), whereas on conventional T cells it is only upregulated after stimulation of the T cell receptor. Due to its greater affinity and avidity, CTLA4 outcompetes the homologous T-cell co-stimulatory protein CD28 for binding to CD80 and CD86 on antigen-presenting cells (APC) and transmits an inhibitory signal to T cells, acting as an "off" switch. Ipilimumab blocks this interaction and lifts the inhibition of T-cell activation, resulting in the resumption of proliferation, tumour infiltration and cytotoxic activity [42–44]. PD1 is a membrane-bound protein on the surface of many immune cells, particularly on T cells, B cells, NK cells, monocytes and dendritic cells (DC) [45], and binds its two ligands PDL1 and PDL2, both of which are predominantly (but not exclusively) expressed on the surface

of various tumour cells. Interaction of PD1 with PDL1 appears to be more relevant than that with PDL2, inducing self-tolerance and leading to the exhaustion of antigen-specific T cells while simultaneously reducing apoptosis of suppressive Tregs [46, 47]. In line with this, a high proportion of PD1-positive tumour-infiltrating lymphocytes is associated with poor prognosis [55], whereas increased anti-tumour immune activity is observed when blocking the PD1/PDL1 axis [56]. Currently, there are six immune-checkpoint inhibiting mAbs of the PD1/PDL1 axis approved for clinical use, three of which are directed against PD1 (nivolumab, pembrolizumab, cemiplimab) and the other three against PDL1 (atezolizumab, durvalumab, avelumab). Among other criteria, the combination of antibody isotype and targeted antigen must be considered when developing new antibodies for checkpoint inhibition. In order to prevent the unwanted elimination of PD1-expressing immune cells via the interaction of bound anti-PD1 mAbs with the FcgR on NK cells or monocytes, all anti-PD1 mAbs utilised so far are of isotype IgG4 which has negligible affinity for FcgR (Fig. 1.2(a) in Section 1.1.2). In contrast to PD1, PDL1 is primarily expressed on tumour cells and their FcgR-dependent elimination may be even desirable to augment the pure blocking of the PD1/PDL1 axis. While the IgG1 portion of both atezolizumab and durvalumab is nonetheless modified to prevent any FcgR-dependent interactions, avelumab stands out as the only currently approved anti-PDL1 mAb with a functioning IgG1-type Fc fragment. Thus, a higher anti-tumour activity of avelumab compared with the other mAbs could be shown in FcgR-humanised mice [57] and its ability of inducing ADCC was proven beyond reasonable doubt, both in vitro and in vivo [58–60]. It is worth noting that, albeit PDL1 is also expressed to some extent on peripheral immune cells, avelumab administration could be confirmed to be safe as PDL1 expression density on these cells is too low to trigger measurable ADCC activity [61, 62].

1.2 Metastatic colorectal cancer

1.2.1 Guideline-based treatment recommendations

With approximately 60,000 newly diagnosed cases per year, the colorectal carcinoma (CRC) is the second highest cause of cancer occurrence in Germany, only surpassed by prostate carcinoma in men and breast carcinoma in women, respectively (Fig. 1.6) [63]. While

a colonoscopy-based statutory screening programme for the early detection of colorectal cancer is ubiquitously available in Germany and high 5-year survival rates of 70-90% are achieved for localised tumours with or without local lymph-node involvement (stage I-III), the 5-year survival drastically drops to 16% for the approximately 20% of patients with distant metastases (stage IV) at diagnosis [63].

Such poor prognosis with a median overall survival of only 15-22 months underlines the pressing need for novel therapeutic approaches in the metastatic setting [64]. Current clinical guidelines for first-line therapy of metastatic CRC (mCRC) patients with good general performance status (ECOG score of 0-2) advocate the routine use of several combination chemotherapy regimens, namely FOLFOX (folinic acid, 5-fluorouracil, oxaliplatin), FOLFIRI (folinic acid, 5-fluorouracil, irinotecan), CAPOX (capecitabin, oxaliplatin) or FOLFOXIRI (folinic acid, 5-fluorouracil, oxaliplatin, irinotecan) [64–67]. This chemotherapy backbone may be further augmented through the addition of targeted molecular therapies against (1) the vascular endothelial growth factor (VEGF) or (2) EGFR. The anti-VEGF monoclonal antibody bevacizumab is approved as add-on to chemotherapy for all patients with metastatic colorectal cancer regardless of the presence of specific concurrent mutations, tumour mutational burden (TMB) or microsatellite instability (MSI) status and significantly increases median progression-free survival. Although not consistent in all studies, bevacizumab was generally found to also prolong overall survival, namely by 4 to 8 months with first-line therapy and by 2.1 months with second-line therapy [68–72].

Unlike for bevacizumab, the anti-EGFR monoclonal antibodies cetuximab and panitumumab are only used in mCRC patient cohorts with RAS and BRAF wild-type status, where they prolong both PFS and OS compared with chemotherapy alone [73]. Since the RAS and BRAF proteins are located downstream of the EGFR receptor, mutations in either of them result in a permanent activation of the cellular signal transduction pathway that is not amenable to inhibition by EGFR blockade and consequently lead to treatment resistance [74–78]. Regarding comparative effectiveness of EGFR inhibition versus VEGF inhibition in RAS/BRAF wild-type patients, a clinical benefit for cetuximab over bevacizumab with respect to overall survival, objective response rate and early tumour shrinkage was observed in retrospective meta analyses of head-to-head multi-cohort studies [79–81],

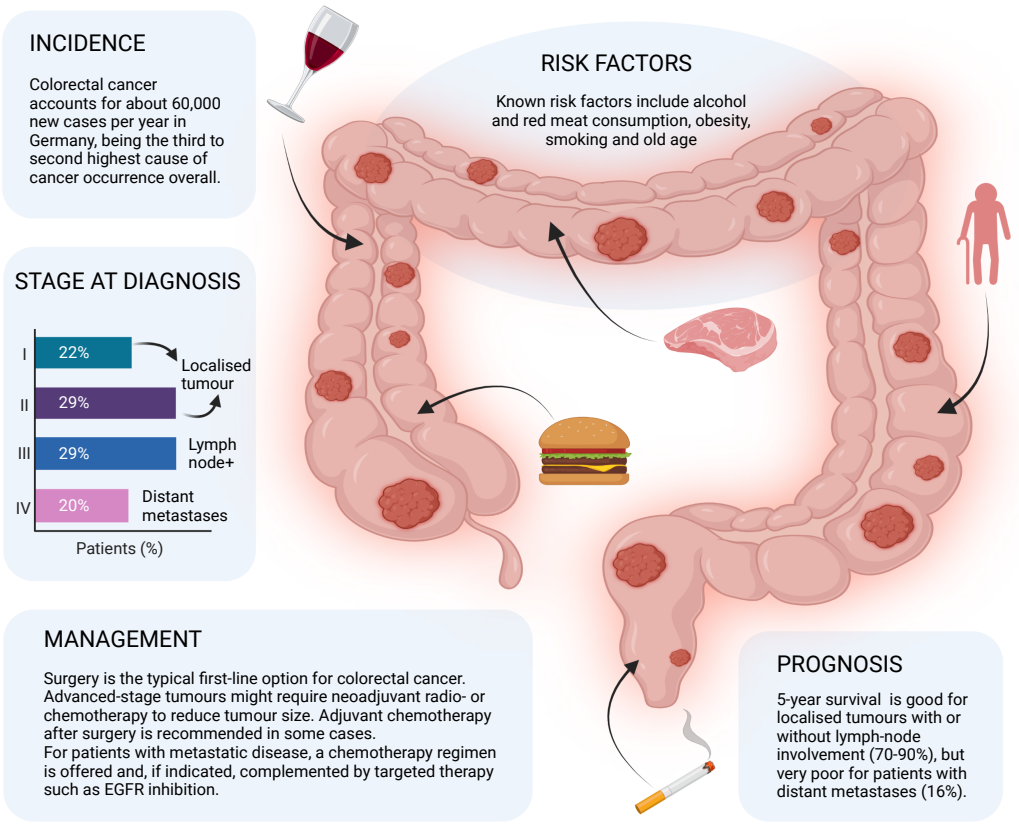

Figure 1.6: Overview of colorectal cancer. Despite increasing incidence due to life-style related risk factors and an ageing population, the long period of disease development generally allows a high likelihood of curative treatment as long as the tumour is still localised. However, once patients present with distant metastases, prognosis is poor and there is an urgent need for new therapy options.

except for the subset of right-sided tumours where cetuximab showed poorer outcomes [82]. Since the inhibition of a single signal transduction pathway is unlikely to provide optimal results, the combination of several targeted agents presents an appealing strategy. Surprisingly however, combining cetuximab with bevacizumab plus chemotherapy led to lower efficacy than single-agent treatment with either monoclonal antibody [83]. This negative finding notwithstanding, there is a clear need for further research to identify and test potential partner drugs to be used in combination with cetuximab and chemotherapy. Encouraged by the success of immune checkpoint blockade therapies for a variety of tumour entities in recent years, these drugs are of particular interest for such combination approaches.

1.2.2 Rationale for addition of Avelumab to FOLFIRI plus Cetuximab

As outlined in Section 1.1.4, immune checkpoint inhibitors (ICIs) are a new and exciting treatment option and are utilised in a growing number of tumour entities, yet the improvements in clinical outcomes are limited in some tumour entities, including HNSCC and mCRC. In several clinical trials, anti-PD1 monotherapy with nivolumab or pembrolizumab for patients affected by mCRC did not improve clinical outcome compared with guideline-based standard chemotherapy plus cetuximab [84, 85]. For combination therapy with nivolumab and ipilimumab, a high response rate (55%) and encouraging progression-free survival at 12 months (71%) was observed, but limited to a cohort of patients with DNA mismatch repair-deficient/microsatellite instability-high mCRC, resulting in high immunogenicity [86]. Overall, the results obtained for pure ICI therapies in mCRC may be described as largely unsatisfactory to date and many experts advocate combining ICIs and the existing standard-of-care chemotherapy plus cetuximab for the treatment of mCRC [33].

There are several important mechanisms by which cetuximab may turn an immunologically cold into a hot tumour, thereby making it more amenable to anti-tumour immune activity of co-administered ICIs than in the setting of ICI monotherapy (Fig. 1.7). In the process of cetuximab-mediated ADCC, NK cells are activated and release $IFN\gamma$ and other cytokines (e.g. IL2, IL12, IL15) to facilitate maturation of dendritic cells as well as crosstalk with other immune cells (macrophages, neutrophils) which in turn secrete chemoattractant molecules. This crosstalk is crucial for triggering EGFR-specific recruitment of cytotoxic T cells from the peripheral blood to the intratumoral space where they can carry out their lytic activity against tumour cells and contribute to the generation of new tumour antigens [87, 88]. The presentation of these tumour antigens by mature dendritic cells activates pre-existing and primes newly recruited cytotoxic T cells for further tumour lysis, ideally stimulating a long-term immune response [34, 89–94].

However, the desired stimulation of immunogenic tumour cell death via cetuximab comes at the cost of concurrently triggered immunosuppressive feedback mechanisms that tend to counteract cytotoxic tumour cell lysis [95–101]. Treatment with cetuximab plus chemotherapy was shown to significantly increase the frequency of Tregs, crucial players in the

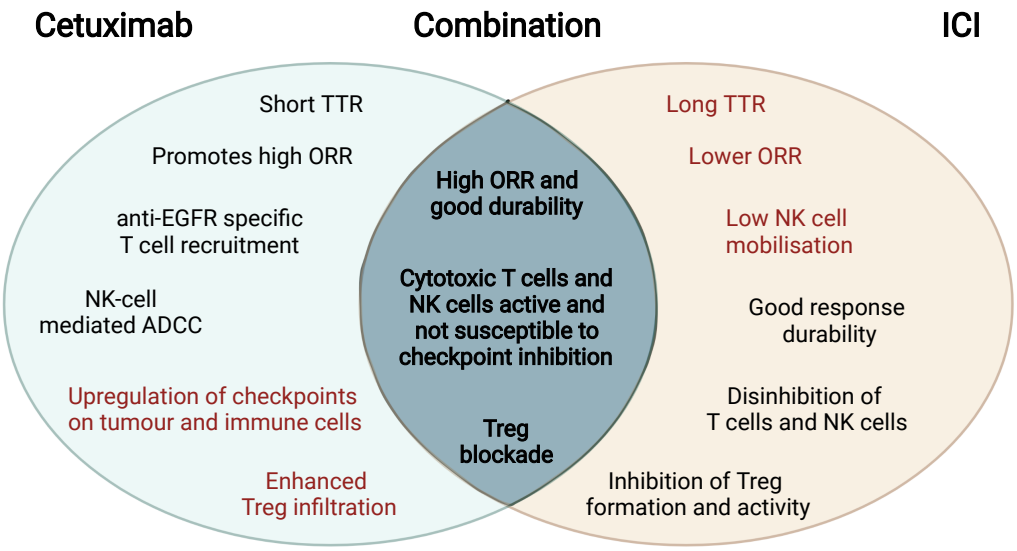

Figure 1.7: Rationale for combination therapy based on complementary and synergistic activities of cetuximab and ICI therapy. In combination treatment, their complementary advantages (black) may act synergistically to overcome the challenges (red) associated with either therapy alone and thus result in a durable response in a high proportion of patients. Abbreviations: TTR = time to response; ORR = objective response rate. Figure adapted from Ferris et al. [33].

suppression of anti-tumour activity, within lymphocyte populations in both the peripheral blood and tumour microenvironment [95]. In addition, cetuximab monotherapy increased the expression of the immunosuppressive markers $TGF\beta$, CTLA4 and PDL1 on Tregs [92] and, fittingly, this subpopulation was particularly enriched in patients who failed to respond to cetuximab treatment [95]. Thus, ICI treatment in combination with cetuximab appears to be a logical therapeutic approach as it may not only inhibit the suppressive CTLA4+/PDL1+ Treg population but may also reduce the infiltration of Tregs into the tumour microenvironment by preventing the peripheral induction of this population [102]. Along with Tregs, myeloid-derived suppressor cells (MDSCs) are another cell population that dampens anti-tumour immune activity. Their numbers were elevated in HNSCC patients treated with cetuximab, particularly so in nonresponders, and their expression of $TGF\beta$ is known to aid in tumour immune escape [35, 103]. Additionally, MDSCs inhibit cytotoxic T cells via PDL1 upregulation and secretion of cytokines that bind to T-cell chemokine receptors such as CXCR3 or CXCR4 [104, 105]. Hence, successful blocking of the PD1/PDL1 axis with ICI therapy carries the promise to relieve MDSC-mediated suppression of cytotoxic T cells. Finally, cetuximab-mediated $IFN\gamma$ secretion by activated NK cells upregulates PDL1 expression on tumour cells via the JAK2/STAT1 pathway,

Clinical trial	Identifier	MSI status	Line	Chemo-therapy	mAb	1° EP
FIRE6	NCT05217069	MSS/MSI	1st line	FOLFIRI	cetuximab and avelumab	PFS
AVETUX	NCT03174405	MSS/MSI	1st line	FOLFOX	cetuximab and avelumab	PFS
CAVE	NCT04561336	MSS/MSI	2nd line	–	cetuximab and avelumab	OS
AVETUXIRI	NCT03608046	MSS	2nd line	Irinotecan	cetuximab and avelumab	ORR
SAMCO	NCT03186326	MSI	2nd line	FOLFOX, FOLFIRI	cetuximab or avelumab	PFS

Table 1.1: Overview of currently ongoing clinical trials of mCRC patients treated with cetuximab and/or avelumab.
Abbreviations: EP = end point; MSI = microsatellite instability; MSS = microsatellite stable.

another immune-evading mechanism that may be counteracted through the concurrent use of ICIs [36, 93].

Taken together, there is a strong scientific rationale to complement the use of cetuximab with an ICI monoclonal antibody because (1) the wanted immunostimulatory effect of cetuximab (e.g. recruitment and priming of cytotoxic T cells) could be exploited to achieve the full potential of checkpoint blockade and (2) the unwanted immunosuppressive effects of cetuximab (Tregs, MDSCs, increased expression of checkpoint molecules on immune and tumour cells) may be alleviated by checkpoint blockade. In selecting a specific ICI agent to partner with cetuximab for such combination treatment, the PDL1 inhibiting IgG1 monoclonal antibody avelumab represents a particularly appealing choice since the concurrent use of two ADCC-inducing monoclonal antibodies may have the added benefit of cooperatively activating NK cells. Importantly, the combination of avelumab and cetuximab has been found to be safe for patients [60, 106] and raises the possibility of true synergy via fully activating the components of the innate and adaptive immune systems, widely engaging multiple types of immune cell populations. Several prospective clinical trials are currently evaluating the combination of cetuximab and avelumab plus chemotherapy in cohorts of mCRC patients (Table 1.1), with the FIRE6 study [107] being the focus of this scientific work. While the details of the study will be presented in Section 3.1 below, it is worth mentioning, from an immunological point of view, that cetuximab and avelumab are co-administered as first-line treatments, meaning they are given when the immune system is most likely to mount an effective anti-tumour response [108].

2 Aim of Study

As described in detail in Chapter 1, therapeutic mAbs are increasingly being used for the clinical treatment of cancer patients. While remarkable results - even including long-lasting complete remissions - are achieved in some, the benefit for the majority of patients is rather limited. Furthermore, predictive biomarkers for routine patient stratification are still largely unknown. Focusing on IgG1 mAbs in the context of mCRC, this work consists of three closely connected parts aiming to shed light on these aspects (Fig.2.1).

Establishing a FACS-based method of determining the FcgRIIIa-158 polymorphism In the first part of this work, we strive to develop and thoroughly validate a flow cytometric experimental method capable of reliably identifying a patient's FcgRIIIa-158 polymorphism. As outlined in Section 1.1.2, the scientific community is still deeply divided with regards to the influence of a patient's FcgRIIIa-158 polymorphism on both treatment response and clinical outcome measures under IgG1 mAb therapy. Thus, a scientifically rigorous elucidation of its role is crucial. With the current gold standard for determining the FcgRIIIa-158 polymorphism being rather costly and laborious PCR-based approaches, there is a yet unmet need for a quick, cost-effective and ubiquitously available technique to swiftly infer a patient's FcgRIIIa-158 polymorphism. Flow cytometric (FACS) measurements are routinely performed even in small hospitals around the world and, hence, the successful establishing of a FACS-based method could fill this niche and pave the way for widespread routine assessment of the FcgRIIIa-158 polymorphism from limited patient material ($< 100\,\mu l$ of blood) with short turn-around time (ca. 30 minutes) and at a fraction of the costs of PCR-based techniques. Having such a technique at hand is pivotal in order to (1) resolve the conflict emerged from contradictory findings reported in the literature and (2) provide a perfectly suited tool for determining the FcgRIIIa-158 polymorphism that could be integrated into routine clinical practice with ease if it turns

out to be of relevance for clinical decision-making or prognostic stratification.

Establishing an in vitro assay to detect ADCC The second part of this work is centered around establishing an in vitro experimental setup comprising (1) a lactate dehydrogenase (LDH) release assay to determine tumour cell death via ADCC and (2) a flow-cytometry based panel to study the phenotypes and activation of the involved immune cells. As described in Section 1.1.2, the class of IgG1 mAbs carries the promise to directly induce tumour cell death via ADCC, in addition to mere receptor inhibition (e.g. by targeting EGFR) or checkpoint blockade (e.g. by targeting PD1 or PDL1). However, to date, it is still unclear how important a role such NK-cell mediated ADCC plays in the clinical treatment of oncologic patients with IgG1 mAbs - it could range from having a negligible effect to being a major determinant of clinical response and outcome. With the basis of the experimental setup being the co-culturing of a suitable CRC cell line with patient-

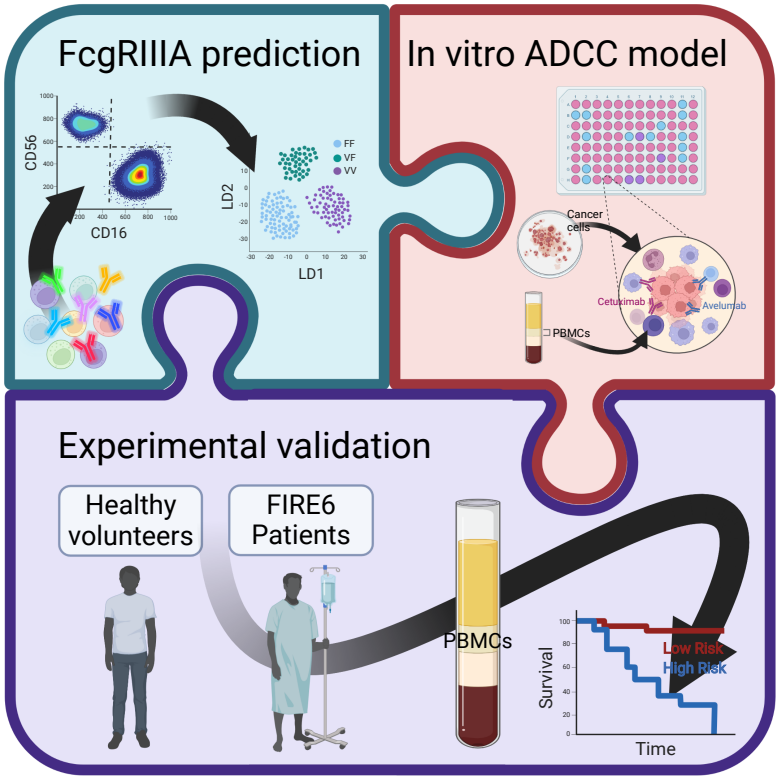

Figure 2.1: Overview of research objectives. The project is comprised of three closely connected parts, namely the establishing of a FACS-based prediction of FcgRIIIa-158 polymorphism (top left), the development of an in vitro ADCC model for colorectal cancer (top right) as well as the application of these two experimental methods to cohorts of healthy volunteers and colorectal cancer patients (bottom).

derived PBMCs, tweaking of culturing conditions and further experimental parameters should culminate in an optimised in vitro screening platform to assess a patient's ADCC capability.

Application of established methods to a clinical study cohort Successful completion of the first and second part forms the foundation of this project. Building upon this, validation of the established methods on a clinical study cohort constitutes its final litmus test. To this end, the experimental setup will be applied to patient-derived PBMCs obtained from peripheral blood sampling at various treatment time points of a cohort of 55 mCRC patients receiving cetuximab and avelumab combination therapy in addition to standard chemotherapy. Within this context, the major focus of the project is to determine whether any of a patient's FcgRIIIa-158 polymorhpism, in vitro ADCC activity or specific NK-cell phenotypes correlates with clinical response and/or outcome. These results promise to advance our current understanding by revealing new clues about patient-specific factors governing the interplay of IgG1 mAbs with the patient's immune system.

In summary, the overall aim of this study is to develop a robust experimental setup which could provide a fast, reliable and easily deployable screening test with prognostic value regarding the response to cetuximab and avelumab combination therapy, potentially useful for patient stratification prior to or during the initial phase of therapy.

3 Materials and Methods

3.1 Selection of study participants and their characteristics

Patients The patients examined in this scientific work were recruited within the framework of the non-randomised, single-arm, multi-centre, phase-II FIRE6 study (Fig. 3.1) which was approved by the Ethics Committee of Charité Universitätsmedizin Berlin and registered on the EU Clinical Trials Register as *EudraCT 2018-002010-12* [109]. Informed consent from all study participants was obtained regarding the prospective blood sampling and review of clinical data. A total of 55 patients with previously untreated RAS/BRAF wild-type mCRC were enrolled between the first quarter of 2019 and the third quarter of 2021 across 16 participating recruitment sites in Germany. As shown in Fig. 3.1, the patients received induction therapy of FOLFIRI and the anti-EGFR antibody cetuximab for

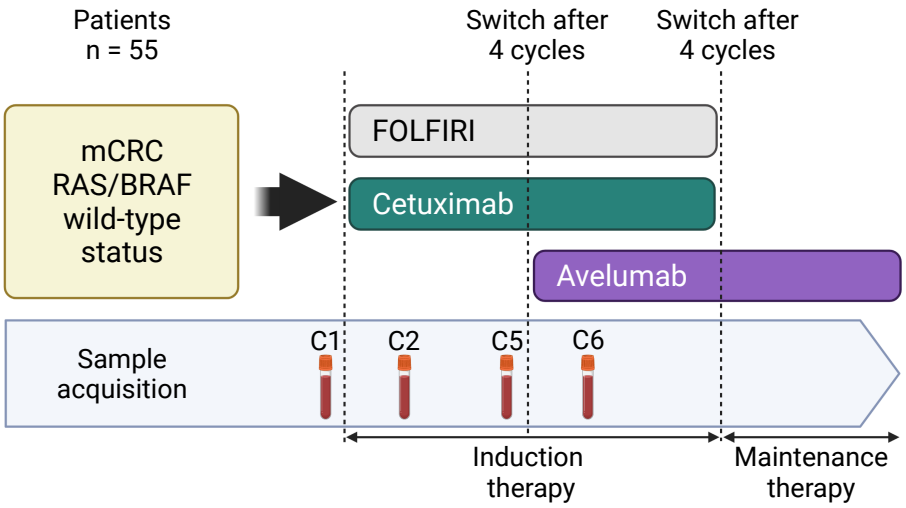

Figure 3.1: Design of FIRE6 study. 55 mCRC patients with RAS/BRAF wild-type status were treated with FOLFIRI and cetuximab for 4 cycles before avelumab was added to this regimen for another 4 cycles. After that, single-agent avelumab treatment was continued for 16 further months or until tumour progression. Peripheral blood samples were acquired at 4 critical timepoints during induction therapy.

the first 4 cycles, each with a duration of two weeks. Patients without tumour progression after cycle 4 received the anti-PDL1 antibody avelumab in addition to the combination of FOLFIRI and cetuximab for another 4 cycles. In the absence of tumour progression, patients were subsequently switched to single-agent maintenance therapy with avelumab only. The treatment ended after 16 months of said maintenance therapy or earlier if tumour progression or inacceptable toxicity occurred. Progression-free survival (PFS) was the primary endpoint of this study, with tumour progression being assessed according to irRECIST v1.1 [110]. Secondary endpoints were PFS rate after 12 months, objective response rate (ORR) and overall survival (OS). Peripheral blood samples from each patient were collected at four critical time points during the induction therapy (defined, based on the nearest treatment cycle, as C1, C2, C5 and C6) and processed according to Section 3.2:

- **C1**: at baseline before treatment initiation
- **C2**: after the first cycle of FOLFIRI plus cetuximab
- **C5**: before the addition of avelumab to the treatment regimen
- **C6**: after the first cycle of combination therapy of FOLFIRI, cetuximab and avelumab

Healthy volunteers To serve as a control group for the patient cohort at baseline (C1), one-off peripheral blood samples from 10 age-matched healthy controls were obtained. In addition, peripheral blood samples from a total of 29 further but not age-matched healthy volunteers were collected to establish a flow-cytometry based prediction of the FcgRIIIa-158 polymorphism. The recruitment of these healthy volunteers was approved by the Ethics Committee of Charité Universitätsmedizin Berlin under application number *EA4/219/20* and written informed consent from all study participants was obtained before blood sampling. Symptoms of acute infection at the time of blood withdrawal were ruled out for all volunteers by anamnesis and the blood samples were processed according to Section 3.2.

3.2 Handling of cell lines and human primary materials

Tumour cell lines As a first step, all colorectal cancer (CRC) cell lines (Table 3.1) were tested for mycoplasma contamination (MycoAlert^{TM} Mycoplasma Detection Kit, Lonza,

Cell line	Disease	a/s	Medium	Additives (% in v/v)	RRID [111]
CACO2	colorectal adenocarcinoma	a	DMEM	10% FBS, 1% P/S, 1% GlutaMax	CVCL_0025
DLD1	Dukes' type C, colorectal adenocarcinoma	a	RPMI-1640	10% FBS, 1% P/S, 1% GlutaMax	CVCL_0248
HT29	colorectal adenocarcinoma	a	DMEM	10% FBS, 1% P/S, 1% GlutaMax	CVCL_0320
HCT116	colorectal adenocarcinoma	a	DMEM	10% FBS, 1% P/S, 1% GlutaMax	CVCL_0291
LS174T	Dukes' type B, colorectal adenocarcinoma	a	DMEM	10% FBS, 1% P/S, 1% GlutaMax	CVCL_1384
RKO	carcinoma, papilloma	a	DMEM	10% FBS, 1% P/S, 1% GlutaMax	CVCL_0504
SnuC5	cecum adenocarcinoma	a	RPMI-1640	10% FBS, 1% P/S, 1% GlutaMax	CVCL_5112
SW48	Dukes' type C, colorectal adenocarcinoma	a	Leibovitz's L-15	10% FBS, 1% P/S, 1% GlutaMax	CVCL_1724
SW403	Dukes' type C, colorectal adenocarcinoma	a	Leibovitz's L-15	10% FBS, 1% P/S, 1% GlutaMax	CVCL_0545
SW480	Dukes' type B, colorectal adenocarcinoma	a	Leibovitz's L-15	10% FBS, 1% P/S, 1% GlutaMax	CVCL_0546
SW620	Dukes' type C, colorectal adenocarcinoma	a	Leibovitz's L-15	10% FBS, 1% P/S, 1% GlutaMax	CVCL_0547
SW837	colorectal adenocarcinoma	a	Leibovitz's L-15	10% FBS, 1% P/S, 1% GlutaMax	CVCL_1729
SW1417	Dukes' type C, colorectal adenocarcinoma	a	Leibovitz's L-15	10% FBS, 1% P/S, 1% GlutaMax	CVCL_1717

Table 3.1: Overview of the characteristics of the 13 colorectal cancer cell lines which were screened in this work to assess their suitability for in-vitro ADCC experiments. Further cell line details of interest may be retrieved via the respective RRIDs.
Abbreviations: a = adherent; RRID = Research Resource Identifier; P/S = Penicillin-Streptomycin; FBS = fetal bovine serum; DMEM = Dulbecco's Modified Eagle's Medium.

#LT07-318) before being cultured in flat-sided culture flasks with a growth area of 25 or 150 cm^2 (Corning, #CLS430372-500EA and #CLS430824-50EA) and placed in an incubator at 37°C, 5% CO_2 and 95% relative humidity. As all cell lines were growing in an adherent manner, cells were detached from the flask surface every 3-4 days at a confluence of 70-90% using phenol-red free TrypLE^{TM} (Life Technologies, #12604-013) and culturing was continued after splitting the cells in a ratio ranging from 1:2 to 1:10. The Luna-FL Automated Cell Counter (Logos Biosystems) was used for cell counting, following staining with the AO/PI Cell Viability Kit (Logos Biosystems, #F23001). As a safeguard measure to prevent the accumulation of genetic changes due to long-term cell culturing, cell cultures were discarded after a maximum of 30 passages and new cultures were established from samples preserved in a cryogenic storage tank at −180°C. As indicated in Table 3.1, CRC cell lines were generally kept in culture using either of DMEM (Gibco, #21885-025), RPMI-1640 (Gibco, #310870-025) or Leibovitz's L-15 medium (Sigma, #L5520), supple-

mented with 10% fetal bovine serum (FBS; Sigma, #F7524), 1% Penicillin-Streptomycin (P/S; Sigma, #P4333) and 1% GlutaMax^{TM} (Gibco, #35050061). All co-culturing experiments with human PBMCs were performed in phenol-red free DMEM (Gibco, #11880028) with only 1% FBS (Sigma, #F7524), unless specified otherwise in the respective section.

Primary materials Peripheral blood mononuclear cells (PBMCs) were isolated from heparinised whole blood by density centrifugation (Biocell, #L6115) according to our laboratory's standard protocol (20 ml of whole blood mixed with 20 ml of PBS and layered on top of 10 ml BioColl solution mixed with; centrifugation for 20 min at 2800 g). After an additional washing step (10 min at 500 g), the isolated PBMCs were resuspended in freezing medium (15% RPMI 1640 medium (Gibco, #12055), 75% FBS (Sigma, #F7524), 10% DMSO (Sigma Aldrich, #D2650)), aliquoted at $2.5 * 10^6$ cells per cryovial and, after rate-controlled cooling at $-1°C/min$ in a CoolCell^{TM} (Corning, #15542771) to $-80°C$, transferred to a cryostorage tank at $-180°C$. At the time of sample freezing, PBMC viability ranged from 30 to 95%. For thawing of cryoconserved PBMCs, the vials were placed in a heat bath at $37°C$ for 2 minutes and the cell suspension washed twice in 10 ml of RPMI 1640 with 20% of FBS pre-warmed at $37°C$. Subsequently, the recovered PBMCs were again resuspended in 10 ml of RPMI 1640 with 20% of FBS and placed in an incubator at $37°C$, 5% CO_2 and 95% relative humidity for 30 minutes before conducting the respective experiments.

3.3 Therapeutic antibodies

The two therapeutic antibodies used in this research project were supplied via the pharmacy of Charité Universitätsmedizin Berlin: The anti-EGFR antibody cetuximab is distributed under the commercial name Erbitux (Merck KGaA, #PZN-0493528), whereas the anti-PDL1 antibody avelumab is sold as Bavencio (Merck KGaA, #NDC-44084-3535-1). In the experiments to screen the various CRC cell lines for their suitability as in vitro ADCC model, both antibodies were used at a concentration of $1000\,ng/ml$ to make sure to saturate all available EGFR and PDL1 receptors on every cell line. Once SnuC5 was chosen as preferred cell line, the concentration of both antibodies was titrated in the range from 0.8 to $1000\,ng/ml$ with regards to ADCC lysis according to the protocol stated in

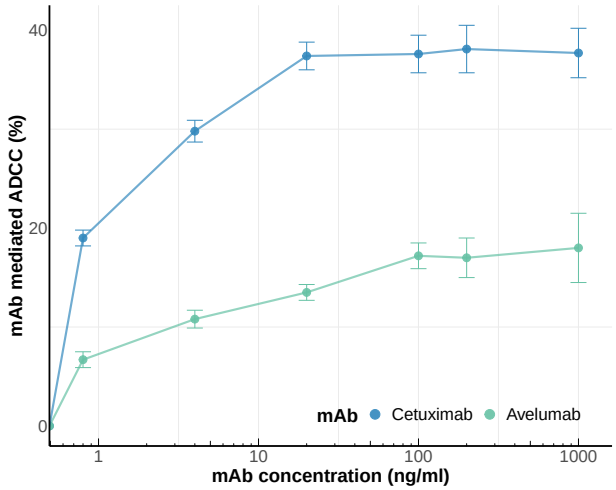

Figure 3.2: Titration of the antibody concentration with regards to ADCC lysis for the SnuC5 cell line. As is evident, ADCC lysis reaches a plateau for 100 ng/ml for both cetuximab and avelumab. Hence, this concentration was used for all further experiments with the SnuC5 cell line.

Section 3.7. As illustrated in Fig. 3.2, ADCC lysis reached a plateau for a concentration of 100 ng/ml for both cetuximab and avelumab. Hence, this concentration was used in all further experiments employing the SnuC5 cell line.

3.4 Flow cytometry (FACS)

Throughout this work, the flow cytometric measurement of all experimental samples (described in detail in Sections 3.5 to 3.7 below) were exclusively acquired using a CytoFLEX LX cytometer (Beckman Coulter). Instrument performance was monitored daily with CytoFLEX daily QC fluorospheres (Beckman Coulter, #B53230). A defined volume of 150 μl per sample was measured at a constant acquisition rate of 150 $\mu l/min$, keeping the abort rate $< 1\%$ over the course of the measurement. Flow cytometry data was analysed using CytExpert Software Version 2.4 (Beckman Coulter) and FlowJo Version 10.8.1 (Becton Dickinson).

3.5 Cell line characterisation

The 13 CRC cell lines listed in Table 3.1 in Section 3.2 were screened for the expression of an array of 9 surface markers that were hypothesised to be implicated in the NK-cell mediated ADCC of tumour cells (Table 3.2). Most importantly, EGFR and PDL1 expres-

Antibody	Fluorochrome	Clone	Dilution	Catalog No.	Company
EpCam	AF700	9C4	1:400	324243	Biolegend
EGFR	PE	AY13	1:100	352903	Biolegend
PDL1	PE	MIH3	1:100	374512	Biolegend
HLA-A,B,C	PE	W6/32	1:50	311406	Biolegend
HLA-E	PE	3D12	1:100	342603	Biolegend
MICA/B	PE	6D4	1:100	320906	Biolegend
CD137L	PE	5F4	1:100	311504	Biolegend
CD40	PE	5C3	1:100	334308	Biolegend
OX40L	PE	11C3.1	1:100	326307	Biolegend

Table 3.2: Overview of the antibodies used to screen for the surface expression of markers on CRC cell lines potentially implicated in ADCC.

sion was determined as they present the primary targets for the therapeutic antibodies cetuximab and avelumab, respectively. In addition, expression of the epithelial cell adhesion molecule (EpCam) was assessed in order to confirm that its ubiquitous presence on epithelium of the gastrointestinal tract, as suggested by the literature, could serve as a reliable marker for a FACS-based discrimination of tumour cells from immune cells in co-culture experiments. High levels of the supreme "self-markers" HLA-A/B/C are known to inhibit NK-cell mediated lysis [112, 113], whereas HLA-E and MICA/B may exhibit diverse effects through binding to the checkpoint receptors NKG2A and NKG2D on NK cells, respectively [112, 114, 115]. In a similar fashion, CD40, OX40L and CD137L expression on tumour cells have been shown to be to associated with tumour elimination by binding to their respective ligands CD40L, OX40 and CD137 expressed on the surface of NK cells and other immune cells [116–121].

In single-stain experiments for each combination of surface marker and cell line, approximately 50,000 tumour cells were stained for 15 minutes at room temperature in the dark with 50 μl of the antibody dilution and subsequently washed twice in 200 μl of phosphate buffered saline (PBS; Gibco, #14190-094) containing 0.5% bovine serum albumin (BSA; MACS, #130091376) for 5 minutes at 300 g. Comparison with appropriate isotype control stains allowed to calculate the proportion of cells expressing each respective surface marker. In addition, the median fluorescence intensity (MFI) of the cells was determined for each stained marker in order to serve as a surrogate for surface expression density.

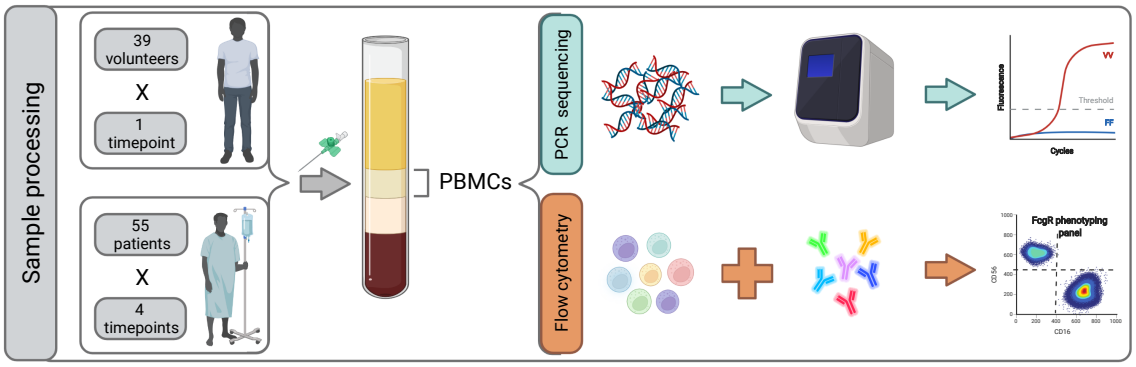

Figure 3.3: Schematic representation of the workflow of determining the FcgRIIIa-158 polymorphism of study participants from PBMCs via a PCR-based (top) and FACS-based approach (bottom).

3.6 Analysis of FcgRIIIa-158 polymorphisms

To determine the FcgRIIIa-158 polymorphism for each study participant as well as a cohort of healthy volunteers, two different approaches were employed in parallel as outlined in Fig. 3.3. It is worth noting that the tissue source for FcgRIIIa phenotyping is crucial. Since the phenotype of the NK cells is determined by the germline genotype present in normal tissue, PBMCs were employed in this work rather than cells from the tumour microenvironment that are more prone to carrying somatic mutations.

3.6.1 PCR-based approach

Currently, PCR amplification and subsequent melting curve analysis are the standard procedure widely employed to infer the presence and identity of single nucleotide polymorphisms (SNP), such as the G559T SNP underlying the three different FcgRIIIa-158 phenotypes. In a first step, a sufficient amount of DNA was purified from approximately 10^5 participant-derived PBMCs using the QIAamp UCP DNA Micro Kit (Qiagen, #56204) on a QIAcube (Qiagen, #QIAG990395). All further steps were carried out externally as a contract service by the Glycotope GmbH (Berlin, Germany) [122], namely melting curve analysis using the High Resolution Melting Kit (Roche Life Science, #50-720-3243) on a Light-Cycler 480 instrument (Roche Life Science).

Antibody	Fluorochrome	Clone	Dilution	Catalog No.	Company
Cell lineage					
CD3	BV421	UCHT1	1:50	300434	Biolegend
CD14	BV785	M5E2	1:50	301840	Biolegend
CD56	BUV395	NCAM16.2	1:200	563554	BD Biosciences
FcgRIIIA-binding antibodies					
CD16	FITC	**MEM154**	1:50	sc-51525 FITC	Santa Cruz
CD16	AF647	**LNK16**	1:50	MCA1193A647T	BioRadAntibodies

Table 3.3: Overview of the flow cytometric antibodies used to infer the FcgRIIIa-158 phenotypes. Two different FcgRIIIa-binding CD16 clones were used, namely *MEM154* and *LNK16*. Clone *MEM154* only binds FcgRIIIa receptors with a valine (V) but not a phenylalanine (F) residue at amino acid position 158, whereas *LNK16* binds in the presence of either residue.

3.6.2 FACS-based approach

Complementing the PCR-based method, a self-developed flow cytometry panel was used to distinguish the different FcgRIIIa-158 phenotypes (Table 3.3). For each patient, 10^5 PBMCs were stained in 50 μl of PBS with five fluorescent antibodies against four characteristic cell surface proteins (CD3, CD14, CD56, CD16) for 15 minutes and resuspended in 150 μl of PBS after being washed twice for 5 minutes at 300 g. As shown in Table 3.3, antibodies were titrated in dilutions from 1:50 down to 1:200 in order to find the best compromise between maximising the signal-to-noise ratio (S/N ratio) and keeping the experiments cost-efficient.

Two distinct CD16 clones were selected to be used simultaneously in this panel due to their differences in terms of binding to the FcgRIIIa receptor [12, 123, 124]. Clone *MEM154* is reported in the literature to bind the FcgRIIIa receptor at an epitope in close proximity to amino acid residue 158 and, thus, its binding is heavily influenced by the FcgRIIIa-158 polymorphism. In the presence of a valine (V) residue at this position, *MEM154* binds very strongly, whereas its binding is almost completely abolished in the presence of a phenylalanine (F) residue. In contrast, the binding epitope of clone *LNK16* lies far away from amino acid position 158 and binds in the presence of either amino acid. Yet, *LNK16* shows a somewhat higher binding affinity for an F residue rather than a V residue. Hence, we hypothesised that binding might differ to a certain extent between individuals with a heterozygote VF or a homozygote VV phenotype. Integrating the information obtained through the staining behaviour of these two CD16 antibodies forms the basis for the attempt of a FACS-based prediction of an individual's FcgRIIIa-158 phenotype.

3.7 Antibody-dependent cellular cytotoxicity

To assess the effect of ADCC activity, 24h co-cultures of tumour cells and PBMCs were carried out in 96-well flat bottom plates as showcased in Fig. 3.4. Unless stated otherwise in the respective sections, PBMCs and tumour cells were always seeded in an effector-to-target ratio (ETT ratio) of 10:1, namely 300,000 PBMCs were added to 30,000 tumour cells. Phenol-red free DMEM (Gibco, #11880028) with only 1% fetal bovine serum (FBS; Sigma, F7524-500ML) was chosen as culture medium to allow the fluorometric detection of LDH release cytotoxicity assays. The therapeutic antibodies were added at a final concentration of 100 ng/ml (as determined in Section 3.3) and 1% Triton-X-100 was added to the wells set aside as positive controls. The antibody binding the NK-cell activation marker CD107a was added immediately at the start of the co-culturing, whereas the protein-transport inhibitor GolgiStop (BD BioSciences, #554724) was added in 1:2500 dilution 4h before the end of incubation in order to prevent internalisation of CD107a

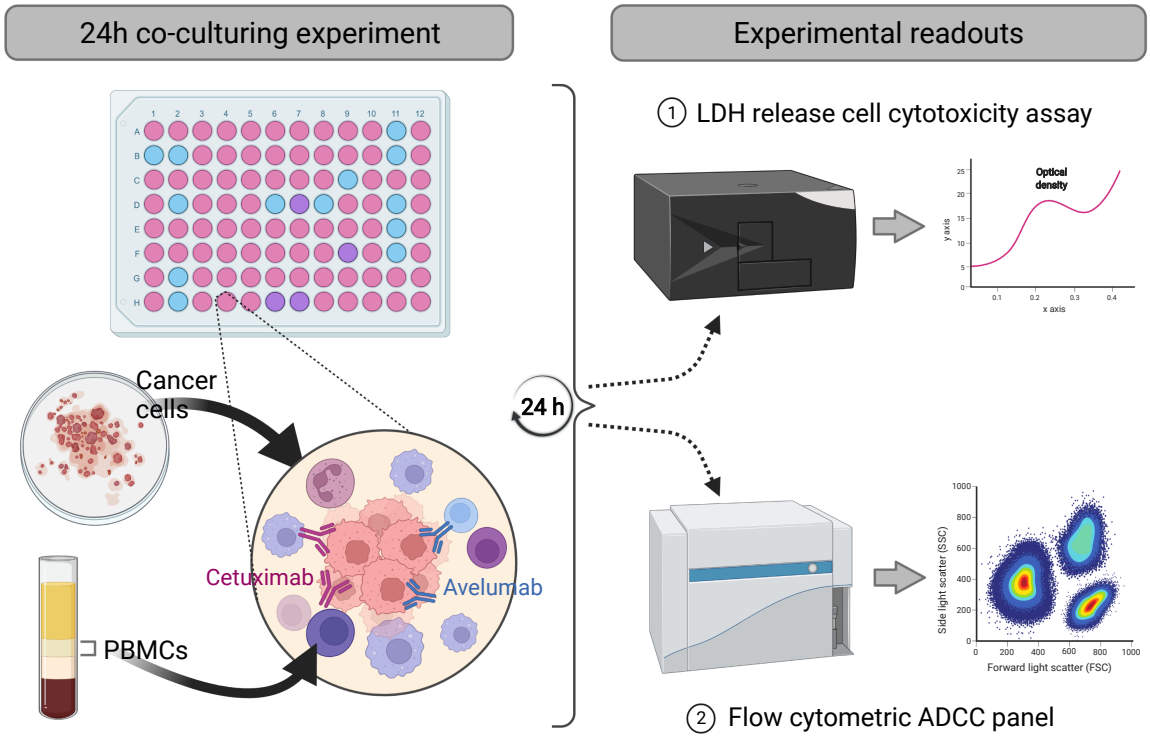

Figure 3.4: Schematic representation of the experimental workflow. CRC cancer cells are co-cultured with patient-derived PBMCs in an effector-to-target ratio of 10:1 with or without the addition of the therapeutic antibodies (left). After 24 hours, an LDH release cell cytotoxicity assay (top right) and a flow cytometric panel (bottom right) are performed in parallel to yield a double readout to assess ADCC activity.

from the cell surface. All wells were brought to a total volume of 220 μl and the plate sealed with an adhesive foil (Thermo Scientific, #10130853) to limit evaporation losses. After brief centrifugation for 2 minutes at 200 g to facilitate tumour cell adhesion to the plate bottom, the plate was kept in an incubator at 37°C, 5% CO_2 and 95% relative humidity for a co-culturing time of 24h. As a general rule, experiments were performed in triplicates whenever possible; for some patients, the scarcity of recovered PBMCs did only allow duplicates or in rare cases only single samples.

3.7.1 Lactate dehydrogenase release cytotoxicity assay

With the help of a cytotoxicity detection kit (Roche, #11644793001), the release of LDH from tumour cells into the medium was measured as a surrogate marker for cytotoxicity. LDH-catalysed oxidation of lactate to pyruvate yields a concomitant reduction of nicotinamide adenine dinucleotide, resulting in a broad absorption maximum at about 500 nm. According to the manufacturer's instructions, reagents and medium supernatants were mixed (75 μl culture medium supernatant mixed 1:1 with 75 μl LDH reaction mix; 25 minutes of incubation in the dark) before the absorbance was quantified in terms of optical density units using a microplate spectrophotometer system (Tecan). The specific PBMC-induced tumour lysis due to administration of the therapeutic antibodies was calculated as percent cytotoxicity according to the formula:

$Specific\,Lysis\,[\%] = (PTA - PT)/(T_{max} - T_{min}) * 100$, where

- **PTA**: LDH value of co-culture of **P**BMCs and **t**umour cells with therapeutic **a**ntibody
- **PT**: LDH value of co-culture of **P**BMCs and **t**umour cells alone
- $\boldsymbol{T_{max}}$: LDH value of **t**umour cells with 1% Triton-X-100 (positive control)
- $\boldsymbol{T_{min}}$: LDH value of **t**umour cells alone (negative control).

3.7.2 FACS assay

After removal of medium supernatant for the LDH assay, the remaining volume was transferred to a 96-well round bottom plate. Since all of the 13 screened CRC cell lines grow in an adherent manner, 50 μl of TrypLE (Life Technologies, #12604-013) were added to

each well of the original 96-well flat bottom plate and incubated for 15 minutes. Then, the detached tumour cells were also transferred to the corresponding wells of the 96-well round bottom plate and the plate centrifuged for 5 minutes at 300 g to discard any supernatant. The left-over cell pellets (consisting of both PBMCs and tumour cells) were stained in $50\,\mu l$ of Annexin V Binding Buffer (Biolegend, #422201) with a panel of 15 fluorochrome-conjugated antibodies (Table 3.4). The staining was performed in darkness at room temperature for 15 minutes. Subsequently, samples were washed once in $200\,\mu l$ PBS for 5 minutes at 300 g, then resuspended in $150\,\mu l$ Annexin V Binding Buffer and immediately measured on the CytoFLEX LX cytometer.

Table 3.4 summarises the employed antibodies and their final dilutions that were chosen with regards to achieving a suitable S/N ratio. As illustrated by the gating scheme in Fig. 3.5, the core of the FACS panel is formed by the 4 major cell lineage markers CD3 (T cells), CD14 (Monocytes), CD56 (NK cells) and EpCam (tumour cells). These cell populations are then examined in a more detailed fashion according to the gating scheme presented in Fig. 3.6. Most notably, tumour cells are assessed for cell death (DAPI and

Antibody	Fluorochrome	Clone	Dilution	Catalog No.	Company
Cell lineage					
CD3	BV421	UCHT1	1:50	300434	Biolegend
CD14	BV785	M5E2	1:50	301840	Biolegend
CD56	BUV395	NCAM16.2	1:200	563554	BD Biosciences
EpCAM	AF700	9C4	1:400	324243	Biolegend
NK-cell checkpoint & activation markers					
CD16	APC-Fire750	3G8	1:100	302060	Biolegend
CD107a	AF488	H4A3	1:100	328610	Biolegend
CD137	APC	4B4-1	1:200	309809	Biolegend
CD62L	BV605	DREG-56	1:200	304834	Biolegend
NKG2A	PE-Cy5	S19004C	1:200	375112	Biolegend
NKG2D	BV510	1D11	1:50	320815	Biolegend
PD1	BV650	EH12.1	1:100	3564104	Biolegend
Tumour-cell & monocyte markers					
PD-L1	PE	MIH3	1:200	374512	Biolegend
CD40	PE-Cy7	5C3	1:200	334322	Biolegend
Cell-death markers					
DAPI	–	–	$0.4\mu M$	D9542-5MG	Sigma-Aldrich
Annexin V	PeDazzle	–	1:50	640956	Biolegend

Table 3.4: Overview of the flow cytometric antibodies of the FACS ADCC panel. The panel primarily consists of cell-lineage markers as well as NK-cell activation and checkpoint markers. Furthermore, additional markers are used to characterise tumour cells and cell death.

Annexin V stains) and the expression of PDL1 and CD40, whereas NK cells are screened for FcgRIIIa receptor engagement and subsequent activation (CD16, CD107a, CD137). In addition, the expression of checkpoint molecules (PD1, NKG2A, NKG2D) and phenotypic markers (CD62L) is quantified on NK cells and T cells. In contrast, monocytes are gated for CD40, PDL1, CD62L and PD1 expression.

3.8 Data analysis, management and statistics

The aim of this explorative experimental work was the description of previously unknown effects. Hence, the performed statistical analyses (e.g. p-values) are not to be considered of confirmatory character, but rather to be seen as descriptive. Unless stated otherwise in the respective section, all results presented in this work are means (μ) and standard

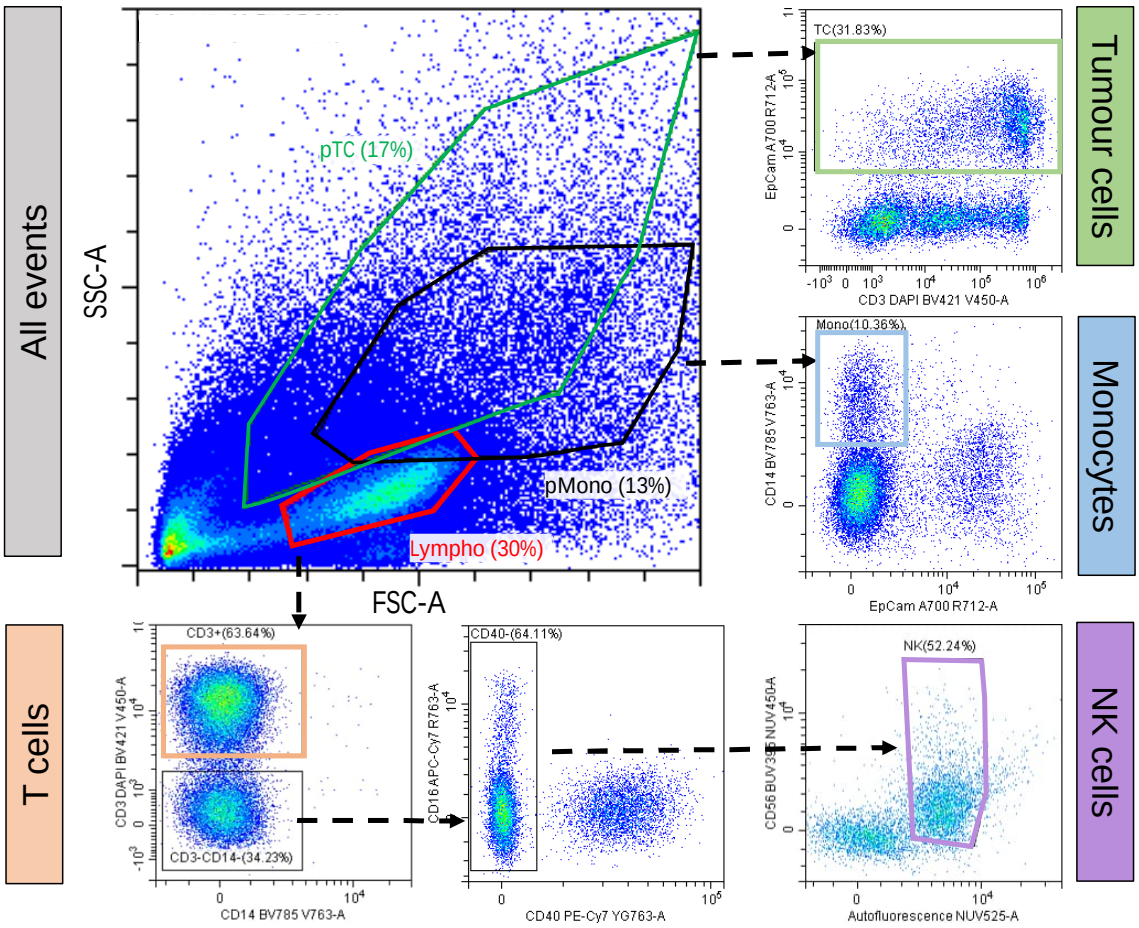

Figure 3.5: Gating scheme of the FACS ADCC panel for tumour cells and the major immune cell populations. The different subsets are distiguished as follows: tumour cells (pTC, EpCam+), monocytes (pMono, EpCam-, CD14+), T cells (Lympho, CD14-, CD3+), NK cells (Lympho, CD3-, CD14-, CD56+).

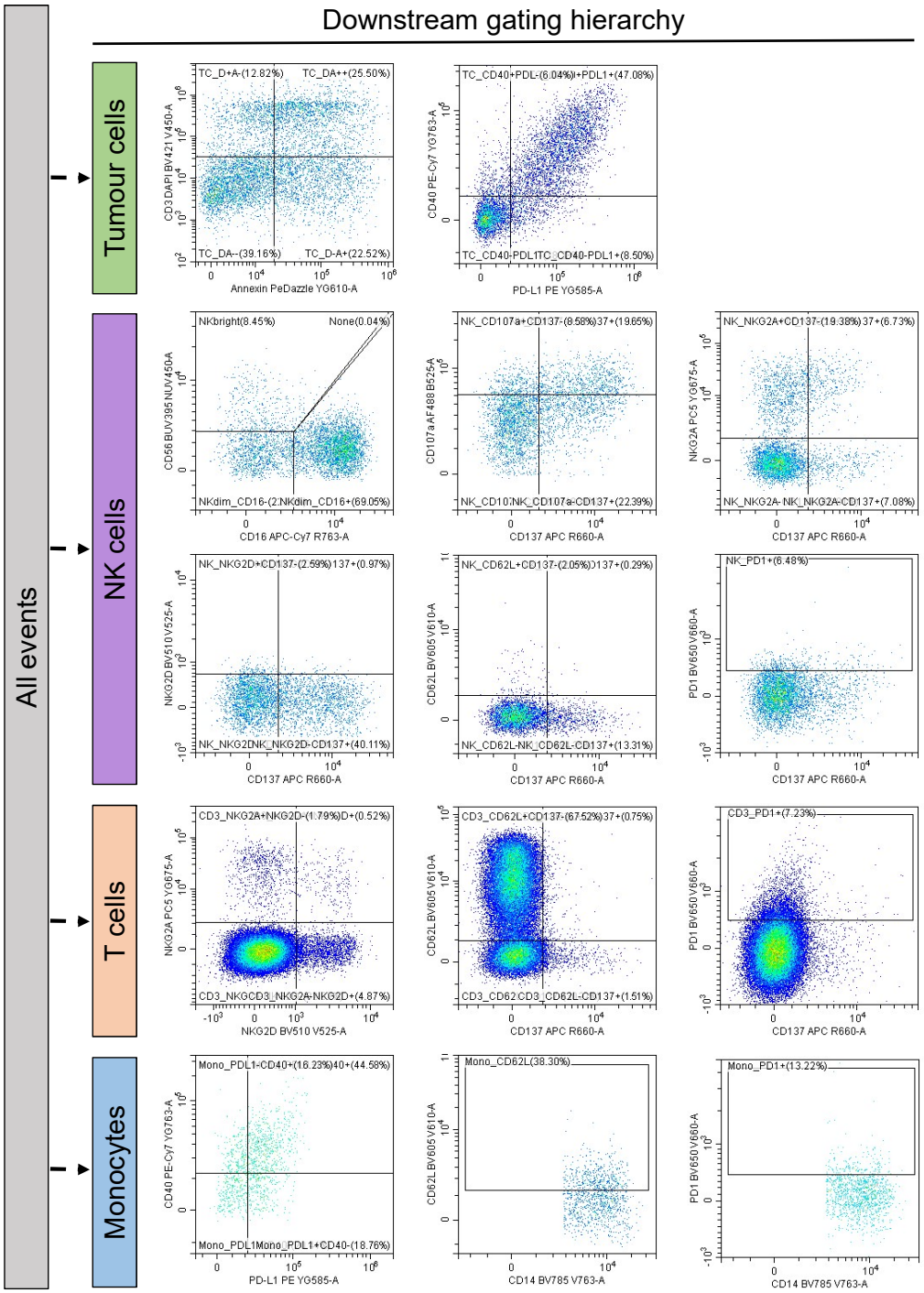

Figure 3.6: Downstream gating scheme for tumour cells and immune cell subsets. Following the gating of Fig. 3.5, tumour cells are examined for cell death (DAPI and Annexin V stains) and the expression of PDL1 and CD40. NK cells are assessed for FcgRIIIa receptor engagement and subsequent activation (CD16, CD107a, CD137). In addition, the expression of checkpoint molecules (PD1, NKG2A, NKG2D) and phenotypic markers (CD62L) was quantified on NK cells and T cells. Monocytes are gated for CD40, PDL1, CD62L and PD1.

error of mean (SEM) derived from technical and/or biological replicates. Comparisons between two dependent or independent groups were made using a two-tailed Welch's t-test (parametric; normally-distributed variables) or the Brunner-Munzel test (non-parametric; non-normally distributed variables). Comparisons between three or more groups were made by one-way ANOVA tests (parametric; normally-distributed variables) or Kruskal-Wallis tests (non-parametric; non-normally distributed variables). The linear mixed-effects model in Section 4.3.3 was fitted employing a restricted maximum likelihood approach (REML) and the Kenward-Roger approximation to compute p-values. As criterion for statistical significance, a p-value < 0.05 was considered throughout this work, whereas *ns* was used to denote statistically non-significant differences. Due to the descriptive nature of this work, it is worth noting that adjustment for multiple testing was not generally performed, unless explicitly stated. In some sections, 95% confidence intervals around the mean are stated to better interpret observed differences rather than considering mere p-values alone. Data analysis was performed using R (v.4.0.0) [125] with RStudio [126] including the packages brunnermunzel [127], caret [128], ComplexHeatmap [129], cowplot [130], dplyr [131], EnhancedVolcano [132], faraway [133], ggord [134], ggplot2 [135], klaR [136], lme4 [137], lmerTest [138], magick [139], magrittr [140], party [141], tibble [142], tidyr [143], tidyverse [144], Rtsne [145] and RVAideMemoire [146]. All visualisations including illustrations of scientific content were created with BioRender [147].

4 Results

4.1 FACS-based prediction of FcgRIIIa-158 phenotypes

In the first part of this work, a FACS-based antibody panel was developed and tested with regards to its ability to infer FcgRIIIa-158 phenotypes from collected PBMC samples as an easily accessible, fast and cost-effective method to replace PCR sequencing.

4.1.1 PCR sequencing forms ground truth for FcgRIIIa-158 phenotypes

As described in Section 3.6.1, PCR sequencing was performed on the cohorts of healthy volunteers and FIRE6 study participants. The unequivocal assignment of the FcgRIIIa-158 phenotypes was feasible for all 39 healthy volunteers as well as all 52 of the 55 patients, for whom sufficient primary material for DNA isolation (i.e. approximately 10^5 PBMCs) was available in our biobank storage facility. Within the scope of this work, the results determined via PCR sequencing forms the ground truth against which the FACS-based phenotype predictions are to be compared. The frequencies of the PCR-determined phenotypes are displayed in Fig. 4.1 for both patients and healthy volunteers, showing a close match in the distribution of phenotypes. This is an important confirmatory check that allows us to deem the group of healthy volunteers as sufficiently representative of the enrolled patient cohort in order to be used to train a prediction model in Section 4.1.3, which may then be validated using the patient cohort as a test set. An additional indicator that the employed PCR sequencing approach is reliable and does not suffer from methodological flaws (e.g. some PCR methods are prone to overcalling VF heterozygotes and undercalling FF homozygotes [148]) is that our data does not show any deviation from the Hardy-Weinberg equilibrium. From the determined FcgRIIIa-158 phenotypes, the allele frequencies for V and F, here denoted as v and f, can be derived, which in turn allows to calculate the ex-

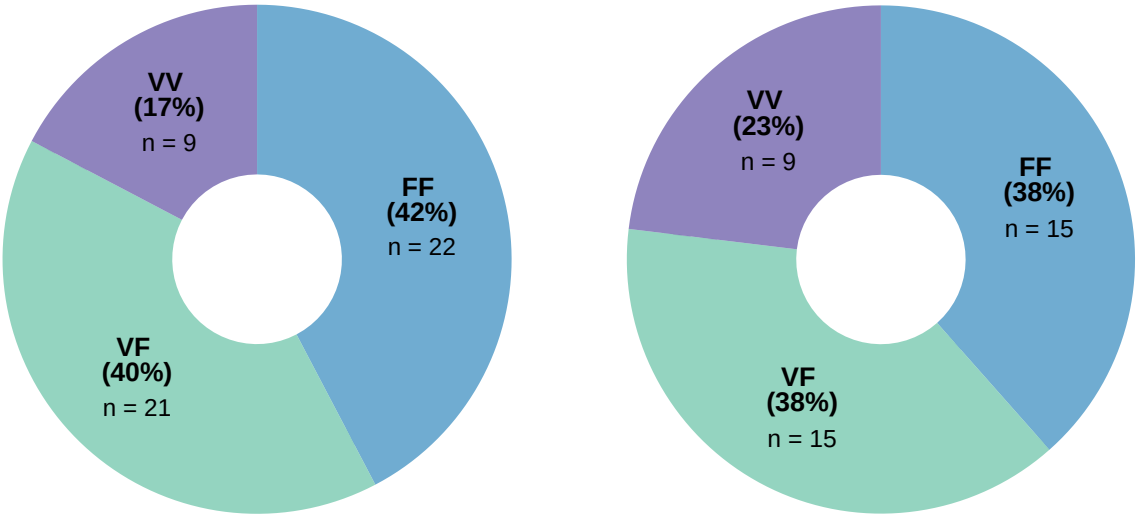

(a) Patients (b) Healthy volunteers

Figure 4.1: Frequency of FcgRIIIa-158 phenotypes determined via PCR sequencing for (a) FIRE6 patients and (b) healthy volunteers. The distribution of the three different phenotypes are similar between both cohorts and in good agreement with the Hardy-Weinberg equilibrium and the literature [149–151].

pected numbers for each FcgRIIIa-158 phenotype by applying the principles of Mendelian inheritance according to the formula $v^2 + 2vf + f^2 = 1$ (Hardy-Weinberg equilibrium) [149]. No significant difference between expected and measured phenotypes is found for patients ($\chi^2/f = 0.99$, p = 0.32) and healthy volunteers ($\chi^2/f = 1.75$, p = 0.19), respectively, confirming that the Hardy-Weinberg equilibrium holds true. Furthermore, it is worth noting that the observed frequencies are in good agreement with the prevalence of the three FcgRIIIa-158 phenotypes in the Caucasian population reported in the literature, ranging from 38-50% (FF), 39-47% (VF) and 11-14% (VV) [150, 151].

4.1.2 MFIs of CD16 clones alone not sufficient to assign FcgRIIIa-158 phenotypes

In Fig. 4.2, the gating scheme for determining the MFIs of the two distinct CD16 clones, LNK16 and MEM154, on the population of NK cells is shown. Starting from a lymphocyte gate on the SSC-A/FSC-A plot, NK cells were subsequently gated as CD3-CD14-CD56+ cells. Within the NK-cell population, it was taken advantage of the fact that $CD56_{bright}$ NK cells are known to be CD16- and, thus, used as a reference to set the gate for CD16+$CD56_{dim}$ NK cells. For each of the three FcgRIIIa-158 phenotypes, Fig. 4.2

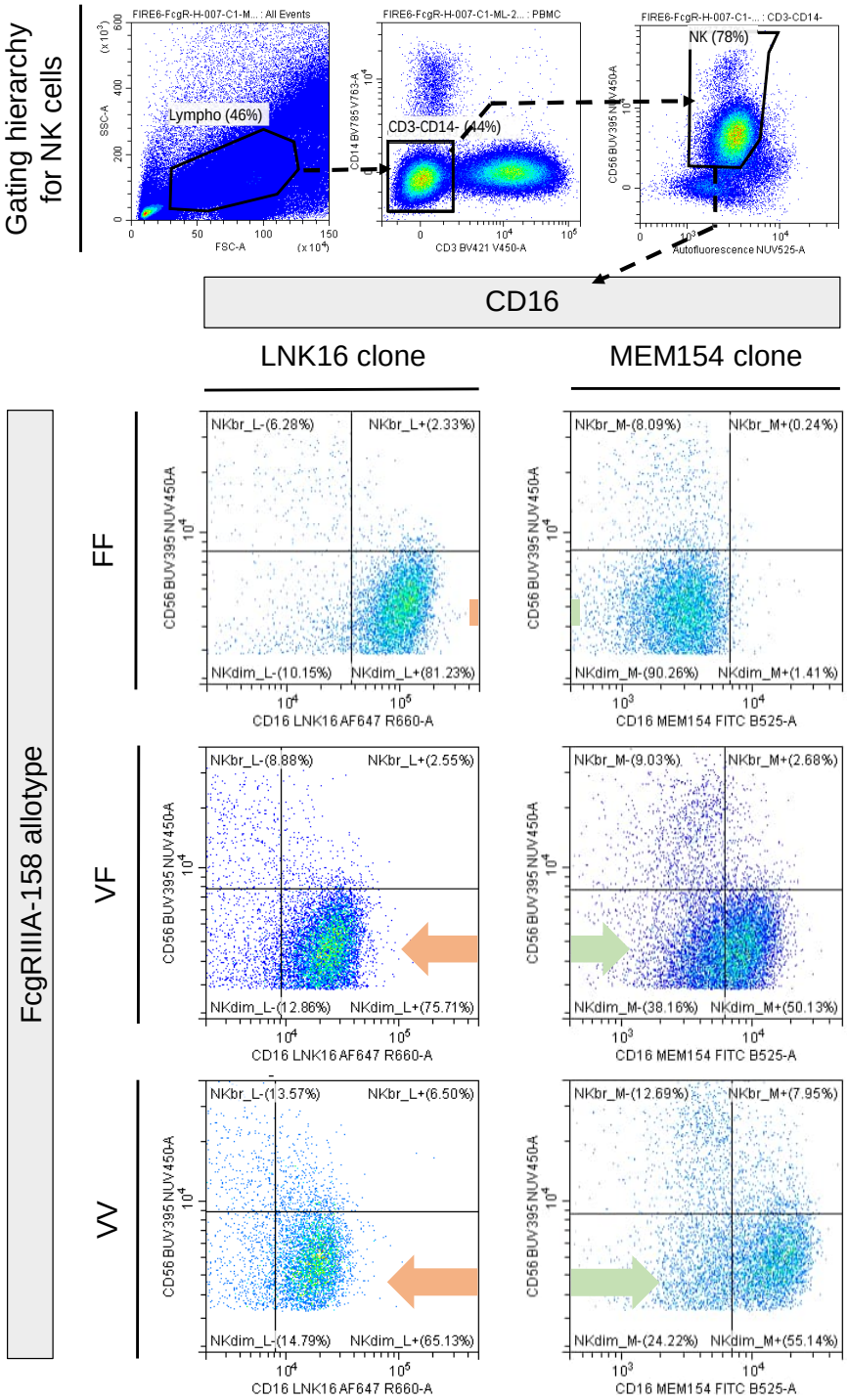

Figure 4.2: Gating scheme of the FcgRIIIa-158 FACS panel and representative examples for each phenotype. For gated NK cells, the MFI for the LNK16 clone is highest for FF individuals and decreases for VF and, even more so, VV individuals (orange arrow). As expected, FF individuals show negligible binding of the MEM154 clone, while the MFI for the MEM154 clone is evidently increased for VF individuals and reaches a maximum for VV individuals (green arrow).
Abbreviations: NKdim = $CD56_{dim}$ NK cells; NKbr = $CD56_{bright}$ NK cells; L+/- = LNK16+/-; M+/- = MEM154+/-.

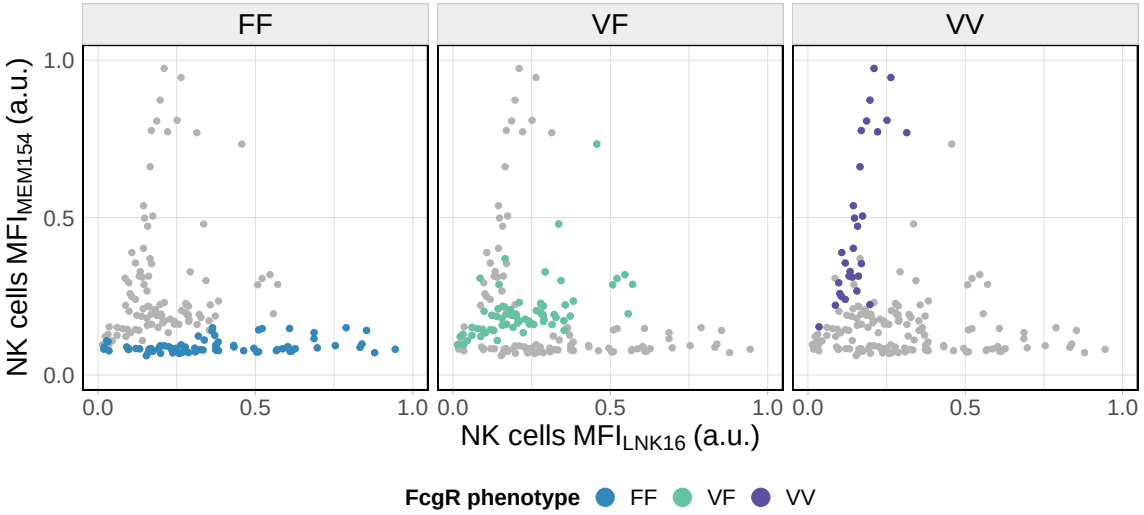

Figure 4.3: Scatterplot of MFI$_{MEM154}$ and MFI$_{LNK16}$ on NK cells. Dots represent single individuals and FcgRIIIa-158 phenotypes are colour-coded. Clustering of the three phenotypes towards different areas of the scatterplot is visible. However, separation between the phenotypes is not sufficient to allow unambiguous assignment of individuals to either group.

displays a representative example of LNK16 and MEM154 binding to CD16 on NK cells, rendering evident two general trends. Firstly, individuals with the FF phenotype exhibit a strikingly higher MFI for the LNK16 clone than do VF and, even more so, VV individuals. In agreement with the literature, this finding confirms that LNK16 doubtlessly reacts with both isoforms of FcgRIIIa-158, but that its binding affinity is nonetheless higher in the presence of the F residue. Secondly, comparing CD56$_{bright}$ to CD56$_{dim}$ NK cells in Fig. 4.2, no binding of the MEM154 clone to NK cells of FF individuals is apparent. In contrast, MEM154 binds to both the VF and VV phenotypes, with the latter showing the highest MFI overall. Yet, this general trend notwithstanding, considerable overlap of MEM154 MFIs between VV homozygotes and VF heterozygotes is observed and prevents the unambiguous assignment of phenotypes solely based on the MEM154 MFI.

To further investigate whether combining the MFI information from the LNK16 and MEM154 clones may be sufficient for an unequivocal distinction of phenotypes, a scatterplot comparing these two MFIs for the combined cohort of healthy volunteers and patients was computed (Fig. 4.3). In general, individuals of each phenotype tend to cluster together towards distinct regions of the plot: FF homozygotes are spread out along the bottom of the plot (MFI_{MEM154} low; MFI_{LNK16} variable), whereas VF heterozygotes are located in the middle-left region (MFI_{MEM154} medium; MFI_{LNK16} medium) and VV homozygotes

accumulate towards the top left part (MFI_{MEM154} high; MFI_{LNK16} low). While some extent of clustering may be appreciated, it is immediately evident that there is a lack of sufficient separation between the three phenotypes in order to allow the placement of class boundaries without misclassification of many individuals. Hence, it can be concluded that this rather simplistic approach is not adequate and a more elaborate analysis is warranted if FcgRIIIa-158 phenotypes are meant to be assigned on the basis of the acquired FACS data.

4.1.3 LDA model allows FACS-based prediction of FcgRIIIa-158 phenotypes

As described in Section 4.1.2, reliable assignment of the FcgRIIIa-158 phenotypes could not be achieved by a mere comparison of the MFIs for the binding of the LNK16 and MEM154 clones alone. Taking advantage of the fact that the acquired flow cytometry data contains a myriad of information which goes far beyond the sheer MFIs for these two clones, a total of 30 features were extracted and/or constructed from the measurements in a more sophisticated approach (outlined in Fig. 4.4). Among others, these features comprised simple parameters such as the frequencies and MFIs (both LNK16 and MEM154) of the different NK-cell subsets (CD56$_{bright}$; CD56$_{dim}$CD16+, CD56$_{dim}$CD16-) as well as combination features such as the MFI or frequency ratios between LNK16 and MEM154 on these subsets. In a next step, the relevance of the individual features had to be de-

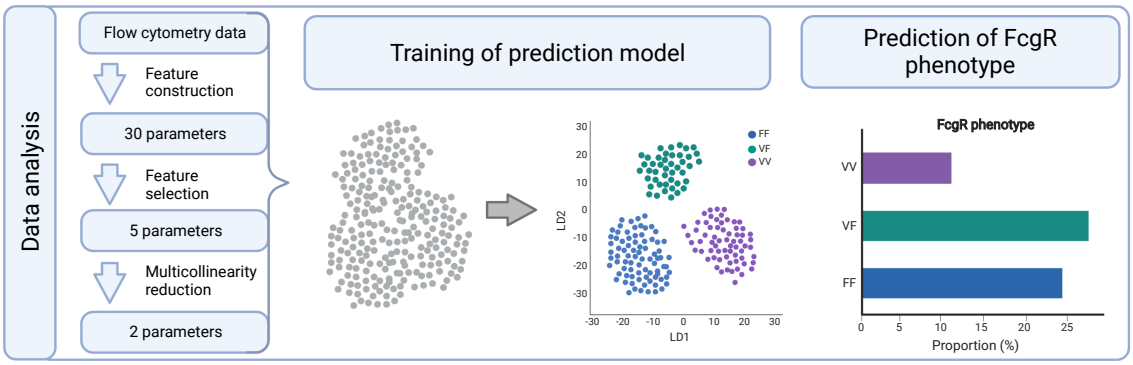

Figure 4.4: Schematic representation of the data analysis workflow to predict the FcgRIIIa-158 phenotypes from FACS data. A total of 30 parameters were extracted from the acquired flow cytometry data. After pre-processing steps involving feature selection and multicollinearity reduction, the two remaining parameters were used to train a prediction model applying Linear Discriminant Analysis (LDA) on the training set of healthy volunteers. Subsequently, FcgRIIIa-158 phenotypes of the patient cohort could be predicted with the LDA-derived model.

termined. As is common in a data-science workflow, a conditional random forest model was applied in order to select the five most important features. The tree-based strategy underlying the random forest model naturally orders features based on how much they improve the purity of the node, bringing the better performing features as closely as possible to the root of the tree. Therefore, to build a decision tree, we need to compute the most predictive features, from which the importance of the features is in turn derived. A high degree of multicollinearity was inherent in our method of feature construction that included the generation of new variables as a combination of others and its presence might adversely affect the performance of the prediction model. To address issues of multicollinearity between the five selected features, the variance inflation factor (VIF) was estimated for each feature. The VIF gives an estimate of how much the variance of a feature is inflated due to multicollinearity with the remaining variables of the model. Values for VIF range from 1 upwards, with higher values indicating a higher degree of multicollinearity. Exactly how large a VIF has to be before it becomes problematic is a subject of debate. Taking a conservative approach, an upper threshold of VIF<5 was applied in this work, in accordance with the literature [152–154]. After these rigourous pre-processing steps, the selection was narrowed down to the following two features:

- $\boldsymbol{rMFI_{NKdim_{ML}}}$: MFI ratio of MEM154 to LNK16 on CD56$_{dim}$CD16+ NK cells
- $\boldsymbol{rF_{NKdim_{ML}}}$: frequency ratio of CD56$_{dim}$CD16+ NK cells (as percentage of all NK cells) between MEM154 and LNK16

Next, these parameters were fed into a model built on linear discriminant analysis (LDA). Among the virtually limitless number of machine-learning algorithms out there, we do not claim that LDA necessarily represents the optimum solution for our scenario. However, as a proof of concept, the application of LDA is appealing because it is (1) a supervised learning algorithm that aims to (2) minimise within-class differences while (3) maximising between-class differences, thus favouring class separation. It is worth mentioning that LDA generally requires the input data to be normally distributed within classes and the variances to be equal between classes. While the former assumption could be confirmed to be true, the variances between the classes differed significantly (p-value >0.05). Nonetheless, it is known that the algorithm is rather robust to violations of the

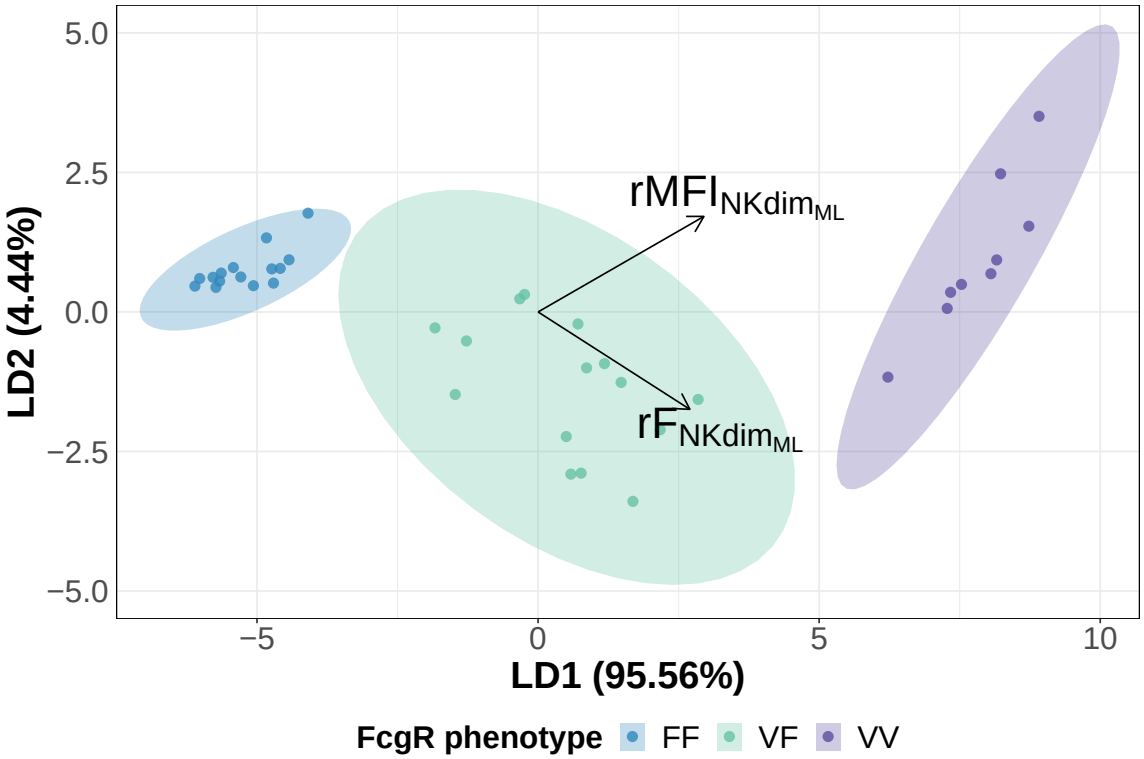

Figure 4.5: Linear Discriminant Analysis (LDA) model computed on a training set of 39 healthy volunteers. The model is based on two previously selected features, $\text{rMFI}_{NKdim_{ML}}$ and $\text{rF}_{NKdim_{ML}}$, and shows excellent separation between the three phenotype classes. Most importantly, the samples of each phenotype cluster together and not a single sample is misclassified.

equal-variance assumption and this violation could likely be tolerated. Fig. 4.5 shows a visualisation of the resulting LDA model computed from the training set of the 39 healthy volunteers. The samples of each phenotype cluster together nicely, showing excellent separation between the three classes. Most importantly, compared to the scatterplot of the MFI_{MEM154} and the MFI_{LNK16} in Fig. 4.3 in Section 4.1.2 above, not a single sample is mistakenly assigned to the wrong class. Instead, class boundaries that perfectly distinguish the phenotypes could be drawn around the clusters, as exemplified by the three shaded colour-coded ellipses overlaid onto the figure.

4.1.3.1 Correct phenotype predictions for >90% of validation set

While the LDA model generated in Section 4.1.3 does hold considerable promise, it must be applied to an appropriate test set for validation in order to confirm its reliability. Hence, it was employed to predict the FcgRIIIa-158 phenotypes of the 52 individuals of the FIRE6 patient cohort (Fig. 4.6(a)). Across all phenotypes, an overall prediction accuracy of

91% was achieved. Examining these results more in detail, it is worth noting that the model classified 100% of FF individuals correctly. In contrast to such perfect results for FF homozygotes, only 91% of all VV homozygotes and 82% of VF heterozygotes were classified correctly. Misclassification of individuals occurred exclusively between VF and VV individuals, with a small but substantial number of samples being assigned to an incorrect phenotype. This finding underlines what could already be suspected from the properties of the two chosen CD16 clones MEM154 and LNK16 reported in the literature: Due to the presence of at least one V allele, VF and VV individuals appear more similar and are harder to distinguish from each other than FF individuals who do not bind the MEM154 clone at all.

4.1.3.2 Prediction accuracy does not decrease due to peripheral NK cell activation

Due to the very nature of the clinical study employing the IgG1 mAbs cetuximab and avelumab, which are able to engage with the FcgRIIIa receptor on NK cells and elicit ADCC, activation of peripherally patrolling NK cells may be expected to result in substantial CD16 downregulation over the course of therapy. Such downregulation of CD16 upon binding the therapeutic IgG1 mAbs could potentially impair the labelling of a patient's NK cells with the LNK16 and MEM154 flow-cytometric antibodies and, thus, adversely

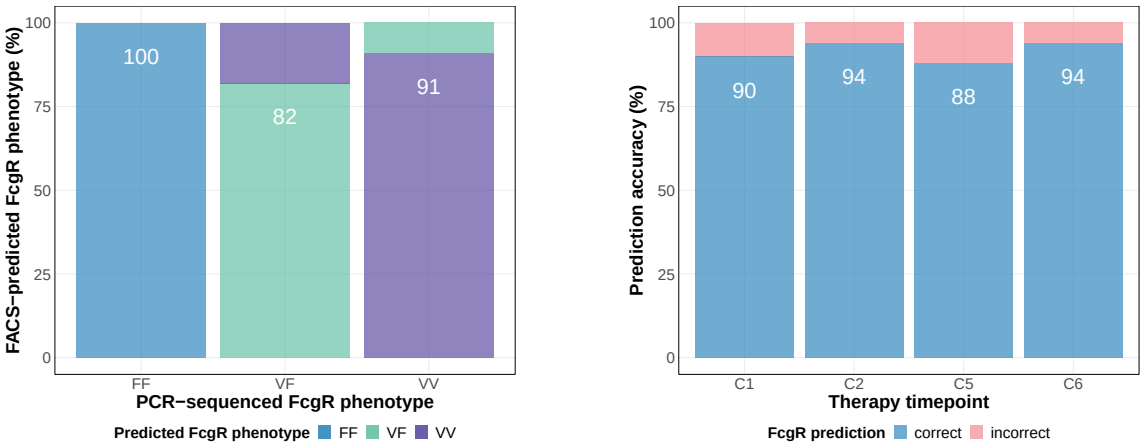

(a) Prediction accuracy per phenotype

(b) Prediction accuracy per timepoint

Figure 4.6: FACS-based FcgRIIIa-158 prediction accuracy for patient cohort. (a) All FF homozygotes are classified correctly, whereas some extent of misclassification is present for VF and VV individuals. (b) Prediction accuracy is comparable over all therapy timepoints, implying that potential CD16 downregulation on peripherally activated NK cell during therapy does not seem to affect prediction accuracy.

affect the FACS-based prediction of FcgRIIIa-158 phenotypes. Much to our reassurance however, the analysis presented in Fig. 4.6(b) confirms that prediction accuracy is comparable over the four examined therapy timepoints, fluctuating only mildly from 88 to 94%. Importantly, prediction accuracy at timepoint C1 before the first administration of any IgG1 mAb is not notably higher than for later timepoints. Hence, the blood sample for the FACS-based FcgRIIIa-158 prediction must not strictly be acquired before the start of therapy and, if pre-emptive sample collection is rendered impossible or impractical, doing so later on is still worthwhile.

4.1.3.3 Training set of 9 samples is sufficient to train LDA model

All of the analysis presented so far heavily relies on flow-cytometric measurements of the MFIs for the LNK16 and MEM154 clones on NK cells. For this reason, it is imperative to mention that measurements of the MFIs are always dependent on the specific flow-cytometry device used as well as its calibration and acquisition settings. This implies that measurements of a training set must be obtained to compute a new prediction model (whether it be LDA or any other algorithm) for each individual machine and its respective settings. While samples of 39 healthy volunteers were used for the model presented in Section 4.1.3, it is of interest to determine the minimum sample size of the training set sufficient to match the prediction accuracy of the model derived by using the full training set. To answer this question, the sample size was gradually reduced from 39 down to only 3 samples in a step-wise fashion.

For each sample size N, picking N samples from the pool of all available samples and subsequent training as well as validation of the LDA prediction model was repeated 100 times in order to minimise uncertainties introduced by "unfavourable picking". Regarding the picking of samples, two different strategies were explored. In the first approach, samples were chosen with FcgRIIIa phenotype proportions FF:VF:VV of 4:4:2, i.e. approximating the reported prevalence of the phenotypes in the Caucasian population. This strategy carries the advantage that volunteers to be included in a new training set could be recruited at random, obviating the need to screen for phenotypes first. In the second approach, equal FcgRIIIa phenotype proportions FF:VF:VV of 1:1:1 were used instead. While for this approach candidates would have to be screened for their phenotype first, it

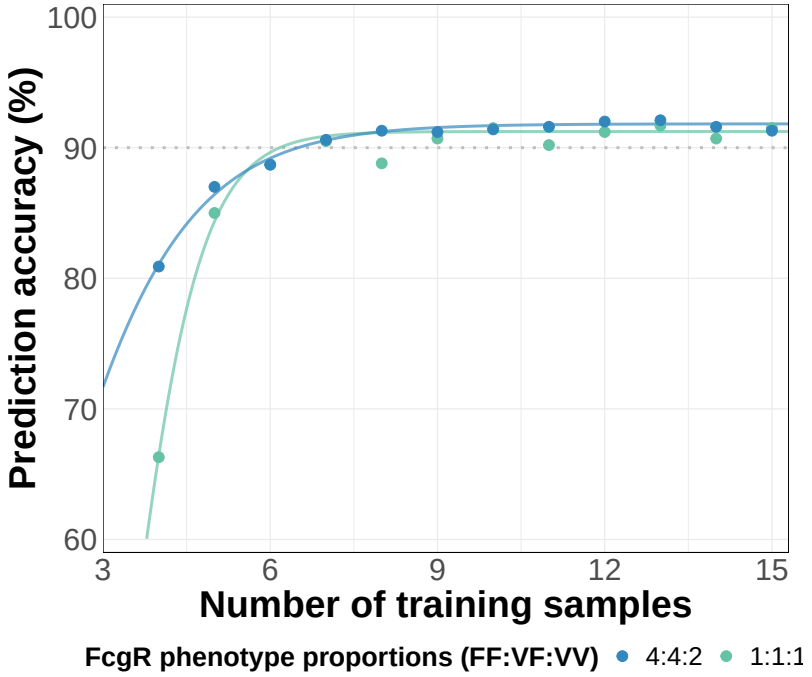

Figure 4.7: Performance of LDA prediction model computed from gradually smaller size of training set. In a step-wise fashion, the sample size is reduced down to only 3 samples. For each sample size, an LDA model is trained and validated on the test set (repetitions n = 100) using two different approaches for FcgRIIIa phenotype proportions: approach 4:4:2 (blue) simulates the approximate prevalence of each phenotype in the Caucasian population, whereas approach 1:1:1 (green) assumes equal proportions of each phenotype in the training set. Both approaches perform similarly well with a prediction accuracy > 90% for sample sizes > 9. For sample sizes smaller than that, prediction accuracy starts to deteriorate for either approach.

is conceivable that an overall smaller sample size could be sufficient to match the prediction accuracy of the first approach. The results displayed in Fig. 4.7 emphasise that for both approaches the prediction accuracy is almost constant and well above 90% for sample sizes > 9. For sample sizes smaller than that, prediction accuracy starts to deteriorate and plummets sharply towards 70% and 60% below 6 samples for the 4:4:2 and 1:1:1 approach, respectively. For such small sample sizes, the 4:4:2 approach performs somewhat better than the 1:1:1 approach. These observations indicate that a size of 9 training samples may be sufficient to compute a well-performing prediction model, independent of the chosen approach.

4.2 Establishing an in vitro ADCC model

To establish a feasible and robust in vitro ADCC model, a total of 13 CRC cell lines were screened to assess their suitability to be used as target cell line in a 24h co-culturing

experiment of tumour cells and patient-derived PBMCs under treatment with IgG1 mAbs. In a first step, the optimum number of tumour cells to be seeded and a feasible ETT ratio were determined. Building upon this, ADCC inducibility was compared for all cell lines and correlated with the expression of a selection of surface markers on the tumour cells. Subsequently, the FACS panel was assessed with regards to its ability to capture ADCC readouts and NK cell activation.

4.2.1 Seeding of 30,000 tumour cells ideal for LDH release assay

Determining the number of tumour cells necessary to obtain a reliable readout from the LDH release assay is crucial. On the one hand, the signal-to-noise (SN) ratio between

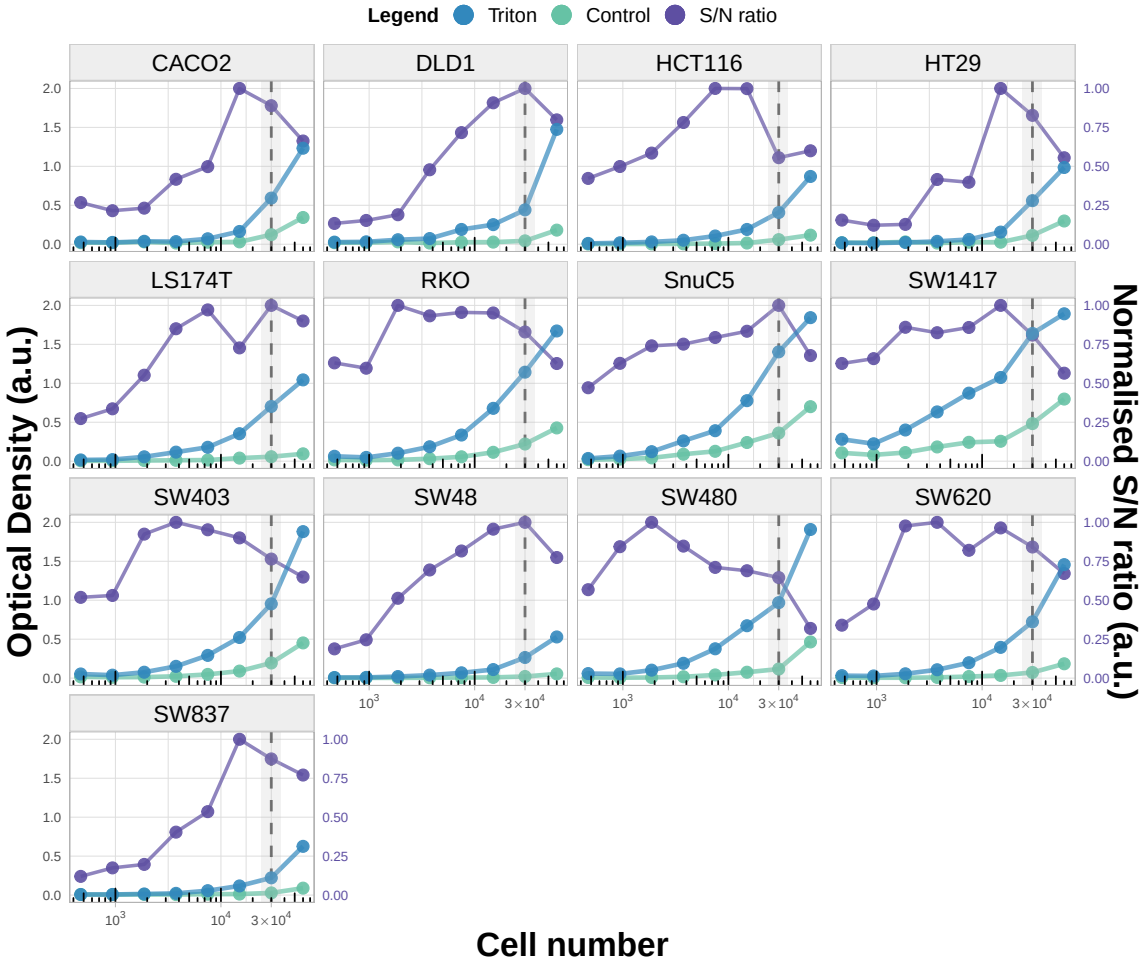

Figure 4.8: Titration of tumour cell number for LDH release assay. Tumour cells of 13 different CRC cell lines were incubated for 24h in culture medium (background control) or culture medium with 1% Triton-X-100 (positive control). Data points shown are the mean of biological triplicates. For most cell lines, the S/N ratio reaches its maximum at around $3*10^4$ tumour cells (vertical dashed line).

complete lysis of all tumour cells and the background LDH level produced by unchallenged tumour cells generally increases as a function of cell number and should ideally be as high as possible. On the other hand, increasing the number of tumour cells goes hand in hand with increasing the number of PBMCs needed to maintain a constant ETT. Given that the number of PBMCs recovered from the primary patient material is a limiting factor of this project, there is a strong incentive to keep the number of tumour cells low. In order to find a sound compromise between the two conflicting aspects, tumour cell number was titrated in the range from $5 * 10^2$ to $6 * 10^4$ cells for each cell line. Triplicates of the respective number of tumour cells were incubated for 24h in culture medium only (background control) or culture medium with cytotoxic 1% Triton-X-100 (positive control) and subsequently an LDH release assay was performed according to the protocol stated in Section 3.7.1. The results of the titrations are shown in Fig. 4.8. Displayed are the mean optical densities measured for the triplicates of positive and background controls as well as the corresponding normalised S/N ratio (defined as the ratio of positive control to background control). While the optical densities are monotonously increasing as a function of cell number, the S/N ratio reaches a maximum near or at approximately $3 * 10^4$ tumour cells for most cell lines (indicated by a vertical dashed line in the figure). Based on this finding, it was decided to use $3 * 10^4$ tumour cells for all further experiments.

4.2.2 Effector-to-target ratio of 10:1 reliably induces ADCC

Naturally, the number of PBMCs recovered from the primary patient material is a limiting factor of this project. Having settled for the seeding of $3 * 10^4$ tumour cells in Section 4.2.1, the next step was to determine the number of PBMCs necessary to induce ADCC in the co-culturing experiments. As per the protocol stated in Section 3.7.1, PBMCs of a healthy volunteer and tumour cells were co-cultured for 24h with a cetuximab concentration of $1000\,ng/ml$, varying the ETT ratio from 5:1 to 10:1 (corresponding to $1.5 * 10^5$ and $3 * 10^5$ PBMCs, respectively). Cetuximab-mediated ADCC was computed from an LDH release assay according to the formula described in Section 3.7.1 and results are shown in Fig. 4.9. Three cell lines are highlighted in Fig. 4.9(a) in an exemplary manner: Cell line RKO (red shading) appears to be resistant to ADCC, presenting a negligible level of lysis that remains constant regardless of the ETT ratio. Unlike RKO, SnuC5 (light-green shading)

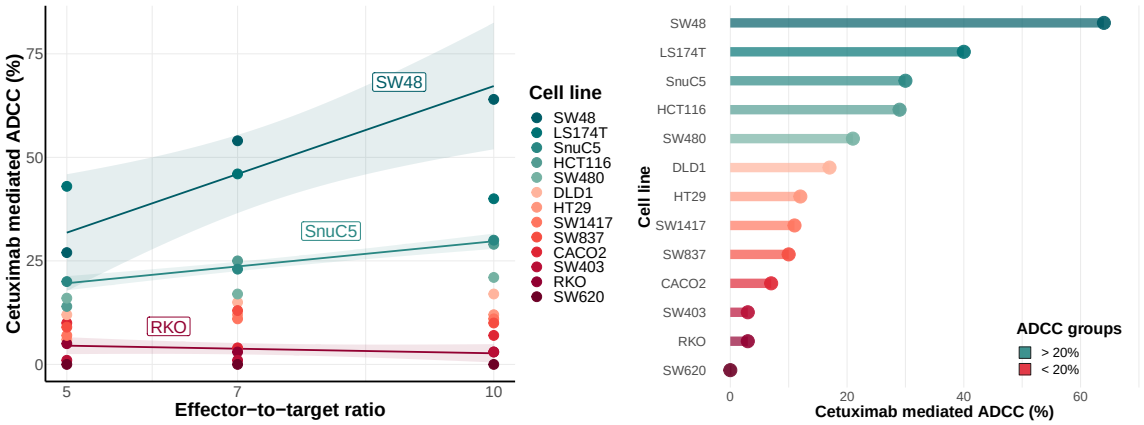

(a) ADCC as function of ETT ratio

(b) Ranked ADCC at 10:1 ETT ratio

Figure 4.9: Cetuximab-mediated ADCC for CRC cell lines. ADCC of PBMCs of healthy donor against each cell line under 1000 ng/ml cetuximab administration was determined in 24h LDH release assays. Each data point represents mean of technical triplicates. (a) ADCC for varying ETT ratios from 5:1 to 10:1. RKO shows low level of ADCC that remains constant regardless of ETT ratio, whereas SnuC5 is more susceptible to ADCC and exhibits a linear relationship with ETT ratio. SW48 is the cell line most susceptible to ADCC overall. (b) Cell lines ranked in descending order according to ADCC at 10:1 ETT ratio. Classification based on ADCC $> 20\%$ (green scale) and ADCC $< 20\%$ (red scale).

shows considerable ADCC in the range from 18% to 30%, increasing in a highly linear fashion with increasing ETT ratio. At the top of the group, SW48 (dark-green shading) is the cell line most susceptible to ADCC, reaching a level of 64% at an ETT ratio of 10:1. However, the relationship between ADCC and ETT ratio is less linear than for SnuC5. It was decided to employ an ETT ratio of 10:1 for all future experiments and Fig. 4.9(b) ranks the cell lines according to the amount of ADCC induced at such an ETT ratio, with colour coding classifying cell lines as highly susceptible or moderately susceptible to ADCC (green scale = ADCC $> 20\%$; red scale = ADCC $< 20\%$). Among the three best performing cell lines, SnuC5 was chosen to be used for the in vitro model despite not having the highest level of ADCC overall. This decision was based on the fact that (1) there was the highest confidence for lysis to be readily quantifiable for donors with both high and low ADCC-inducing potential and (2) handling of this cell line was better manageable than for the other two cell lines which showed a strong tendency to clump after detachment from the flask bottom, being prone to higher uncertainty with regards to the cell counting step before seeding.

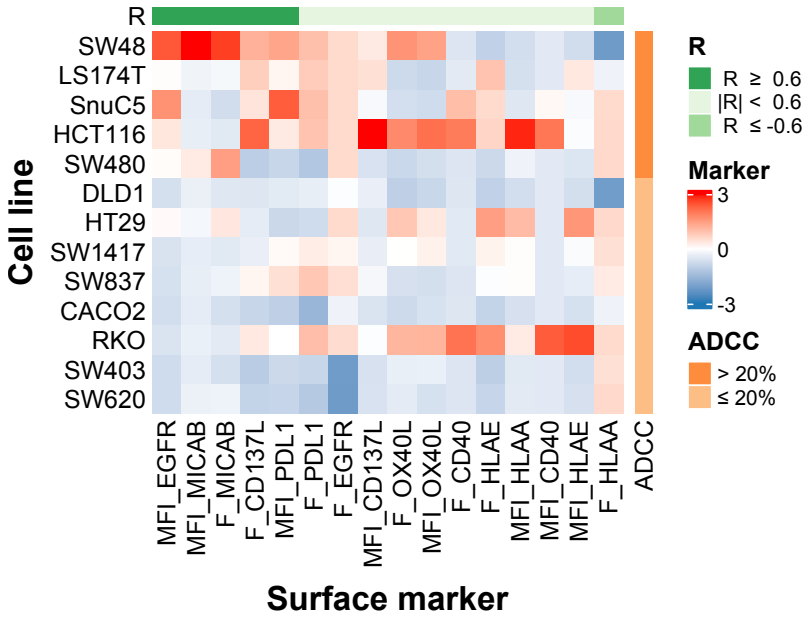

Figure 4.10: Heatmap of surface marker expression and ADCC inducibility for 13 CRC cell lines. Cell lines (rows) are ordered by decreasing cetuximab-mediated ADCC, surface markers (columns) by decreasing correlation coefficient R. Values for surface markers are transformed to z-scores. Strong positive correlation with ADCC exists for expression of EGFR, MICA/B, CD137L and PDL1 on tumour cells, whereas HLA-A/B/C is the only marker showing a strong negative correlation.
Abbreviations: MFI = median fluorescent intensity; F = frequency of positive cells; R = Pearson's correlation coefficient.

4.2.3 Surface marker expression correlates with ADCC inducibility of cell lines

The observation of notable differences in ADCC between the different CRC cell lines raises the question whether these differences may be explained by the differential expression of surface markers on the tumour cells that inhibit or facilitate NK cell activation. Hence, all cell lines were screened for the expression of a selection of 8 surface markers (EGFR, PDL1, HLA-A/B/C, HLA-E, MICA/B, CD40, OX40L and CD137L) via flow cytometry (Fig. 4.10). Marker expression and expression density were assessed as the percentage of cells positive for a marker and the MFI of the positive cell population for that marker, respectively. In the heatmap, cell lines are ordered row-wise with respect to decreasing ADCC and the markers are arranged column-wise in the order of descending Pearson's correlation coefficient R. The MFI of EGFR, MICA/B and PDL1 as well as the frequency of MICA/B+ and CD137L+ positive tumour cells show strong positive correlation with ADCC activity ($R \geq 0.6$; Fig. 4.11 (a)-(d)).

In contrast, the frequency of HLA-A/B/C+ cells is the only parameter that exhibits

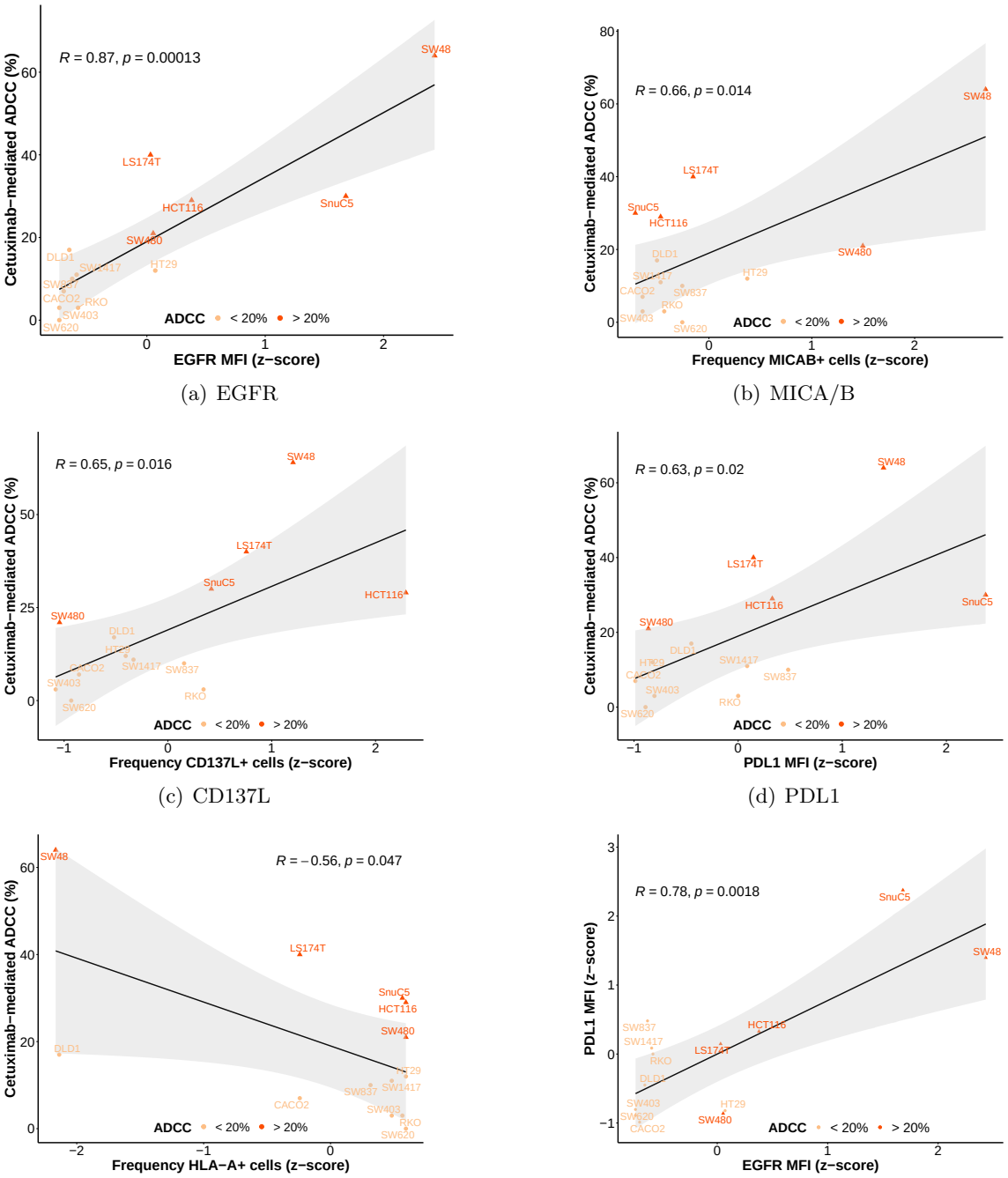

Figure 4.11: Relationship of tumour-expressed surface markers and ADCC activity. (a)-(e) Correlation of respective surface markers with cetuximab-mediated ADCC. Only markers that exhibit a strong positive correlation (EGFR, MICA/B, CD137L, PDL1) or strong negative correlation (HLA-A/B/C) with cetuximab-mediated ADCC are shown. (f) PDL1 expression is positively correlated with EGFR expression on tumour cells. This finding may explain why PDL1 expression correlates with cetuximab-mediated ADCC (PDL1 was not targeted directly in this experiment).
Abbreviations: MFI = median fluorescent intensity; F = frequency of positive cells; R = Pearson's correlation coefficient.

a strong negative correlation with ADCC activity ($R \leq -0.6$; Fig. 4.11(e)). It is worth noting that in the ADCC experiment only EGFR was targeted by cetuximab administration, whereas the anti-PDL1 antibody avelumab was not used. Yet, PDL1 expression correlated with ADCC, albeit less strongly than EGFR expression. This correlation may be merely due to the fact that PDL1 expression is also associated with EGFR expression according to the literature [155–157], which we could confirm for the cell lines screened in this work (Fig. 4.11(f)).

4.2.4 Effect of cetuximab and avelumab combination treatment on ADCC

Since a key objective of the FIRE6 study is to investigate whether the concurrent treatment of mCRC patients with a cetuximab + avelumab combination therapy confers a clinical benefit, it is of interest to compare the amount of in vitro ADCC mediated by cetuximab and avelumab alone as well as the combination of both. To do so, ADCC mediated by PBMCs of a healthy volunteer against the cell line SnuC5 for a 10:1 ETT ratio was determined in a 24h LDH release assay under the three conditions of administrating $100\,ng/ml$ cetuximab, $100\,ng/ml$ avelumab or the combination of $100\,ng/ml$ cetuximab and $100\,ng/ml$ avelumab (Fig. 4.12). As can be readily seen, single-agent avelumab treatment is considerably less potent at inducing ADCC than single-agent cetuximab treatment, with the ADCC level for cetuximab being approximately 2-fold that of avelumab (37% versus 17%, respectively). In the case of combination treatment, ADCC increases from 37% for cetuximab alone to 42% for cetuximab+avelumab treatment. The most straight-forward explanation for this rather small, albeit recognisable, additive effect is that the majority of SnuC5 tumour cells which express enough PDL1 in order to be lysed by avelumab-mediated ADCC is also successfully targeted by cetuximab due to the concurrent expression of EGFR (as already established in Fig. 4.11(f)). Whether this effect seen here for a single healthy volunteer is of relevant consequence for the FIRE6 patient cohort will be investigated in Section 4.3.

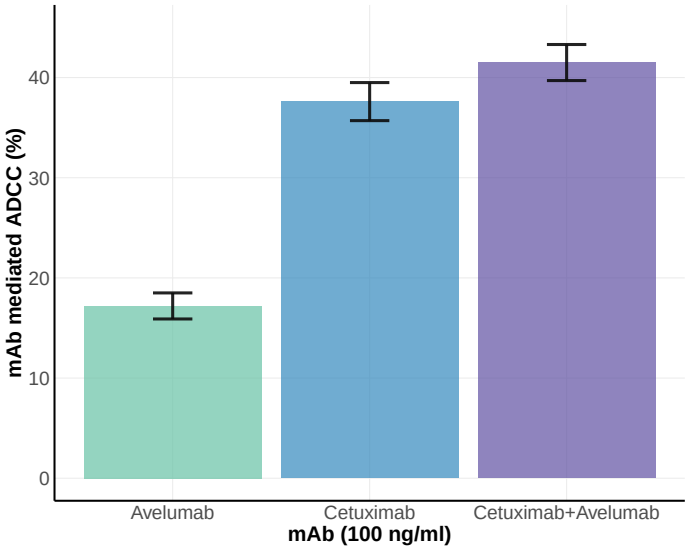

Figure 4.12: Small additive effect on ADCC of cetuximab and avelumab combination treatment. ADCC of PBMCs of a healthy volunteer against the cell line SnuC5 for a 10:1 ETT ratio was determined in a 24h LDH release assay for 100 ng/ml cetuximab alone, 100 ng/ml avelumab alone or the combination of 100 ng/ml cetuximab + 100 ng/ml avelumab. ADCC induced by avelumab alone is about half of that induced by cetuximab alone. Combination treatment with both antibodies results in highest level of ADCC overall. Data shown are mean ADCC ± SEM of biological triplicates.

4.2.5 FACS-based ADCC readouts show good agreement with LDH release assay and reliably capture NK-cell activation

As the final step in establishing the in vitro ADCC model, a robust FACS antibody panel had to be developed and tested with regards to its ability to provide more in-depth information on the mechanisms involved in ADCC, such as the activation of immune cell subsets and changes in the expression of tumour surface markers. First and foremost, it was of interest whether the FACS ADCC panel is capable of detecting tumour cell death as reliably as the LDH release assay. Having a second readout to quantify ADCC activity to confirm the LDH results would not only increase the confidence in the experimental method, but also provide a reassuring level of redundancy in case of sporadic failure of either approach for a given patient. In this regard, the relative decrease in live tumour cells (defined as DAPI-AnnexinV- tumour cells) between control samples and those treated with the therapeutic antibodies may be considered such a suitable readout of the FACS ADCC panel. Fig. 4.13 compares the FACS-quantified tumour cell death (termed Δ Tumour cells$_{FACS}$) with the ADCC lysis determined by LDH release assay (termed ADCC Lysis$-LDH$) for both healthy volunteers and patients. A strong positive linear relationship between the two parameters with a correlation coefficient of $R = 0.72$ is evidence of excellent agree-

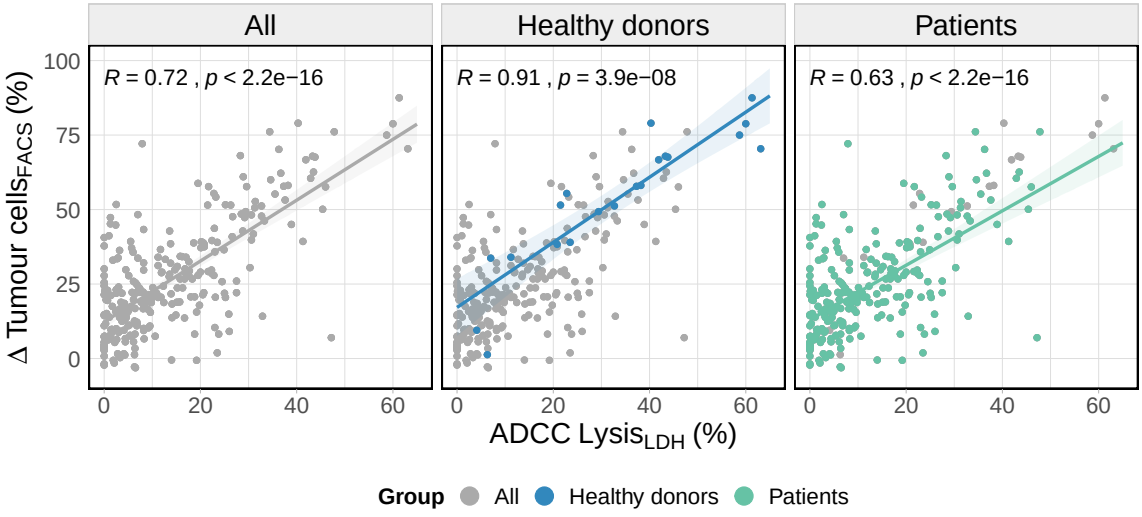

Figure 4.13: FACS-quantified tumour cell death strongly correlates with ADCC lysis determined via LDH release assay. Data show the positive linear relationship between the relative decrease in live tumour cells (FACS) and ADCC lysis (LDH) of SnuC5 tumour cells after 24h of co-culture with PBMCS from healthy volunteers (middle panel) and patients (right panel) following treatment with cetuximab and/or avelumab.
Statistics: R = Pearson's correlation coefficient

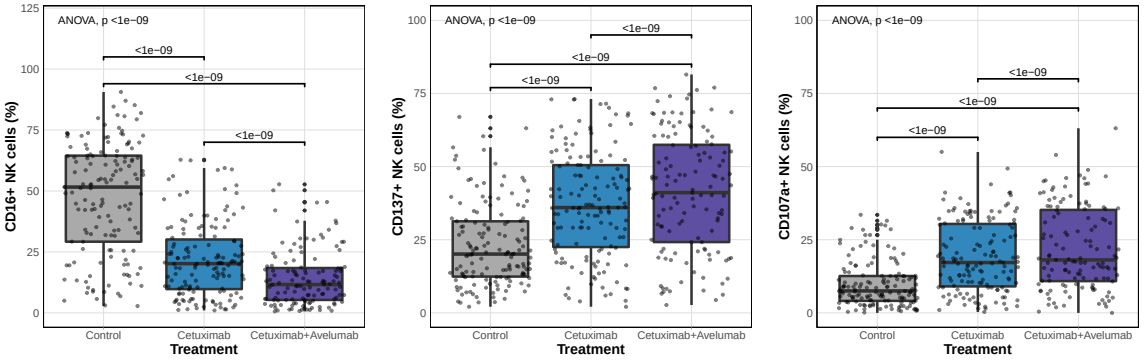

Figure 4.14: In vitro evidence of NK cell engagement and activation after incubation with cetuximab and/or avelumab. Flow cytometric analysis of CD16 (left), CD137 (middle) and CD107a (right) on NK cells of healthy volunteers and patients that were co-cultured with SnuC5 tumour cells. The data reveal significant CD16 downregulation as well as concurrent CD137 and CD107a upregulation in the presence of IgG1 monoclonal antibodies. These effects are the strongest for cetuximab+avelumab combination treatment. Statistics: one-way ANOVA; pairwise t-test with post-hoc Bonferroni adjustment

ment between the FACS-based and LDH-based approaches ($p < 2.2 * 10^{-16}$). It is worth mentioning that the correlation is even stronger for the healthy volunteers ($R = 0.91$; $p < 3.9 * 10^{-8}$) than the patients ($R = 0.63$; $p < 2.2 * 10^{-16}$). This observation may be largely explained by the overall better sample quality for the healthy volunteers than for the patients. All healthy volunteers were recruited close to a single site where the samples could be processed immediately following their retrieval, whereas patient samples had to be shipped across Germany before being processed, incurring delivery delays ranging from 1 to 3 days.

Both approaches confirming that ADCC does take place in our in vitro model sparked the curiosity whether the FACS ADCC panel could gather further insights on the interaction between tumour and immune cells. As NK cells are known to be the key players in this interaction, a closer look at their fate was warranted (Fig. 4.14). Comparing CD16 expression on NK cells between control samples and those exposed to cetuximab or cetuximab+avelumab treatment shows a highly significant downregulation of CD16 from the cell surface with treatment ($p < 10^{-9}$), being strongest in case of combination treatment. This downregulation may be interpreted as a clear sign of binding of the therapeutic IgG1 mAbs to the FcgRIIIa receptors on NK cells, which in turn become internalised. Further substantiating this claim is the concurrent observation of significant upregulation of CD137 (marker for NK cell activation) and CD107a (marker for NK cell degranulation) on these cells with treatment ($p < 10^{-9}$).

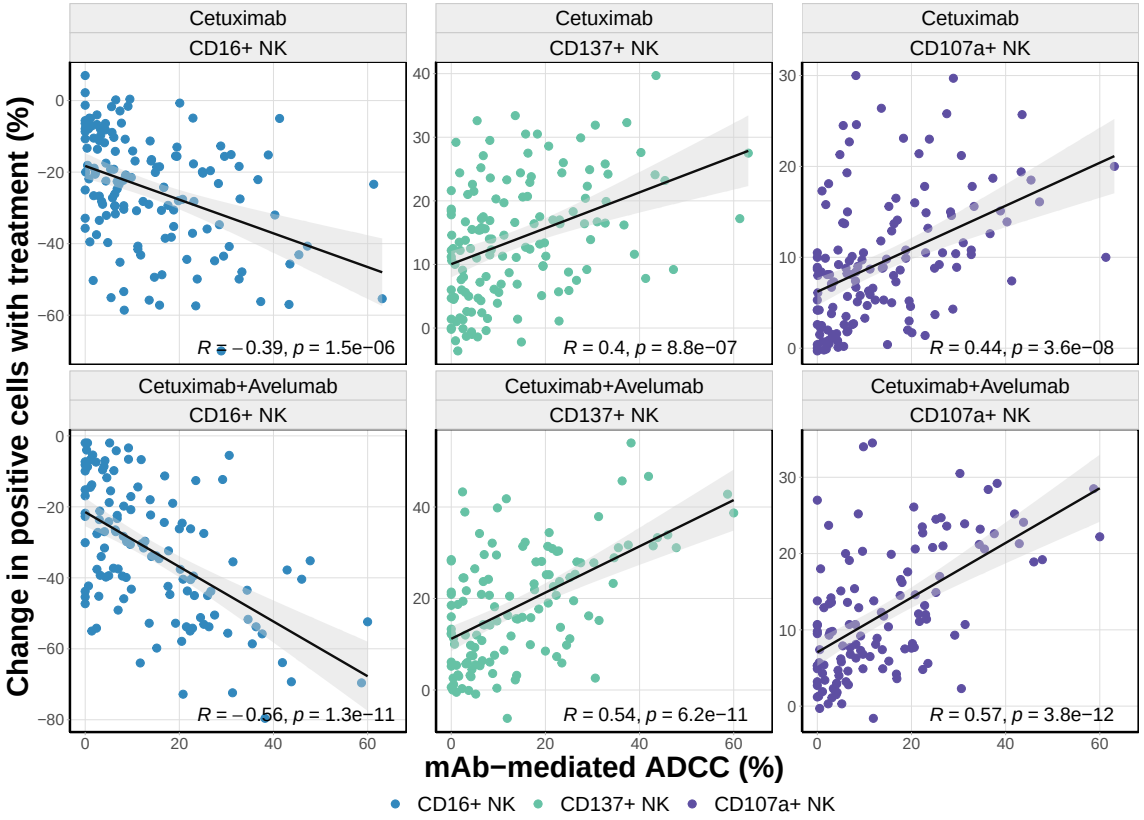

Figure 4.15: NK cell activation correlates with ADCC for cetuximab treatment (top) and cetuximab+avelumab treatment (bottom), respectively. The correlation shows that higher mAb-mediated ADCC goes along with more pronounced downregulation of CD16 on NK cells, which in turn become increasingly activated (CD137+) and degranulate (CD107a+). Abbreviations: R = Pearson's correlation coefficient.

As displayed in Fig. 4.15, the downregulation of CD16 and the concurrent upregulation of CD137 and CD107a exhibit a linear relationship with increasing ADCC for both cetuximab and cetuximab+avelumab treatment. Generally speaking, the higher the ADCC, the more pronounced is the respective down- or upregulation of these markers of NK cell engagement and activation. Taken together, these findings provide evidence beyond reasonable doubt that IgG1 mAb binding induces NK cell mediated ADCC in our in vitro model and that the developed FACS ADCC panel is able to reliably capture this process.

4.3 Results of FIRE6 study

4.3.1 FcgRIIIa-158 phenotype correlates with ADCC, but does not confer clinical benefits

From the literature, it is known that the binding affinity of NK cells to IgG1 mAbs differs based on FcgRIIIa-158 phenotype, with receptors comprised of proteins with a valine residue at position 158 binding more strongly [12, 158, 159]. As shown in Fig. 4.16, this stronger binding translates to significantly higher baseline ADCC lysis for VF and VV individuals compared to FF individuals of our patient cohort ($p < 0.022$, ANOVA). Interestingly, no noticeable difference is apparent between VF heterozygotes and VV homozygotes, implying that the presence of a single V allele is already sufficient for a donor's NK cells to obtain their full ADCC potential.

Having confirmed the relevance of the FcgRIIIa-158 polymorphism for NK-cell induced ADCC, another intriguing question is whether it also correlates with clinical outcome measures (Fig. 4.17). Within the context of the FIRE6 study, tumour response to treat-

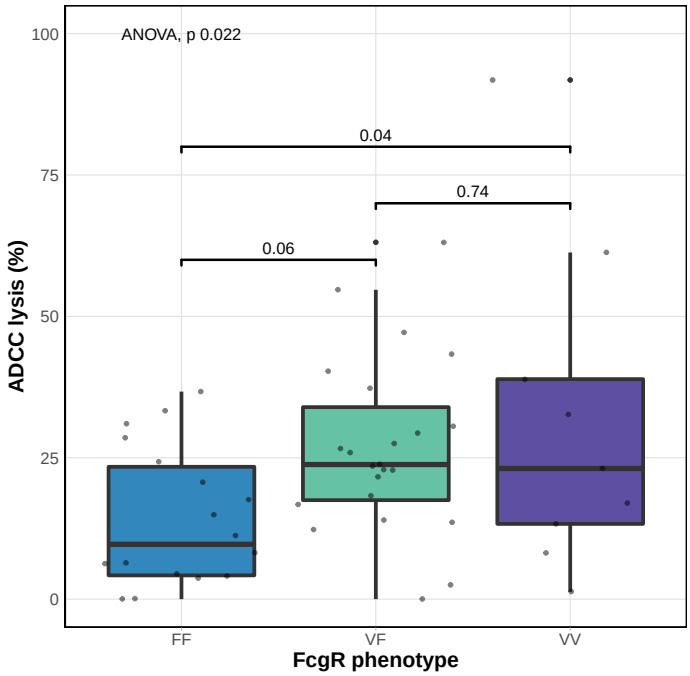

Figure 4.16: FcgRIIIa-158 phenotype correlates with in vitro ADCC at baseline. Cetuximab-mediated ADCC at timepoint C1 is significantly lower for FF individuals than for VF or VV individuals. Among the latter two groups, no difference in ADCC is discernible.
Statistics: one-way ANOVA; post-hoc unpaired t-test with Bonferroni adjustment.

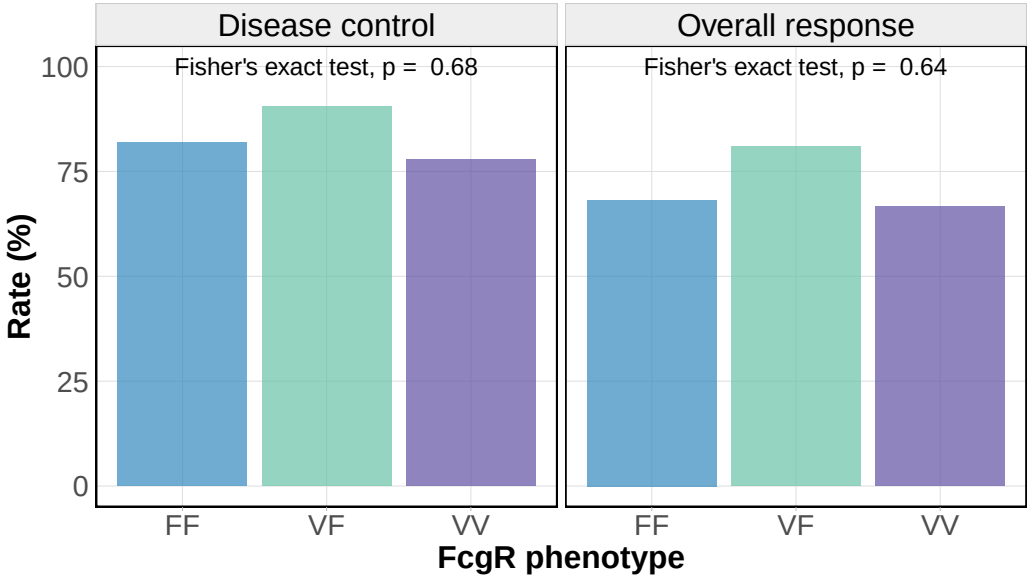

(a) Response rates

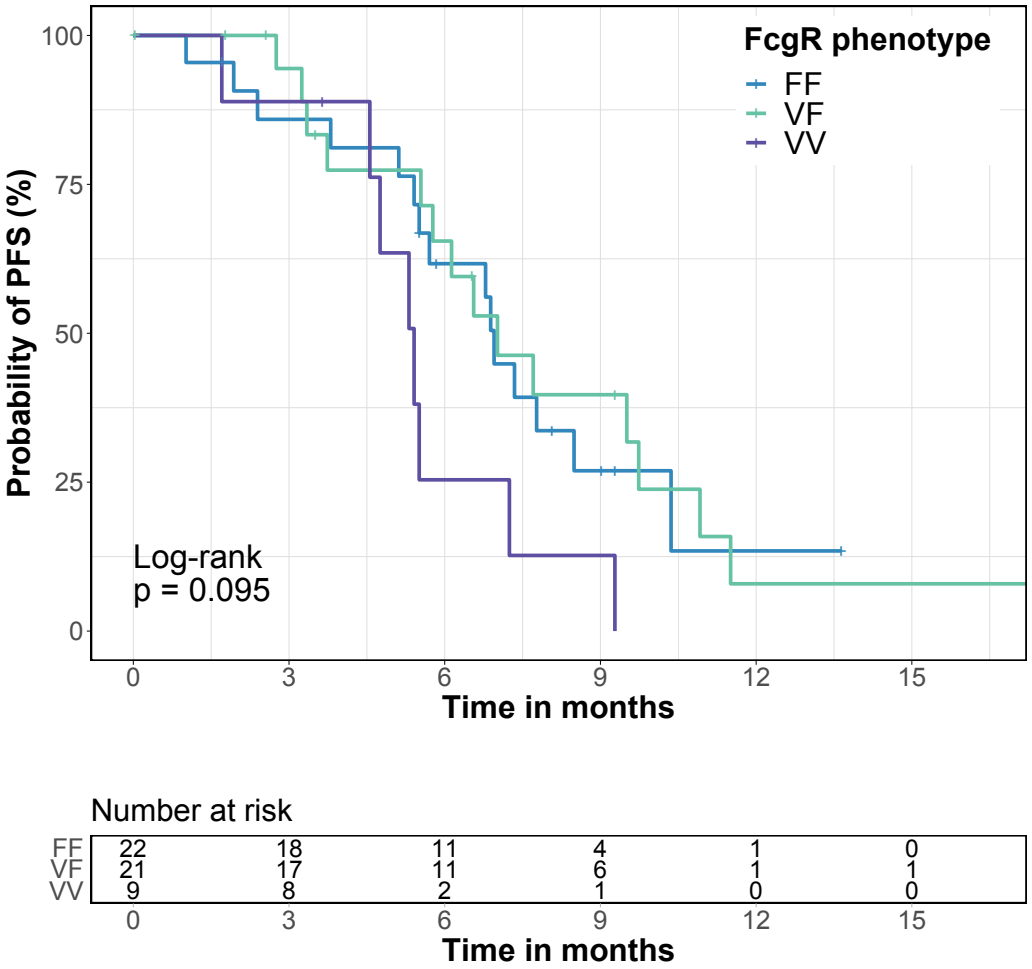

(b) Progression-free survival

Figure 4.17: FcgRIIIa-158 phenotype does not correlate with clinical outcome of FIRE6 patients. (a) No significant differences in DCR and ORR between FF, VF and VV individuals. (b) Progression-free survival is similar for the three phenotypes. Statistics: (a) Fisher's exact test; (b) log-rank test.

ment was evaluated centrally as best overall response (BOR) according to irRECIST v.1.1 criteria. For the patient cohort, it was that both disease control rate (DCR; defined as rate of patients with complete response, partial response or stable disease) and objective response rate (ORR; defined as rate of patients with complete or partial response) did not show any significant differences based on FcgRIIIa-158 phenotype (Fig. 4.17(a); Fisher's exact test; $p = 0.68$ and $p = 0.64$, respectively). Taking the analysis yet a step further, it was also confirmed via Kaplan-Meier survival analysis that the groups of the three different phenotypes did not differ in terms of PFS, the primary endpoint of the clinical study (Fig. 4.17(b); log-rank test; $p = 0.095$). As a word of caution, it is worth mentioning that 10 patients had not yet progressed at the time of analysis and their PFS had to be censored at the most recent follow-up visit.

4.3.2 ADCC and NK cell activation at baseline do not correlate with clinical outcome

A key hypothesis of this work was that IgG1-antibody mediated ADCC might play an important role in the treatment of mCRC patients with such antibodies. Exploiting the in vitro ADCC model established in Section 4.2, ADCC of PBMCs collected at baseline (timepoint C1) against the CRC cell line SnuC5 was determined and analysed for the three groups of healthy volunteers, responding and non-responding patients (Fig. 4.18). While a trend towards higher ADCC for healthy volunteers compared to patients is visible, no significant differences are observed between the patient groups. In agreement with this, NK cell engagement and activation as measured by changes in CD16, CD137 and CD107a expression were also of comparable magnitude between responding and non-responding patients.

As a next step, it was assessed whether in vitro ADCC at baseline may nonetheless be associated with the duration of progression-free survival. To this end, receiver operating characteristic (ROC) analysis was employed to identify the ADCC cut-off that best separates responding from non-responding patients (data not shown). This ADCC cut-off was found to be at 20% lysis and was used to classify each patient to either of the low or high ADCC category. We performed survival estimations by using the Kaplan-Meier analysis

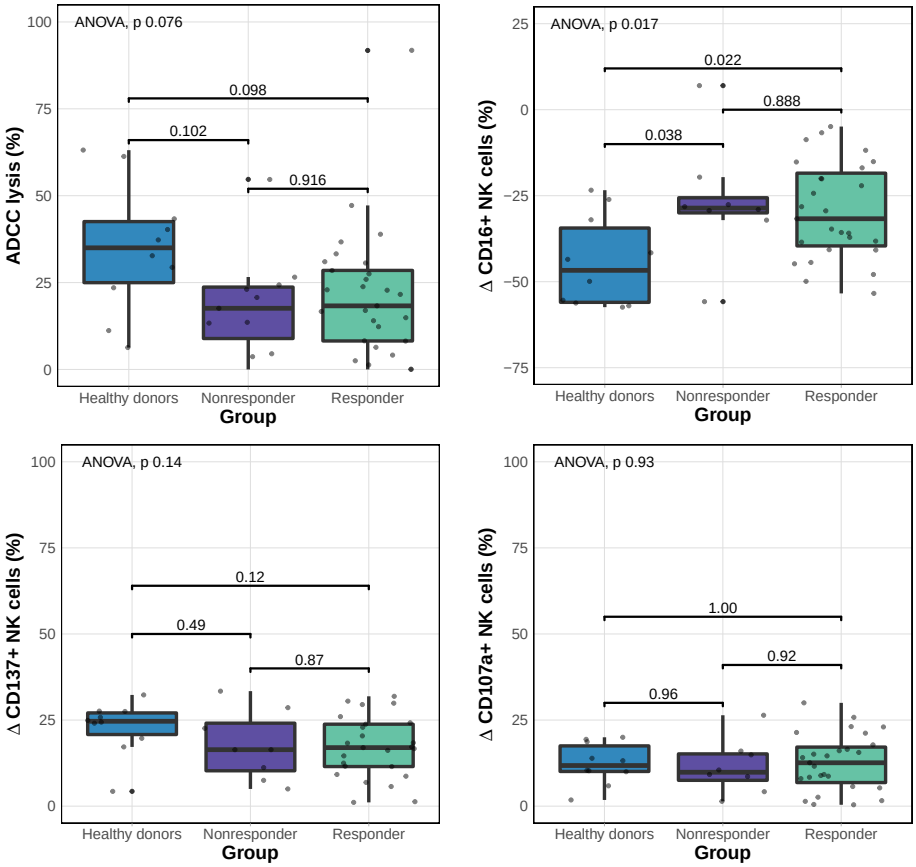

Figure 4.18: Baseline cetuximab-mediated ADCC and NK cell activation do not differ between responding and non-responding patients. A non-significant trend towards higher levels of ADCC for healthy volunteers compared to patients is visible.
Statistics: one-way ANOVA; post-hoc unpaired t-test with Bonferroni adjustment.

to assess whether the distinction into patients with low and high ADCC would be prognostic of prolonged PFS of patients treated with the FIRE6 therapy regimen (Fig. 4.19). However, we did not observe any statistically significant differences between patients with low and high ADCC ($p = 0.58$, log-rank test).

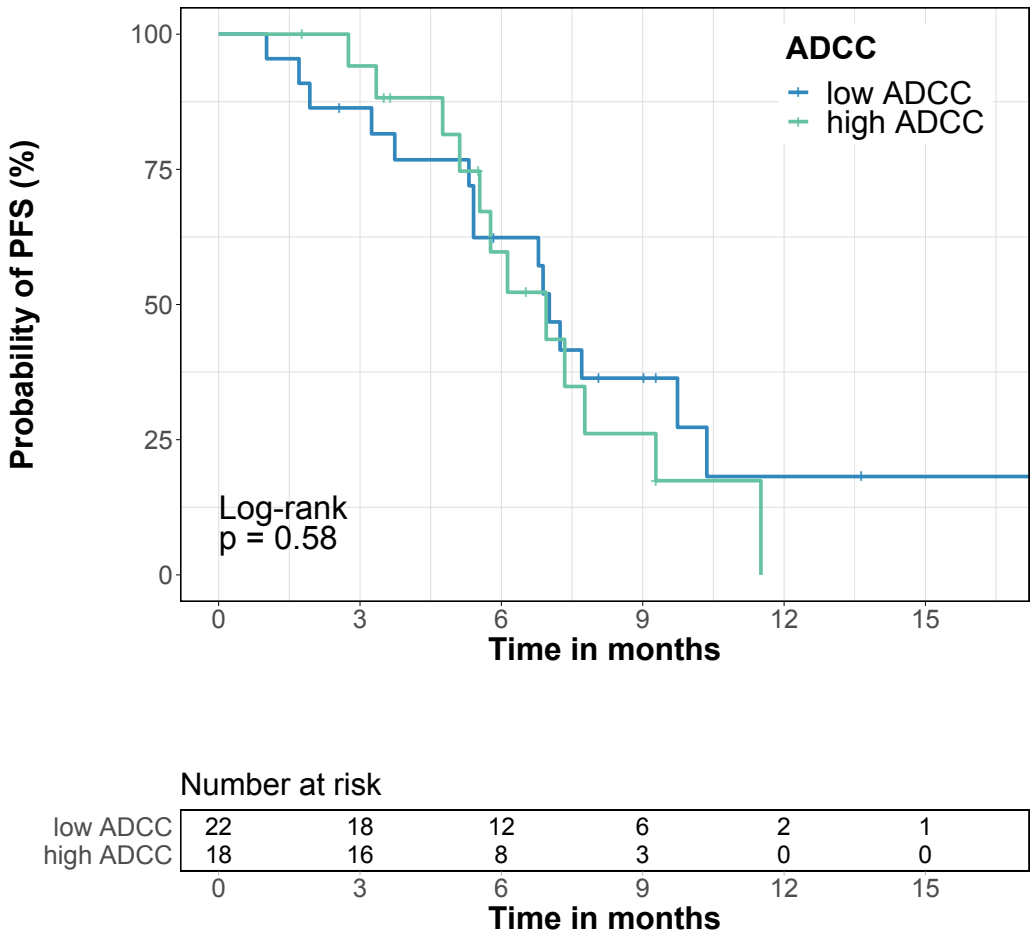

Figure 4.19: Progression-free survival does not differ for patients with low ADCC ($\leq$ 20%) and high ADCC ($>$ 20%). ADCC cut-off was determined by ROC analysis as the value that best separates responding from non-responding patients.
Statistics: log-rank test

4.3.3 ADCC and NK cell activation decrease during therapy for all patients

In the previous Section 4.3.2, we have determined that our in vitro ADCC model did not reveal any differences in baseline ADCC lysis and NK cell activation between responders and nonresponders within our FIRE6 study cohort. This means that we cannot infer based on these parameters whether a patient is likely (or not) to respond to therapy before starting the treatment. However, having at our disposal PBMCs withdrawn from each patient at various timepoints during therapy gives us the opportunity to investigate if and when these parameters change over the course of therapy. Of particular interest in this context are changes in these parameters that differ between responders and nonresponders, potentially preceding radiologic evidence of response to treatment.

In order to appropriately analyse this longitudinal data, we implemented a linear mixed-effects model. Such models are increasingly being used in settings where repeated measurements are made on the same statistical unit (e.g. a single person), as is the case in all longitudinal studies, and they are typically preferred over more traditional approaches, such as repeated measures ANOVA, because of their advantage in handling missing val-

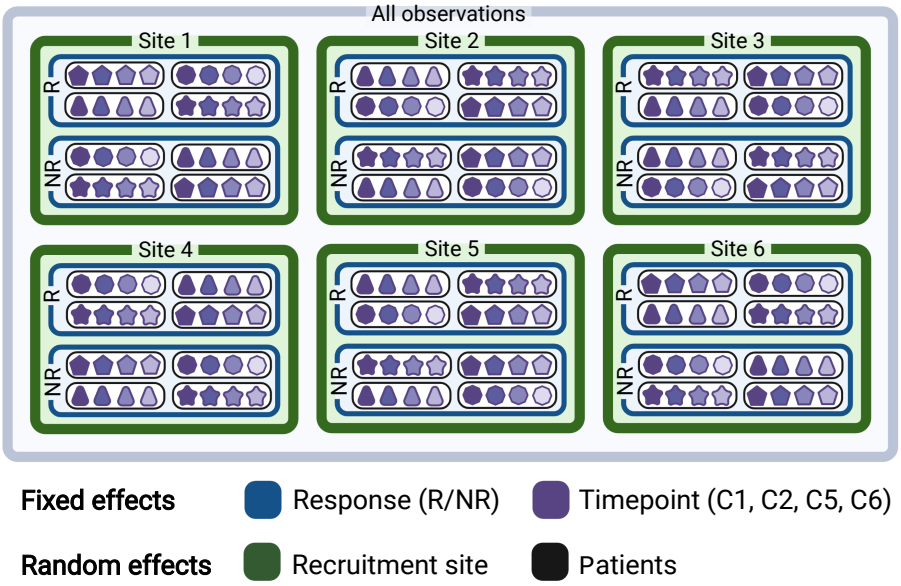

Figure 4.20: Schematic visualisation of developed mixed-effects model for longitudinal data analysis. The aim of the model is to determine the influence of two fixed effects, namely a patient's response status (blue) and timepoint (purple) on the measured parameters of interest. Since patients were recruited by a range of sites (green) and measurements were repeated at four timepoints for each patient (black), correlations for these two variables had to be taken into account as random effects.

ues. Fig. 4.20 illustrates the underlying basis of the mixed-effects model for our study cohort. Patients were recruited across a range of different recruitment sites (green) and each patient (black) was sampled up to four times, meaning that correlations between measurements of the same patient as well as between patients of the same recruitment site do exist and must be taken into account as random effects in our model. Since we are interested in observing differences depending on response status (blue), timepoint (purple) and their interaction, these two variables were modelled as fixed effects. Following from these considerations, the implementation of the full model in R is of the form:

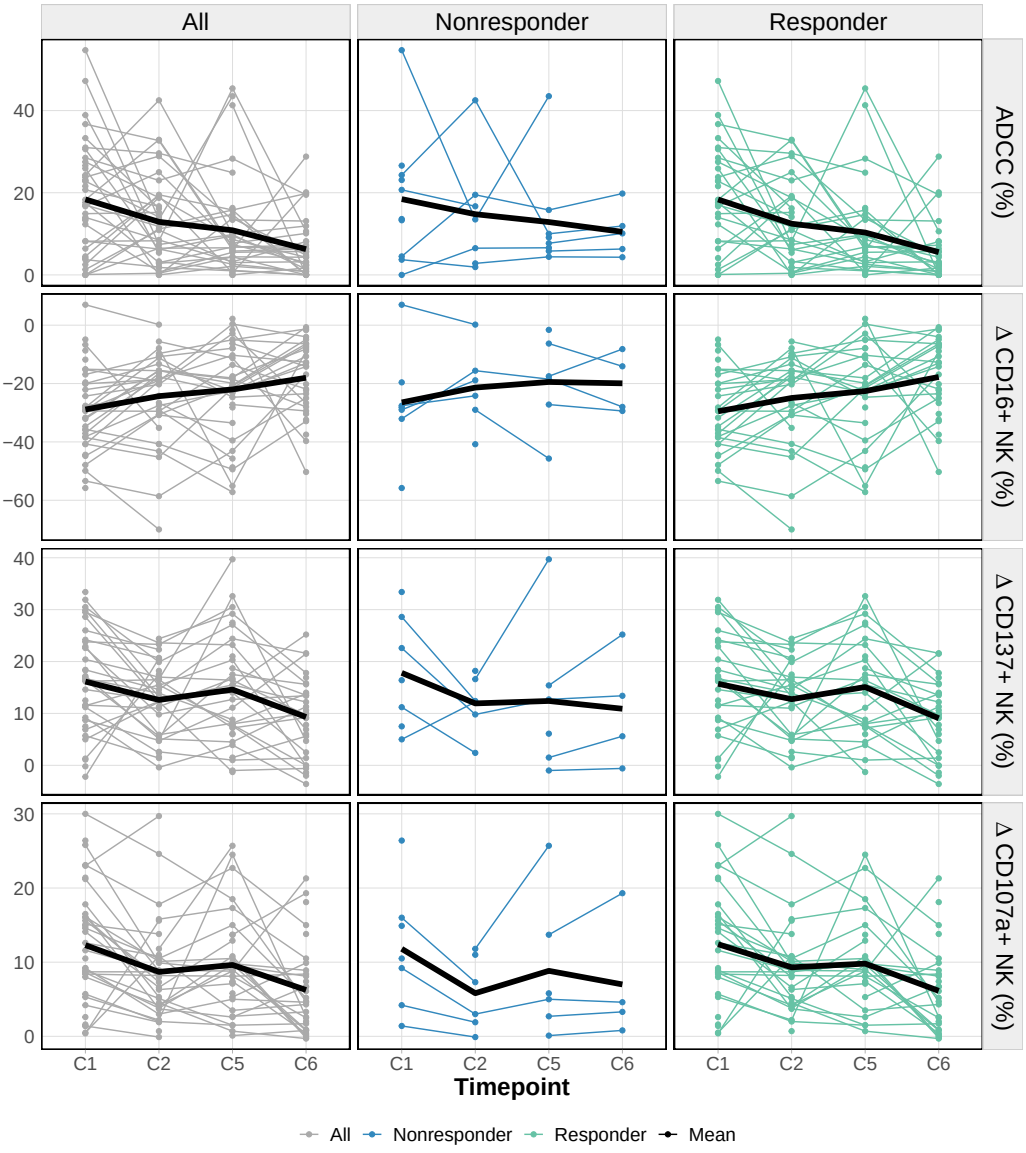

Figure 4.21: Longitudinal evolution of ADCC and NK cell activation during therapy. Both responders (green) and nonresponders (blue) show an overall similar trend of gradually decreasing ADCC and NK cell activation during treatment.

	Cetuximab				Cetuximab+Avelumab			
	ADCC	$\Delta CD16$	$\Delta CD137$	$\Delta CD107$	ADCC	$\Delta CD16$	$\Delta CD137$	$\Delta CD107$
response	0.91	0.97	0.99	0.99	0.93	0.99	0.96	0.96
timepoint	$<10^{-4}$	$<10^{-4}$	$<10^{-4}$	$<10^{-4}$	$<10^{-4}$	$<10^{-4}$	$<10^{-4}$	$<10^{-4}$
response:timepoint	0.99	0.99	0.72	0.88	0.83	0.84	0.83	0.83

Table 4.1: Results of linear mixed-effects model. Shown are p-values derived using the Kenward-Roger approximation for the fixed effects response, timepoint and their interaction. ADCC and all NK-cell activation parameters display a statistically significant decrease with timepoint ($< 10^{-4}$). In contrast, no differences were found for response status and the interaction of response and timepoint.

$$p \sim response + timepoint + response : timepoint + (1|patient) + (1|site),$$

where p is a placeholder for our four parameters of interest, namely ADCC, ΔCD16, ΔCD137 and ΔCD107a. Performing a likelihood ratio test for this full model against the two reduced models neglecting either the recruitment site or the patient (i.e. without the term (1|site) or (1|patient), respectively) revealed that the influence of the recruitment site was not significant ($p > 0.05$) and, thus, should be dropped from the model. In contrast, the influence of the individual patient was found to be a significant random effect ($p < 0.05$) and must be kept, yielding the final model of the form:

$$p \sim response + timepoint + response : timepoint + (1|patient) \tag{4.1}$$

This model was fit in R with the *lme4* package, employing a restricted maximum likelihood approach (REML). The longitudinal measurement data of all four parameters of interest are shown as the difference between cetuximab and untreated control samples in Fig. 4.21 (data for cetuximab+avelumab combination treatment showed the same trend and is omitted here). For the sake of better visualisation, data are grouped and colour-coded according to response status. In the figure, a gradual trend towards decreasing ADCC and less NK cell activation during therapy becomes evident for both responders (green) and nonresponders (blue). Evaluating the statistical significance of fixed effects in linear mixed-effects modelling is a heavily debated issue in the scientific literature. The model output produced by the *lme4* package provides t-values but does not include p-values as the authors argue that for linear mixed models it is not at all clear what the appropriate denominator degrees of freedom to use are (e.g. number of observations, number of subjects, number of grouping factors). However, several approaches have been

developed to address this issue and are reviewed elsewhere [160]. Luke et al. have shown through extensive analysis of simulated data that when linear mixed models are fitted using REML and p-values are derived using the Kenward-Roger approximation, realistic type 1 error rates were obtained even for small sample sizes. Applying the Kenward-Roger approximation to our data (Table 4.1) confirms that the visually discernible decrease in ADCC and NK cell activation during treatment is indeed statistically significant for both experimental conditions (cetuximab and cetuximab+avelumab, respectively). In stark contrast, no significant differences in any parameter were found based on response status alone as well as the interaction of response status and timepoint (modelled by the term response:timepoint in Eq. 4.1), meaning responders and nonresponders essentially exhibit the same longitudinal trend.

4.3.4 Exploratory analysis at baseline

Apart from investigating the impact of the FcgRIIIa-158 polymorphism, ADCC and NK cell activation on clinical outcome of the study patients, the developed FACS ADCC panel was designed to produce some "bycatch", i.e. to offer the great advantage of capturing a vast amount of additional information about the interaction of the immune cell populations and tumour cells (as exemplified by the gating scheme in Fig. 3.6 in Section 3.7.2). Hence, it is conceivable that sifting through these data diligently, we might stumble upon *a priori* unanticipated findings, potentially forming the starting point for generating new hypotheses to be scrutinised and tested in future experiments. As is common for exploratory analyses, it is worth mentioning that this section involves multiple comparisons of a large amount of measured variables. In the field of statistics, rather than a clear consensus, there is an ongoing debate on how and when to adjust for multiple testing [161–164]. In line with Bender et al. [161], we are of the opinion that multiple comparison adjustments are not strictly necessary in an exploratory setting as such corrections inherently increase the likelihood of missing genuine differences (type II errors). Instead, we would like to remind the reader to interpret our findings cautiously and we emphasise that further research with larger sample sizes is without doubt required in order to confirm or refute the findings of this section. Beginning the exploratory screening with Fig. 4.22(a), all donors (patients and healthy volunteers) were clustered in a heatmap according to the subset

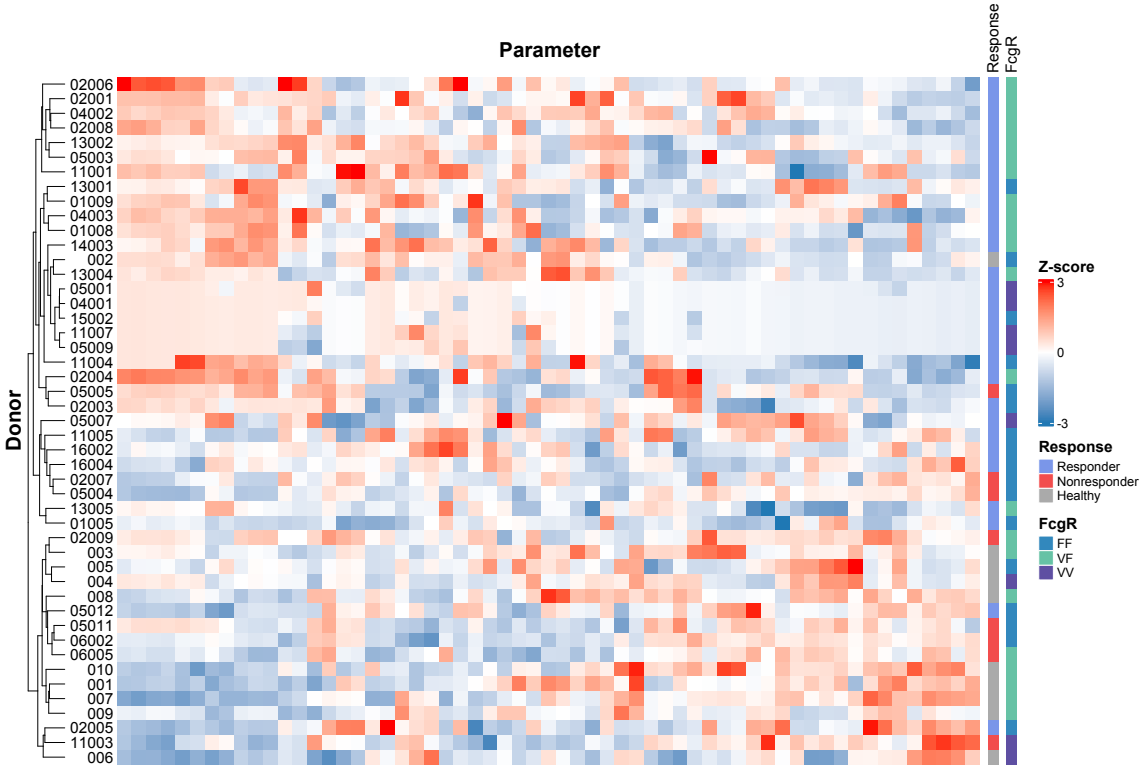

(a) Heatmap

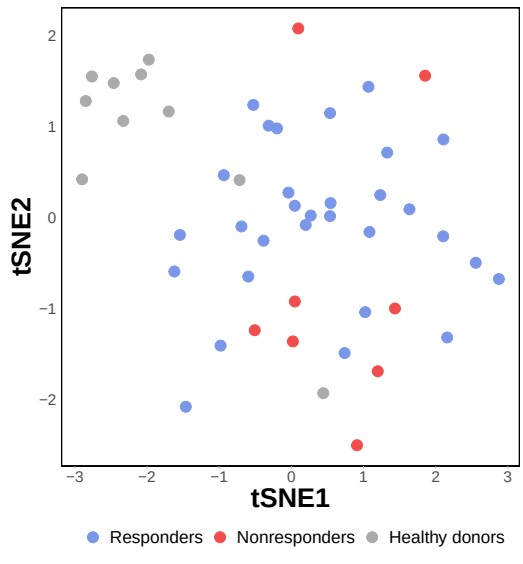

(b) tSNE

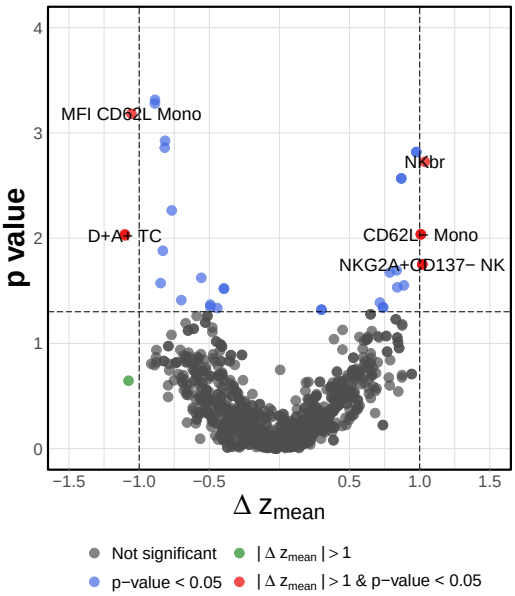

(c) Volcanoplot

Figure 4.22: Exploratory analysis at baseline. (a) Heatmap clustering of patients and healthy volunteers according to the parameters that differ the most between the groups (i.e. $p < 0.1$). (b) tSNE dimensionality reduction shows a moderate amount of clustering of healthy donors, responders and nonresponders. (c) Volcanoplot of the difference in the mean z-scores between responders and nonresponders (Δz_{mean}) with respective p values. Parameters with $| \Delta z_{mean} | > 1$ and $p < 0.05$ are highlighted in red and labelled.
Statistics: (a) Clustering algorithm: ward.D; (c) Brunner-Munzel test

of FACS-derived parameters which differed the most between the groups (i.e. threshold of $p < 0.1$). Within this heatmap, two major clusters can be appreciated: responding patients tend to cluster together towards the top of the heatmap, whereas non-responding patients and healthy volunteers are intermingled at the bottom of the heatmap. Similarly, employing tSNE analysis for dimensionality reduction onto two dimensions, a moderate level of clustering can be recognised in Fig. 4.22(b) where healthy volunteers (top left), responders (centre right) and nonresponders (bottom right) tend to end up in different regions of the plot. To single out the small group of parameters that are chiefly responsible for the differences between responders and nonresponders, a volcanoplot of the difference between the mean z-scores of both groups (Δz_{mean}) and their respective p values was computed for all parameters (Fig. 4.22(c)). As is evident at first glance, the vast majority of parameters does not show significant differences between responders and nonresponders (coloured in grey). Only a handful of parameters differ significantly in their mean z-scores (blue) and, for even fewer parameters, this difference additionally fulfils the condition of $\mid \Delta z_{mean} \mid > 1$ (red).

In the next step, the parameters that differed significantly were divided according to cell type (Fig. 4.23) and separate boxplots were generated for responders and nonresponders. The displayed variables are labelled with a subscript that corresponds to either the treatment condition they were measured for (0 = control sample; C = cetuximab sample; A = cetuximab+avelumab sample) or the difference in that variable between two treatment conditions ($\Delta C0$ = difference between cetuximab and control sample; $\Delta A0$ = difference between cetuximab+avelumab and control sample; ΔAC = difference between cetuximab+avelumab and cetuximab sample). For CD3 cells of nonresponders, a higher change towards more PD1 expression as well as more NKG2D+ and CD137+ cells was observed when avelumab was added ($\Delta A0$ and ΔAC, respectively) with respect to responders. Moving on to monocytes, a higher percentage of CD40+ monocytes in the control samples for responders strikes the eye and a more pronounced change towards more CD62L- monocytes occurred under avelumab administration for responders. Furthermore, responders had more NKG2A+CD137- NK cells in the control sample and a bigger increase in NK_{bright} and CD107a-CD137+ NK cells when avelumab was added than nonresponders. Tumour cells displayed a stronger increase in PDL1 and CD40 expression for

nonresponders when cetuximab was given and the proportion of dead DAPI+AnnexinV+ tumour cells increased more strongly for nonresponders when cetuximab and avelumab were combined. On their own, it is difficult, if not impossible, to tell whether these findings are the result of pure chance alone due to a type I error and, hence, it is worth reiterating that they must be discussed (and will be in Chapter 5) in the context of the existing scientific literature and, where applicable, new hypotheses may be generated and subsequently tested in future experiments.

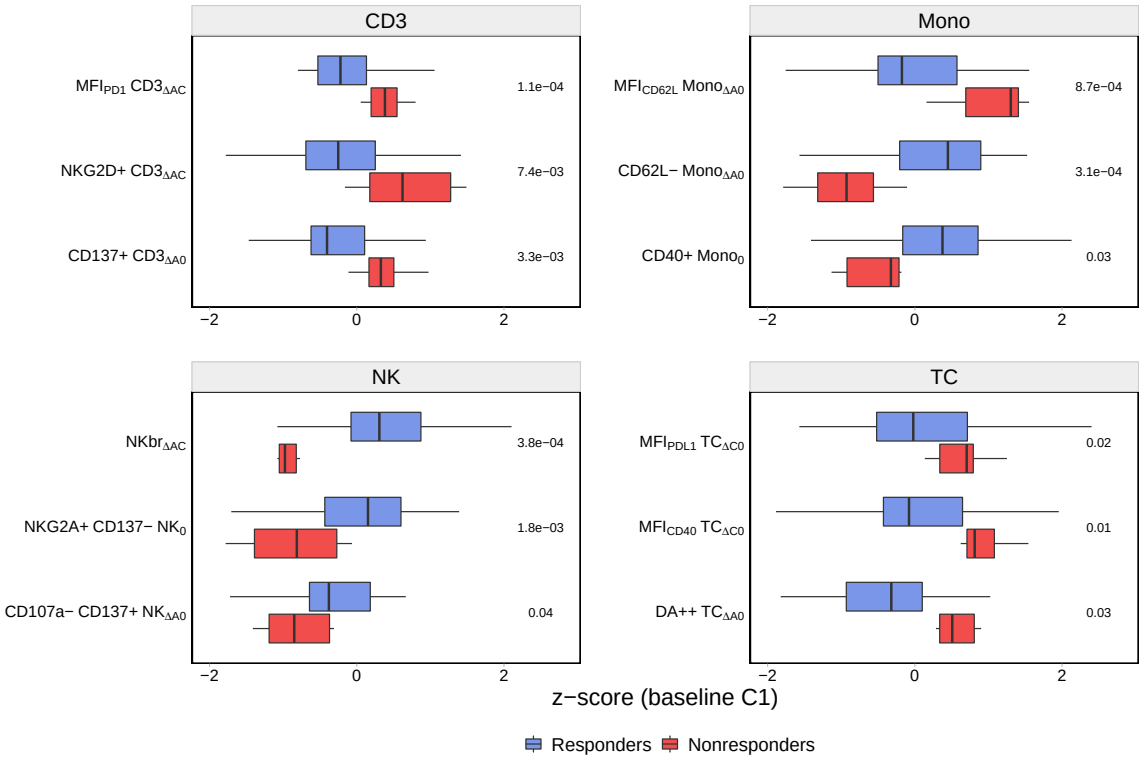

Figure 4.23: Boxplots of the parameters that differ significantly at baseline between responders and nonresponders. Parameters are grouped according to cell type and labelled with a subscript indicating the treatment condition.
Abbreviations: 0 = control sample; C = cetuximab sample; A = cetuximab+avelumab sample; $\Delta C0$ = difference between cetuximab and control sample; $\Delta A0$ = difference between cetuximab+avelumab and control sample; ΔAC = difference between cetuximab+avelumab and cetuximab sample; DA++ = DAPI+AnnexinV+. Statistics: Brunner-Munzel test

5 Discussion

5.1 FACS-based prediction of FcgRIIIa-158 phenotype

The binding affinity of IgG1 mAbs to FcgRIIIa is altered by polymorphisms in the FcgRIIIa-encoding genes and, thus, the presence of various FcgRIIIa phenotypes accounts for differences in immune defense mechanisms. In the literature, the FcgRIIIa-158 V/F polymorphism chiefly investigated in the context of this project has been associated with the susceptibility to a range of different diseases, namely various autoimmune disorders (rheumatoid arthritis, systemic lupus erythematous, immune thrombocytopenic purpura) [13, 165–170] and infectious diseases (infectious adult periodontitis, parasitic infections) [171, 172]. Beyond modulating susceptibility to disease, the FcgRIIIa-158 polymorphism has also been implicated with responsiveness to immunological therapies, such as treatments based on monoclonal antibodies (rituximab, trastuzumab, cetuximab, infliximab) [15, 16, 173–175], cancer vaccinations [176] and oncolytic adenovirus therapy [177] as well as disease progression. With this in mind, it becomes clear that the knowledge of a patient's particular FcgRIIIa-158 phenotype is highly desirable not only in the context of clinical trials but also for informed decision-making in routine clinical practice. In Section 4.1, we have successfully demonstrated that our self-developed FACS panel based on the two CD16 clones LNK16 and MEM154 is capable of determining the correct FcgRIIIa-158 phenotype with an accuracy of 91%. Compared with PCR-sequencing based techniques, our FACS-based approach has the advantage of being considerably less cost-intensive and having a short turn-around time (ca. 30 minutes). In addition, it could be widely employed with relative ease as the equipment and expertise to perform flow cytometric measurements is more readily available even in smaller hospitals, as opposed to PCR-sequencing based techniques. In an approach similar to us, Böttcher et al. have

previously developed a FACS-based assay to infer the FcgRIIIa-158 phenotype [124]. A key difference in their experimental setup is that they use clone MEM154 in combination with clone 3G8 (analogous to LNK16, 3G8 binds all isoforms). Since MEM154 and 3G8 recognise epitopes of the FcgRIIIa receptor in close proximity to each other [123], they compete for binding and cannot be used simultaneously. As a workaround, they processed two separate samples per patient, each featuring only one of the clones. A single-sample approach such as ours is appealing not only because it saves resources and is less laborious but also because it avoids the problem of random fluctuations between samples unintentionally introduced by the experimenter. While Böttcher et al. were able to define MFI thresholds to unambiguously classify 37 healthy volunteers according to their FcgRIIIa-158 phenotype (similar to our training set), they did not proceed to test these thresholds, once defined, on a cohort of individuals with unknown phenotype. Without such validation, the performance of their experimental assay cannot be compared to our approach; however, given the great variances of the MFIs within the groups that were observed both by them and us, it is unlikely that their simplistic model based solely on MFI thresholds would not lead to the misclassification of some individuals. Linked to this statement, it is worth discussing that all samples misclassified by our own prediction model belonged to the VF or VV group. In the literature [158, 178–181] as well as in our own data (Fig. 4.16 in Section 4.3.1), we have seen that the potential to induce ADCC differed significantly between FF individuals and the combined group of VF and VV individuals. The latter two groups showed similar reactivity, suggesting that the presence of one V allele is sufficient to unleash the full ADCC potential. Reasoning on the basis of this finding, we would not expect the incorrect predictions for $<10\%$ of samples by our prediction model to interfere with clinical decision-making. However, should perfect accuracy in the distinction between the VF and VV phenotype gain importance in the future due to advancing scientific knowledge, we would like to emphasise that our prediction model may be further improved. While the LDA model employed in this work certainly confirmed its usefulness, its implementation is merely meant as a proof-of-concept. Delving more deeply into the universe of machine learning, a better performing algorithm may likely be identified for our use case. A weakness of the FACS-based approach is that the measurement of MFIs is dependent on the specific calibration of the flow cytometer, which makes it necessary

to retrain the prediction model in case of changes to these settings or when running the FACS panel on a new machine. Reassuringly, we were able to show that the number of samples sufficient for model retraining is in the order of magnitude of about 9 samples - a number that appears feasible in practice. We would like to conclude the discussion of this part with the remark that successfully applying the FACS-based FcgRIIIa-158 prediction to the cohort of FIRE6 study patients may already be considered a first testimony of its general usefulness.

5.2 In vitro ADCC model

In the field of therapies employing monoclonal antibodies, in vitro ADCC co-culture assays are routinely performed to direct research and development of new therapeutic antibodies as well as used as an experimental tool to predict the clinical prognosis of patients treated with these antibodies. An effective in vitro ADCC assay requires at least three mandatory components: (1) biologically relevant target cells expressing the antigen of interest on their surface, (2) a monoclonal antibody highly specific for the antigen of interest and (3) suitable effector cells that are capable of inducing lysis of the antibody-tagged target cells. The in vitro ADCC assay developed in this work is based on PBMCs as effector cells, two IgG1 mAbs directed against EGFR (cetuximab) and PDL1 (avelumab) as well as a CRC cell line as target cells. To determine an appropriate choice for the latter, we screened a selection of 13 different CRC cell lines in Section 4.2, assessing their susceptibility to cetuximab-mediated ADCC. Having observed a highly variable ADCC response, the CRC cell lines were subsequently characterised with regards to their expression of relevant surface markers. Ranked in decreasing order, expression of EGFR, MICA/B, CD137L and PDL1 showed strong positive correlation with a cell line's sensitivity to ADCC. In addition, HLA-A/B/C expression was found to be associated with relative resistance to ADCC. As will be discussed here, these findings are in excellent agreement with the literature and underpin the reliability of the developed in vitro ADCC assay.

The EGFR receptor is the principal target of the anti-EGFR antibody cetuximab and, thus, it is of little surprise that higher EGFR expression was found to unanimously correlate with better cetuximab-mediated ADCC inducibility for a range of tumour types,

including colorectal cancer [182–184]. In addition, it could be shown that escalation techniques to upregulate surface EGFR expression on CRC cell lines greatly enhanced ADCC sensitivity [185] and that this effect is independent of KRAS/BRAF/ PIK3CA mutational status [184]. Further confirmation of this is the fact that the ADCC results obtained for the specific cell lines screened in this work are in line with results for the same cell lines in the literature. These cell lines may be grouped as EGFR/ADCC high (SW48, SnuC5, LS174T) [186, 187], EGFR/ADCC intermediate (HCT116, HT29, SW480, DLD1) [182, 184, 188] and EGFR/ADCC low (RKO, SW620, SW403) [184].

Similarly to EGFR targeted by cetuximab, expression of PDL1 on tumour cells is widely known to correlate with avelumab-mediated ADCC [189–191]. Interestingly, we could confirm with our in vitro ADCC assays that PDL1 expression was additionally associated with cetuximab-mediated ADCC. PDL1 expression on tumour cells is regulated by a series of factors that are linked to therapies with EGFR-targeting antibodies. In several studies, activating mutations as well as upregulation of EGFR were observed to increase PDL1 expression on tumour cells, which in turn could be reduced via EGFR blockade with tyrosine kinase inhibitors [155, 192–194]. From a mechanistic point of view, activation of the EGFR signalling cascade increases the activity of β-1,3-N-acetylglucosaminyl transferase (B3GNT3) resulting in the glycosylation of PDL1 and blocking its removal from the cell membrane [195, 196]. Supporting these observations, our analysis also determined that CRC cell lines with high EGFR expression in this work exhibited increased co-expression of PDL1. While one may argue that such co-expression of EGFR and PDL1 forms an appealing rationale for cetuximab and avelumab combination therapy, it is just as conceivable that this will have only a limited effect. If EGFR expression on tumour cells alone is already sufficient for NK cells to mount a strong ADCC response, the additional targeting of PDL1 largely expressed on the same share of tumour cells may not translate to significantly improved tumour lysis. When ignoring the potential concurrent effect of avelumab through PD1/PDL1 checkpoint blockade and focussing solely on ADCC, we indeed observed that the level of ADCC against the highly EGFR and PDL1 expressing CRC cell line SnuC5 increased only slightly for cetuximab and avelumab combination treatment compared with cetuximab alone.

The MHC class I chain-related protein A and B (MICA/B) are polymorphic proteins

that are not constitutively expressed by healthy normal cells. Their expression is typically induced upon danger stimuli such as stress, cell damage or malignant transformation of cells and has been reported for most tumour types [112, 114, 115]. Hence, MICA/B are thought to act as "kill me" signals that are bound by the natural-killer group 2, member D receptor (NKG2D) on NK cells and cytotoxic lymphocytes. NKG2D is an activating checkpoint and, upon binding to MICA/B, marks the target cell for NK-cell mediated destruction, resulting in a higher level of ADCC as was observed with our in vitro ADCC assay.

CD137L is a member of the tumour necrosis factor (TNF) receptor superfamily present on antigen-presenting cells such as mature dendritic cells and macrophages [197, 198]. Under physiologic conditions, binding of CD137L by the inducible costimulatory CD137 receptor mainly expressed on activated T cells and NK cells enhances immune responses, leading to upregulation of NKG2D, increased production and secretion of cytokines (e.g. INF-γ) and cytotoxic molecules (e.g. perforin, granzyme B) by NK cells [116–121]. These changes result in strengthening the cytotoxic capacity of NK cells against ADCC-sensitive tumours. CD137L expression is virtually absent on healthy normal tissue but commonly present on tumour cells, where it is correlated with the occurrence of distant metastases. Mechanistically, CD137/CD137L reverse signalling in tumour cells is thought to trigger events favouring the epithelial-to-mesenchymal transition (EMT) necessary to unleash a tumour's potential for metastatisation and invasive growth [199]. Thus, while CD137/CD137L signalling may be beneficial for tumour progression on the one hand, it in turn renders the tumour more vulnerable to NK-cell mediated ADCC on the other hand, as seen in this work. Currently, there are several ongoing clinical trials exploring the effect of agonistic anti-CD137 antibodies, namely urelumab and utomilumab, in combination with already approved tumour-targeted mAbs in diverse oncological and haematological malignancies. For example, urelumab is used together with cetuximab for head and neck cancer patients (NCT02110082), whereas the combination of utomilumab and cetuximab is under trial for colorectal cancer (NCT03290937).

The three major types of human MHC class I transmembrane proteins HLA-A/B/C are among the most important "self markers" for cells of healthy normal tissue. As such, they play a pivotal role not only in solid-organ transplantation but also tumour progression. The

suppressed expression of HLA-A/B/C on metastatic cancer cells leads to tumour immune evasion due to the failure of antigen presentation of tumour-specific cell surface epitopes to host cytotoxic T cells [200]. This process helps malignant cells to evade host immune responses and promote cell dissemination and invasive growth [201]. Despite seemingly being an advantageous adaptation at first glance (from the tumour's point of view), the downregulation of HLA-A/B/C surface expression to reduce T cell recognition comes at a cost, in this case at the expense of attracting attention from NK cells. The family of killer immunoglobulin-like receptors (KIR) expressed on NK cells recognise HLA molecules as their ligands [202]. In their developmental stages, NK cells undergo a "licensing" phase that induces their tolerance to HLA-A/B/C constitutively expressed on the surface of healthy self cells [112, 113]. When encountering HLA-deficient cells, such as tumour cells, these licensed NK cells are more capable of killing these target cells ("missing-self" hypothesis) [203–205]. With this in mind, it becomes clear why HLA-A/B/C surface expression is negatively correlated with NK-cell mediated ADCC in our assay.

Moving on to the FACS panel that complements the LDH release assay in our in vitro ADCC model, we were able to show a strong positive correlation of tumour cell death - as determined by quantifying the change in DAPI-AnnexinV- viable tumour cells between mAb-treated and control samples - with the results from the LDH release assay. There are many different approaches of in vitro ADCC assays in wide use in laboratories around the world, the majority of which are based on either of LDH release [206], 51 Cr release [207], Europium release [208] or, more recently, flow cytometric measurements of DAPI [209], PI [210] or CFSE uptake [211, 212] as well as staining for calcein AM [213] or AnnexinV [214]. Yet, our approach of combining an LDH release assay with a FACS-based assay into a parallelised workflow is rather unique and, in our opinion, offers a series of advantages. LDH release assays are well established, low-priced and not very time-consuming. A potential downside is that they only provide a single readout, i.e. LDH release as a surrogate for cell death, and that the overall LDH signal must be corrected for the contribution by the effector cells, which may negatively impact on reproducibility. In contrast, FACS-based approaches are more time-consuming and expensive, but allow the concurrent measurement of additional readouts of interest. As demonstrated in this work, our FACS panel further captures NK cell engagement and activation (CD16, CD137,

CD107a) as well as checkpoint markers (PD1, NKG2A, NKG2D) and phenotypic markers (CD62L, CD40) as part of the same experiment. Due to its extensive nature, we consider our FACS panel a great asset for our own projects and certainly able to contend with similar panels from other groups [60, 215–217]. One could make a case for dispensing with the LDH release assay when having the FACS panel at hand, the former, however, was useful to validate the reliability of the newly developed FACS panel in this work and, even for future use case, provides a feasible fall-back readout should anything go awry with the FACS panel.

5.3 FIRE6 study

5.3.1 FcgRIIIa-158 polymorphism

In Section 4.3.1, we have determined for our patient cohort that PBMCs from donors with at least one FcgRIIIa-158 V allele were able to induce significantly higher in vitro IgG1-mediated ADCC than those from FF homozygous donors. This is in line with the literature as the known stronger IgG1 mAb binding affinity of NK cells with a valine residue at position 158 was expected to result in higher ADCC - a finding that has consistently been reported for virtually all clinically used IgG1 mAbs, namely anti-EGFR cetuximab [218, 219], anti-PDL1 avelumab [220], anti-CD20 rituximab [178, 221], anti-HER2 trastuzumab [16] as well as anti-TNF$_\alpha$ adalimumab [181] and infliximab [222]. In line with other reports [181, 220, 221], it is worth noting that we observed no noticeable difference in in vitro ADCC between VF heterozygotes and VV homozygotes, implying that the presence of a single V allele is already sufficient for a donor's NK cells to obtain their full ADCC potential. From an epidemiological point of view, this is worth highlighting as the prevalence of VV homozygotes is relatively low in the general Caucasian population (<20%), whereas VF and VV individuals combined account for more than half of all people [150, 151].

Despite the well-established increased ADCC lysis for donors with the high-affinity VF and VV phenotypes, subsequent analysis did not confirm an association of the FcgRIIIa-158 polymorphism with clinical outcome measures. Within the FIRE6 cohort, both response to treatment and PFS did not differ significantly between the three FcgRIIIa-158

phenotypes. This result adds yet another blur of colour to the inconsistent picture painted by the large body of scientific evidence with regards to the predictive and prognostic value of the FcgRIIIa-158 polymorphism for IgG1-based therapies. Limiting our discussion here to the use of cetuximab in metastatic colorectal cancer (for a broader critical review see Mellor et al. [148]), there are five retrospective studies that observed prolonged progression-free survival for the VV phenotype [218, 223–226], which is in stark contrast to four other retrospective studies that found the low-affinity FF phenotype was most beneficial [227–230]. Since all good things come in threes, the confusion is completed by three further studies that, in line with our own findings, showed no significant association of the FcgRIIIa-158 polymorphism with clinical cetuximab efficacy [231–233]. Among others, the differences between these studies include the line of therapy (from first line to salvage), the clinical setting (adjuvant, neoadjuvant or metastatic), the chemotherapeutic drugs administered in combination with cetuximab as well as the specific parameters assessed to quantify clinical outcome. Further complicating the matter, most of the studies were of retrospective, non-randomised nature and, thus, cannot adequately determine the relationship between the FcgRIIIa-158 polymorphism and clinical outcome under cetuximab therapy. Contributing to the conflicting data is likely the low statistical power of most studies, including ours, due to small sample sizes in the order of less than 100 patients. Importantly, the best-powered of the studies presented here did not find any association of the FcgRIIIa-158 polymorphism with the therapeutic effect of cetuximab [232]. For some of the studies, Mellor et al. identified a deviation of the phenotype distribution from the Hardy-Weinberg equilibrium [148]. While a deviation may naturally occur and may be of no concern when diverse ethnic groups with differing allelic frequencies are mixed in large multi-centre studies, such a deviation may alternatively indicate methodological flaws (e.g. type of tissue used, PCR sequencing method) in the determination of the FcgRIIIa-158 polymorphism. For our patient cohort however, the Hardy-Weinberg equilibrium holds true, raising no doubt in the results of the PCR sequencing.

Overall, the inconsistent findings reviewed here suggest that the FcgRIIIa-158 polymorphism is not currently a useful predictive biomarker of response to cetuximab. While it corresponds with in vitro ADCC activity and may influence the anti-tumour activity of IgG1-based therapies, it may be of lower importance compared with non-ADCC mechan-

isms of action such as the direct effect of the mAb (e.g. EGFR blockade for cetuximab, PD1-PDL1 checkpoint inhibition for avelumab) or complement-dependent cytotoxicity.

5.4 ADCC activity and NK cell activation

With our in vitro model, we were able to show that patient-derived PBMCS are generally capable of mounting an ADCC response against CRC cell lines and that NK cells play a pivotal role in this process as quantified through their widespread engagement (CD16 downregulation), activation (CD137 upregulation) and degranulation (CD107a upregulation), all of which showed strong positive correlation with ADCC. These findings are in excellent agreement with the literature [60, 218, 233, 234]. In comparison with age-matched healthy donors, we observed a clear, albeit non-significant, trend towards lower ADCC at baseline (timepoint C1) for all patients regardless of their later response to the treatment or failure thereof. Kawaguchi et al. reported the same observation when evaluating the in vitro ADCC by PBMCs of 7 healthy volunteers and 7 patients suffering from oesophageal squamous cell carcinoma [183]. Since not only tumour-infiltrating but also peripherally circulating immune cells are known to be dysfunctional in a cancer-induced immunosuppressive environment [235], it may be speculated that this gives rise to a partial impairment of their ADCC capabilities compared with those of healthy volunteers.

Analysing in vitro ADCC activity with respect to clinical outcome, in our patient cohort we did not observe any statistically significant differences (1) in ADCC levels between responders and nonresponders or (2) in progression-free survival between individuals with high or low ADCC levels (i.e. ADCC $<$ or $>$ 20%, respectively). In contrast to our own findings, several authors reported a correlation of in vitro ADCC and diverse clinical outcome measures for cancer patient cohorts treated with cetuximab and/or avelumab therapy [218, 233, 234]. Trotta et al. studied a small cohort of 28 KRAS wild-type mCRC patients receiving standard chemotherapy and cetuximab therapy [218]. Patients who experienced a partial or complete response with cetuximab showed higher in vitro ADCC than those patients who did not. However, it is worth noting that despite the correlation with cetuximab responsiveness, no difference in progression-free survival was found. In a cohort of 41 KRAS wild-type mCRC patients treated with cetuximab and chemotherapy

as second or third line, Lo Nigro et al. detected a significantly improved overall survival of patients with above-median in vitro ADCC compared with the remaining patients [233]. Similarly, Bertino et al. reported a trend, albeit non-significant, towards increased ADCC in 19 KRAS wild-type mCRC patients responding to cetuximab and lenalidomide combination therapy compared with those who failed to respond [234]. A key difference of the aforementioned studies with respect to ours is their use of enriched NK cells that were isolated from patient PBMCs when evaluating ADCC. In our reasoning, we decided to use PBMCs instead of isolated NK cells due to practical limitations, i.e. the fact that for most patients an insufficient number of NK cells would have likely been recovered from the scarce amount of cryostored PBMCs due to the isolation procedure itself incurring additional cell losses. In addition, we sought after more appropriately reflecting the in vivo situation of the peripheral blood by employing PBMCs rather than enriched NK cells in our experimental model. For example, the population of CD16+ non-classical monocytes present in the PBMC samples (experimentally confirmed for our cohort; data not shown) are capable of competing with NK cells for binding of the IgG1 antibodies and, thus, may influence ADCC results [236]. Similarly, the interplay of NK cells with other immune cell subsets, most importantly T cells, may also be expected to have an impact on ADCC. While we attempted to approximate the in vivo situation in the peripheral blood as best as possible with our experimental model, some important shortcomings of our own model as well as those reported by other groups must be discussed. Among others, the patient-specific characteristics of each tumour are ignored by in vitro models simply testing ADCC against a standard CRC cell line (SnuC5 in our case). EGFR and PDL1 expression vary heavily between tumours from different patients and it has been shown both in this work and in the literature that surface expression of the target antigens has a strong impact on ADCC. Underlining this importance for clinical outcome, Lattanzio et al. reported that in vitro ADCC alone did not correlate with response to cetuximab in 28 patients with head and neck squamous cell carcinoma, but predicted response when combined with a score of tumour EGFR expression [237]. Furthermore, individual tumours may differ in their ability to wall themselves off from surrounding tissue and resist immune cell infiltration. Effective tumour lysis by NK cells can only occur if the latter are able to invade the tumour and find themselves in close proximity to

the antibody-coated tumour cells, yet promoting the infiltration of adequate numbers of functionally active NK cells into the tumour milieu remains an obstacle in solid tumours [219]. Not surprisingly, Marechal et al. thus showed that NK cell infiltration of the tumour correlated with increased PFS in 5 mCRC patients receiving cetuximab [238]. Hence, analysing NK cell levels and their functional properties in peripheral blood cannot reveal the whole picture of the activity of tumour-infiltrating NK cells (and other immune cell populations) in patients. Further substantiating this claim, a reduced number of NK cells in the periphery may correspond to an increased number and activity of NK cells in the tumour [239]. Apart from such experimental weaknesses inherent in every in vitro model to a variable extent, it is important to keep in mind that although ADCC may have an impact on the anti-tumour activity and, thus, clinical outcome of patients receiving IgG1-isotype mAbs, there may be an overall predominance of non-ADCC mechanisms of action such as direct cytotoxicity by Fab-mediated binding of the monoclonal antibodies to the target antigen, or complement-dependent cytotoxicity.

Our longitudinal analysis over four timepoints spanning the range from before therapy initiation to chemotherapy and cetuximab therapy to combination treatment of chemotherapy, cetuximab and avelumab therapy detected a gradual decline in ADCC activity and NK cell activation for all patients. Potentially explaining these results, we observed a continuous drop of peripheral NK cell levels for all patients during therapy (data not shown), which might reflect the abovementioned increased recruitment of NK cells to tumour tissues during therapy [239]. In addition to a peripheral reduction of NK cells, our longitudinal screening also found an increase of CD16+ non-classical monocytes under therapy (data not shown) and, as explained above, their scavenging of therapeutic antibodies from NK cells may contribute to a decrease of in vitro ADCC. In line with our findings, Lo Nigro et al. reported for a cohort of mCRC patients that the capacity to perform ADCC decreased during therapy compared to baseline levels [233]. They chiefly attribute the lower therapy-induced ADCC to the known immunosuppressive effect of chemotherapy that is reviewed in detail elsewhere [240] and may also play a role in our cohort. However, there also is at least one report of 16 patients with non-small cell lung cancer treated with cetuximab and avelumab second-line combination therapy, with longterm responders (PFS $>$ 8 months) experiencing a significant increase in ADCC and

nonresponders (PFS < 5 months) showing a trend towards reduced ADCC during therapy [60].

5.5 Exploratory analysis

The exploratory analysis conducted in this work may be compared to searching for a needle in a haystack. As elaborated before, we intentionally did not adjust for multiple testing when screening the measured parameters for significant differences between responders and nonresponders. Due to the non-negligible risk of parameters resulting significant by pure chance alone, the reported findings must be placed in the context of the scientific literature and it must be carefully assessed whether a research hypothesis can be generated that is in line with the findings. Within the scope of this work, we would like to limit the discussion to the potential role of CD40+ monocytes since we cannot make a convincing case for any of the other parameters on the basis of what is known so far. Regarding CD40+ monocytes, we observed that a higher level of circulating CD40+ monocytes in peripheral blood at baseline correlated with a response to treatment in our patient cohort. It is well-known that CD40, a member of the TNF-receptor superfamily, is widely expressed on the surface of antigen-presenting cells including macrophages, dendritic cells and monocytes [241]. Interaction with its ligand CD40L, predominantly expressed on activated T cells, leads to the upregulation of MHC molecules and the release of inflammation-promoting molecules, all of which in turn promotes further T cell activation [242, 243]. The expression of CD40 on both peripherally circulating and intratumoral monocytes was shown to decrease as the tumour progresses and to be paralleled by a reduced co-stimulation of T cells [92, 244]. Furthermore, dense infiltration of colorectal cancer tissues by CD40+ tumour-associated macrophages (TAM) was confirmed to be an independent favourable prognostic marker, which indicates an important role of CD40 in the tumour immunity of colorectal cancer [245]. In several mouse models, the administration of agonistic anti-CD40 monoclonal antibodies was observed to be effective in reprogramming of TAMs towards M1 polarisation, thereby restoring lost tumour immune surveillance and anti-tumour activity [246–248]. Administration of an agonistic anti-CD40 antibody, in combination with an inhibitor of colony stimulating factor 1 (CSF1R), transformed immunologically "cold" into "hot" tu-

mours by enhancing activity of infiltrating T cells and simultaneously diminishing the number of immunosuppressive cells in a preclinical model [249]. While most of this evidence in the literature stems from the investigation of monocytes and macrophages in the intratumoral milieu, it is at least conceivable that the correlation of peripherally circulating CD40+ monocyte levels with the response to cetuximab and avelumab treatment may be intertwined with CD40 expression on intratumoral monocytes and macrophages.

6 Future Work and Outlook

In recent years, the use of therapeutic monoclonal antibodies against tumour-associated antigens and immune-checkpoint molecules has become a mainstay of cancer immunotherapy, nowadays complementing and in some instances even replacing the widespread use of chemotherapy, radiation therapy and surgical interventions. Focussing on a cohort of 55 patients with previously untreated RAS/BRAF wild-type metastatic colorectal carcinoma receiving chemotherapy and the IgG1 mAbs cetuximab (anti-EGFR) and avelumab (anti-PDL1), we successfully developed experimental methods to study the role of the FcgRIIIa-158 polymorphism as well as NK-cell mediated in vitro ADCC with respect to clinical benefit for patients. Having confronted our own findings with those reported in the literature, it is safe to say that - in light of at least partially contradictory results - a final decision on this matter may not yet be taken and future work towards addressing and resolving these discrepancies are warranted.

The analysis presented in this work should not be considered final and will benefit from more detailed data becoming available when the data lock-up period is reached after the conclusion of the clinical trial. For the time being, patients had to be treated as "black boxes", with the only information accessible being a patient's response status and progression-free survival. We expect that better knowledge of the patient characteristics such as epidemiological data and, even more importantly, histological data including tumour type, EGFR/PDL1 expression and tumour immune infiltration will aid interpretation of the results obtained in this work.

A further point worthy of brief mention are the different cytotoxic agents being administered as chemotherapeutic backbone across the various clinical trials employing mAbs. In this context, we tend to ignore agent-specific differences and simply speak of chemotherapy being used in combination with mAb targeted therapy. Yet, the precise choice of

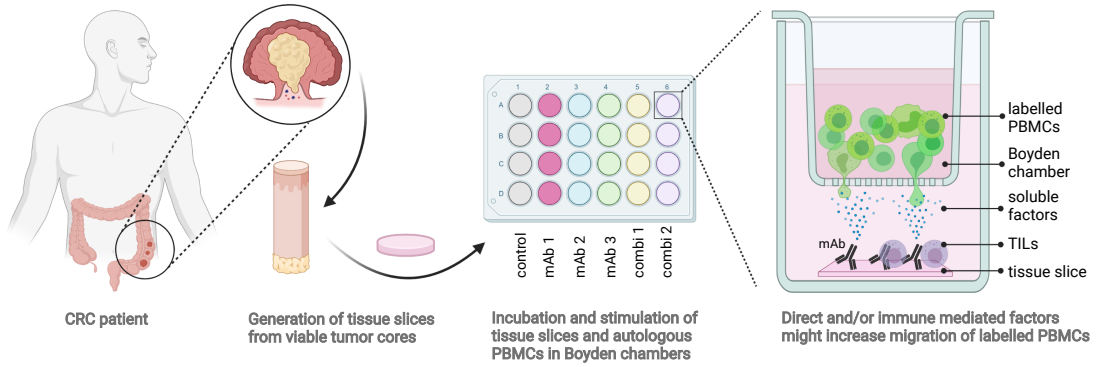

Figure 6.1: Scheme of proposed in vitro ADCC model employing tumour tissue slices to be used in future work. To address tumour heterogeneity between patients, tissue slices could be cut from viable tumour biopsy samples obtained from cancer patients and replace the use of a CRC cell line as target cells. In doing so, the effect of pre-existing immune cell infiltrates could be studied as well as the migration into the tissue slice of autologous PBMCs provided in a Boyden chamber.

cytotoxic agents may impact on the success of concurrent mAb therapy, a field that to date appears to be understudied by the scientific community, albeit it is gaining further importance in the era of immunotherapy as immune cell populations are severely influenced by chemotherapeutics. With this in mind, in vitro models to investigate the influence of the most commonly clinically applied cytotoxic agents on aspects such as tumour composition, immune cell infiltration and activity are certainly warranted.

As discussed in Chapter 5, the current in vitro ADCC model should be further improved in future work to better reflect the in vivo situation. Rather than testing ADCC of patient-derived PBMCs against a CRC cell line, it is desirable to work with tumour biopsies, tumour-derived organoids or developing a tumour-on-a-chip model. As a step in this direction, we propose an improved in vitro model in Fig. 6.1. Generating tissue slices from viable biopsy samples of individual patients, these slices could be incubated and stimulated with and without the addition of autologous PBMCs in Boyden chambers, allowing to better dissect (1) the role and feasibility of immune cell migration into a patient's tumour and (2) the presence or absence of pre-existing immune cell infiltrates in the biopsy samples. To the best of our knowledge, such a model has not yet been extensively studied in the context of CRC and IgG1 mAbs and may potentially help towards reconciling the conflicting reports in the literature.

Bibliography

[1] G. R. Dagenais, D. P. Leong, S. Rangarajan, F. Lanas, P. Lopez-Jaramillo, R. Gupta, R. Diaz, A. Avezum, G. B. Oliveira, A. Wielgosz, L. Wei, M. Kaur and S. Yusuf. 'Variations in common diseases, hospital admissions, and deaths in middle-aged adults in 21 countries from five continents (PURE): a prospective cohort study'. In: *The Lancet* 395.10226 (2020), pp. 785–794.

[2] H. Frank. 'The original 'magic bullet'is 100 years old'. In: *The British Journal of Psychiatry* 195.5 (2009), pp. 456–456.

[3] A. N. Barclay. 'Membrane proteins with immunoglobulin-like domains—a master superfamily of interaction molecules'. In: *Seminars in immunology*. Vol. 15. 4. Elsevier. 2003, pp. 215–223.

[4] E. Market and F. N. Papavasiliou. 'V (D) J recombination and the evolution of the adaptive immune system'. In: *PLoS biology* 1.1 (2003), e16.

[5] A. Kretschmer, R. Schwanbeck, T. Valerius and T. Rösner. 'Antibody isotypes for tumor immunotherapy'. In: *Transfusion Medicine and Hemotherapy* 44.5 (2017), pp. 320–326.

[6] P. Bruhns. 'Properties of mouse and human IgG receptors and their contribution to disease models'. In: *Blood* 119.24 (2012), pp. 5640–5649. ISSN: 15280020.

[7] R. P. Kimberly, J. Wu, A. W. Gibson, K. Su, H. Qin, X. Li and J. C. Edberg. 'Diversity and duplicity: Human Fcγ receptors in host defense and autoimmunity'. In: *Immunologic Research* 26.1-3 (2002), pp. 177–189. ISSN: 0257277X.

[8] K. G. Smith and M. R. Clatworthy. 'FcγRIIB in autoimmunity and infection: Evolutionary and therapeutic implications'. In: *Nature Reviews Immunology* 10.5 (2010), pp. 328–343. ISSN: 14741733.

[9] J. Yu, Y. Song and W. Tian. 'How to select IgG subclasses in developing anti-tumor therapeutic antibodies'. In: *Journal of Hematology & Oncology* 13.1 (2020), pp. 1–10.

[10] S. W. De Taeye, A. E. Bentlage, M. M. Mebius, J. I. Meesters, S. Lissenberg-Thunnissen, D. Falck, T. Sénard, N. Salehi, M. Wuhrer, J. Schuurman, T. Rispens and G. Vidarsson. 'FcγR binding and ADCC activity of human IgG allotypes'. In: *Frontiers in immunology* 11 (2020), p. 740.

[11] N. Van Sorge, W.-L. Van Der Pol and J. Van de Winkel. 'FcγR polymorphisms: implications for function, disease susceptibility and immunotherapy'. In: *Tissue antigens* 61.3 (2003), pp. 189–202.

[12] H. R. Koene, M. Kleijer, J. Algra, D. Roos, A. E. Von Dem Borne and M. De Haas. 'FcγRIIIa-158V/F polymorphism influences the binding of IgG by natural killer cell FCγRIIIa, independently of the FCγRIIIa-48L/R/H phenotype'. In: *Blood* 90.3 (1997), pp. 1109–1114. ISSN: 00064971.

[13] J. Wu, J. C. Edberg, P. B. Redecha, V. Bansal, P. M. Guyre, K. Coleman, J. E. Salmon and R. P. Kimberly. 'A novel polymorphism of FcγRIIIa (CD16) alters receptor function and predisposes to autoimmune disease'. In: *Journal of Clinical Investigation* 100.5 (1997), pp. 1059–1070. ISSN: 00219738.

[14] R. Niwa, S. Hatanaka, E. Shoji-Hosaka, M. Sakurada, Y. Kobayashi, A. Uehara, H. Yokoi, K. Nakamura and K. Shitara. 'Enhancement of the antibody-dependent cellular cytotoxicity of low-fucose IgG1 is independent of FcγRIIIa functional polymorphism'. In: *Clinical Cancer Research* 10.18 (2004), pp. 6248–6255.

[15] W. K. Weng and R. Levy. 'Two immunoglobulin G fragment C receptor polymorphisms independently predict response to rituximab in patients with follicular lymphoma'. In: *Journal of Clinical Oncology* 21.21 (2003), pp. 3940–3947. ISSN: 0732183X.

[16] A. Musolino, N. Naldi, B. Bortesi, D. Pezzuolo, M. Capelletti, G. Missale, D. Laccabue, A. Zerbini, R. Camisa, G. Bisagni, T. M. Neri and A. Ardizzoni. 'Immunoglobulin g fragment c receptor polymorphisms and clinical efficacy of trastuzumab-based therapy in patients with HER-2/neu-positive metastatic breast cancer'. In: *Journal of Clinical Oncology* 26.11 (2008), pp. 1789–1796. ISSN: 0732183X.

[17] D. S. Salomon, R. Brandt, F. Ciardiello and N. Normanno. 'Epidermal growth factor-related peptides and their receptors in human malignancies'. In: *Critical reviews in oncology/hematology* 19.3 (1995), pp. 183–232.

[18] N. Normanno, C. Bianco, A. De Luca and D. S. Salomon. 'The role of EGF-related peptides in tumor growth'. In: *Front Biosci* 6.1 (2001), pp. D685–707.

[19] M. A. Olayioye, R. M. Neve, H. A. Lane and N. E. Hynes. 'The ErbB signaling network: receptor heterodimerization in development and cancer'. In: *The EMBO journal* 19.13 (2000), pp. 3159–3167.

[20] P. Seshacharyulu, M. P. Ponnusamy, D. Haridas, M. Jain, A. K. Ganti and S. K. Batra. 'Targeting the EGFR signaling pathway in cancer therapy'. In: *Expert opinion on therapeutic targets* 16.1 (2012), pp. 15–31.

[21] M. Wieduwilt and M. Moasser. 'The epidermal growth factor receptor family: biology driving targeted therapeutics'. In: *Cellular and molecular life sciences* 65.10 (2008), pp. 1566–1584.

[22] P. Schiele. 'Das Potenzial der Glyko-Optimierung bei kombinatorischen Krebs-Immuntherapien mit monoklonalen Antikörpern'. PhD thesis. 2021.

[23] P. J. Miettinen, J. E. Berger, J. Meneses, Y. Phung, R. A. Pedersen, Z. Werb and R. Derynck. 'Epithelial immaturity and multiorgan failure in mice lacking epidermal growth factor receptor'. In: *Nature* 376.6538 (1995), pp. 337–341.

[24] M. Sibilia and E. F. Wagner. 'Strain-dependent epithelial defects in mice lacking the EGF receptor'. In: *Science* 269.5221 (1995), pp. 234–238.

[25] M. Sibilia, J. P. Steinbach, L. Stingl, A. Aguzzi and E. F. Wagner. 'A strain-independent postnatal neurodegeneration in mice lacking the EGF receptor'. In: *The EMBO journal* 17.3 (1998), pp. 719–731.

[26] D. W. Threadgill, A. A. Dlugosz, L. A. Hansen, T. Tennenbaum, U. Lichti, D. Yee, C. LaMantia, T. Mourton, K. Herrup, R. C. Harris, J. Barnard, S. Yuspa, R. Coffey and T. Magnuson. 'Targeted disruption of mouse EGF receptor: effect of genetic background on mutant phenotype'. In: *Science* 269.5221 (1995), pp. 230–234.

[27] M. Gassmann, F. Casagranda, D. Orioli, H. Simon, C. Lai, R. Klein and G. Lemke. 'Aberrant neural and cardiac development in mice lacking the ErbB4 neuregulin receptor'. In: *Nature* 378.6555 (1995), pp. 390–394.

[28] K.-F. Lee, H. Simon, H. Chen, B. Bates, M.-C. Hung and C. Hauser. 'Requirement for neuregulin receptor erbB2 in neural and cardiac development'. In: *Nature* 378.6555 (1995), pp. 394–398.

[29] J. Baselga. 'Why the epidermal growth factor receptor? The rationale for cancer therapy'. In: *The oncologist* 7.S4 (2002), pp. 2–8.

[30] D. Wujcik. 'EGFR as a target: rationale for therapy'. In: *Seminars in oncology nursing*. Vol. 22. Elsevier. 2006, pp. 5–9.

[31] I. B. Weinstein and A. K. Joe. 'Mechanisms of disease: oncogene addiction—a rationale for molecular targeting in cancer therapy'. In: *Nature clinical practice Oncology* 3.8 (2006), pp. 448–457.

[32] X. Yang, X. Zhang, E. D. Mortenson, O. Radkevich-Brown, Y. Wang and Y.-X. Fu. 'Cetuximab-mediated tumor regression depends on innate and adaptive immune responses'. In: *Molecular Therapy* 21.1 (2013), pp. 91–100.

[33] R. L. Ferris, H. J. Lenz, A. M. Trotta, J. García-Foncillas, J. Schulten, F. Audhuy, M. Merlano and G. Milano. 'Rationale for combination of therapeutic antibodies targeting tumor cells and immune checkpoint receptors: Harnessing innate and adaptive immunity through IgG1 isotype immune effector stimulation'. In: *Cancer Treatment Reviews* 63 (2018), pp. 48–60. ISSN: 15321967.

[34] R. M. Srivastava, S. C. Lee, P. A. Andrade Filho, C. A. Lord, H.-B. Jie, H. C. Davidson, A. López-Albaitero, S. P. Gibson, W. E. Gooding, S. Ferrone and R. Ferris. 'Cetuximab-activated natural killer and dendritic cells collaborate to trigger tumor antigen–specific T-cell immunity in head and neck cancer patients'. In: *Clinical Cancer Research* 19.7 (2013), pp. 1858–1872.

[35] J. Li, R. M. Srivastava, A. Ettyreddy and R. L. Ferris. 'Cetuximab ameliorates suppressive phenotypes of myeloid antigen presenting cells in head and neck cancer patients'. In: *Journal for immunotherapy of cancer* 3.1 (2015), pp. 1–16.

[36] F. Concha-Benavente, R. M. Srivastava, S. Trivedi, Y. Lei, U. Chandran, R. R. Seethala, G. J. Freeman and R. L. Ferris. 'Identification of the cell-intrinsic and-extrinsic pathways downstream of EGFR and IFNγ that induce PD-L1 expression in head and neck cancer'. In: *Cancer research* 76.5 (2016), pp. 1031–1043.

[37] T. Yamaoka, M. Ohba and T. Ohmori. 'Molecular-targeted therapies for epidermal growth factor receptor and its resistance mechanisms'. In: *International journal of molecular sciences* 18.11 (2017), p. 2420.

[38] D. L. Wheeler, E. F. Dunn and P. M. Harari. 'Understanding resistance to EGFR inhibitors—impact on future treatment strategies'. In: *Nature reviews Clinical oncology* 7.9 (2010), pp. 493–507.

[39] V. Agarwal, A. Subash, R. C. Nayar and V. Rao. 'Is EGFR really a therapeutic target in head and neck cancers?' In: *Journal of Surgical Oncology* 119.6 (2019), pp. 685–686.

[40] M. H. Yazdi, M. A. Faramarzi, S. Nikfar and M. Abdollahi. 'A comprehensive review of clinical trials on EGFR inhibitors such as cetuximab and panitumumab as monotherapy and in combination for treatment of metastatic colorectal cancer'. In: *Avicenna journal of medical biotechnology* 7.4 (2015), p. 134.

[41] T. G. Lyons, M. N. Dickler and E. E. Comen. 'Checkpoint Inhibitors in the Treatment of Breast Cancer'. In: *Current Oncology Reports* 20.7 (2018), pp. 1–10. ISSN: 15346269.

[42] D. S. Chen and I. Mellman. 'Elements of cancer immunity and the cancer–immune set point'. In: *Nature* 541.7637 (2017), pp. 321–330.

[43] C. Kyi and M. A. Postow. 'Checkpoint blocking antibodies in cancer immunotherapy'. In: *FEBS letters* 588.2 (2014), pp. 368–376.

[44] S. Menon, S. Shin and G. Dy. 'Advances in cancer immunotherapy in solid tumors'. In: *Cancers* 8.12 (2016), p. 106.

[45] C. Sun, R. Mezzadra and T. N. Schumacher. 'Regulation and function of the PD-L1 checkpoint'. In: *Immunity* 48.3 (2018), pp. 434–452.

[46] M. Baas, A. Besançon, T. Goncalves, F. Valette, H. Yagita, B. Sawitzki, H.-D. Volk, E. Waeckel-Enée, B. Rocha, L. Chatenoud and S. You. 'TGFβ-dependent expression of PD-1 and PD-L1 controls CD8+ T cell anergy in transplant tolerance'. In: *elife* 5 (2016), e08133.

[47] G. J. Freeman, A. J. Long, Y. Iwai, K. Bourque, T. Chernova, H. Nishimura, L. J. Fitz, N. Malenkovich, T. Okazaki, M. C. Byrne and T. Honjo. 'Engagement of the PD-1 immunoinhibitory receptor by a novel B7 family member leads to negative regulation of lymphocyte activation'. In: *The Journal of experimental medicine* 192.7 (2000), pp. 1027–1034.

[48] P.-W. Huang and J. W.-C. Chang. 'Immune checkpoint inhibitors win the 2018 Nobel Prize'. In: *biomedical journal* 42.5 (2019), pp. 299–306.

[49] D. M. Pardoll. 'The blockade of immune checkpoints in cancer immunotherapy'. In: *Nature Reviews Cancer* 12.4 (2012), pp. 252–264.

[50] L. Dyck and K. H. Mills. 'Immune checkpoints and their inhibition in cancer and infectious diseases'. In: *European journal of immunology* 47.5 (2017), pp. 765–779.

[51] C. Robert. 'A decade of immune-checkpoint inhibitors in cancer therapy'. In: *Nature Communications* 11.1 (2020), pp. 1–3.

[52] C. Fellner. 'Ipilimumab (yervoy) prolongs survival in advanced melanoma: serious side effects and a hefty price tag may limit its use'. In: *Pharmacy and Therapeutics* 37.9 (2012), p. 503.

[53] J. Larkin, V. Chiarion-Sileni, R. Gonzalez, J. J. Grob, C. L. Cowey, C. D. Lao, D. Schadendorf, R. Dummer, M. Smylie, P. Rutkowski, P. Ferrucci, A. Hill and J. Wolchok. 'Combined nivolumab and ipilimumab or monotherapy in untreated melanoma'. In: *New England journal of medicine* 373.1 (2015), pp. 23–34.

[54] J. D. Wolchok, H. Kluger, M. K. Callahan, M. A. Postow, N. A. Rizvi, A. M. Lesokhin, N. H. Segal, C. E. Ariyan, R.-A. Gordon, K. Reed, M. Burke and M. Sznol. 'Nivolumab plus ipilimumab in advanced melanoma'. In: *N Engl J Med* 369 (2013), pp. 122–133.

[55] K. C. Ohaegbulam, A. Assal, E. Lazar-Molnar, Y. Yao and X. Zang. 'Human cancer immunotherapy with antibodies to the PD-1 and PD-L1 pathway'. In: *Trends in molecular medicine* 21.1 (2015), pp. 24–33.

[56] G. K. Philips and M. Atkins. 'Therapeutic uses of anti-PD-1 and anti-PD-L1 antibodies'. In: *International immunology* 27.1 (2015), pp. 39–46.

[57] R. Dahan, E. Sega, J. Engelhardt, M. Selby, A. J. Korman and J. V. Ravetch. 'FcγRs modulate the anti-tumor activity of antibodies targeting the PD-1/PD-L1 axis'. In: *Cancer cell* 28.3 (2015), pp. 285–295.

[58] A. J. Giles, S. Hao, M. Padget, H. Song, W. Zhang, J. Lynes, V. Sanchez, Y. Liu, J. Jung, X. Cao, J. Lee and D. Park. 'Efficient ADCC killing of meningioma by avelumab and a high-affinity natural killer cell line, haNK'. In: *JCI insight* 4.20 (2019).

[59] R. Fujii, E. R. Friedman, J. Richards, K. Y. Tsang, C. R. Heery, J. Schlom and J. W. Hodge. 'Enhanced killing of chordoma cells by antibody-dependent cell-mediated cytotoxicity employing the novel anti-PD-L1 antibody avelumab'. In: *Oncotarget* 7.23 (2016), p. 33498.

[60] M. Fasano, C. M. Della Corte, R. Di Liello, G. Barra, F. Sparano, G. Viscardi, M. L. Iacovino, F. Paragliola, V. Famiglietti, V. Ciaramella, F. Cimmino, M. Capasso, A. Iolascon, V. Sforza, A. Morabito, E. Maiello, F. Ciardiello and F. Morgillo. 'Induction of natural killer antibody-dependent cell cytotoxicity and of clinical activity of cetuximab plus avelumab in non-small cell lung cancer'. In: *ESMO Open* 5.5 (2020), pp. 1–10. ISSN: 20597029.

[61] B. Boyerinas, C. Jochems, M. Fantini, C. R. Heery, J. L. Gulley, K. Y. Tsang and J. Schlom. 'Antibody-dependent cellular cytotoxicity activity of a novel anti–PD-L1 antibody avelumab (MSB0010718C) on human tumor cells'. In: *Cancer immunology research* 3.10 (2015), pp. 1148–1157.

[62] R. N. Donahue, L. M. Lepone, I. Grenga, C. Jochems, M. Fantini, R. A. Madan, C. R. Heery, J. L. Gulley and J. Schlom. 'Analyses of the peripheral immunome following multiple administrations of avelumab, a human IgG1 anti-PD-L1 monoclonal antibody'. In: *Journal for immunotherapy of cancer* 5.1 (2017), pp. 1–16.

[63] F. Erdmann, C. Spix, A. Katalinic, M. Christ, J. Folkerts, J. Hansmann, K. Kranzhöfer, B. Kunz, K. Manegold, A. Penzkofer and K. Treml. 'Krebs in Deutschland für 2017/2018'. In: (2021).

[64] C. Tournigand, T. André, E. Achille, G. Lledo, M. Flesh, D. Mery-Mignard, E. Quinaux, C. Couteau, M. Buyse, G. Ganem, B. Landi, P. Colin, C. Louvet and A. de Gramont. 'FOLFIRI followed by FOLFOX6 or the reverse sequence in advanced colorectal cancer: a randomized GERCOR study.' In: *Journal of Clinical Oncology* 22.2 (2004).

[65] W. Schmiegel, B. Buchberger, M. Follmann, U. Graeven, V. Heinemann, T. Langer, M. Nothacker, R. Porschen, C. Rödel, T. Rösch, W. Schmitt, S. Wesselmann and C. Pox. 'S3-leitlinie–kolorektales karzinom'. In: *Zeitschrift für Gastroenterologie* 55.12 (2017), pp. 1344–1498.

[66] A. Sobrero, S. Lonardi, G. Rosati, M. Di Bartolomeo, M. Ronzoni, N. Pella, M. Scartozzi, M. Banzi, M. G. Zampino, F. Pasini, P. Marchetti, A. Cantore and R. Labianca. 'FOLFOX or CAPOX in stage II to III colon cancer: efficacy results of the Italian three or six colon adjuvant trial'. In: *J Clin Oncol* 36.15 (2018), pp. 1478–1485.

[67] A. Falcone, S. Ricci, I. Brunetti, E. Pfanner, G. Allegrini, C. Barbara, L. Crinò, G. Benedetti, W. Evangelista, L. Fanchini, S. Vitello and G. Masi. 'Phase III trial of infusional fluorouracil, leucovorin, oxaliplatin, and irinotecan (FOLFOXIRI) compared with infusional fluorouracil, leucovorin, and irinotecan (FOLFIRI) as first-line treatment for metastatic colorectal cancer: the Gruppo Oncologico Nord Ovest'. In: *Journal of clinical oncology* 25.13 (2007), pp. 1670–1676.

[68] H. Hurwitz, L. Fehrenbacher, W. Novotny, T. Cartwright, J. Hainsworth, W. Heim, J. Berlin, A. Baron, S. Griffing, E. Holmgren, N. Ferrara and G. Fyfe. 'Bevacizumab plus irinotecan, fluorouracil, and leucovorin for metastatic colorectal cancer'. In: *New England journal of medicine* 350.23 (2004), pp. 2335–2342.

[69] F. Kabbinavar, H. I. Hurwitz, L. Fehrenbacher, N. J. Meropol, W. F. Novotny, G. Lieberman, S. Griffing and E. Bergsland. 'Phase II, randomized trial comparing bevacizumab plus fluorouracil (FU)/leucovorin (LV) with FU/LV alone in patients with metastatic colorectal cancer'. In: *Journal of clinical oncology* 21.1 (2003), pp. 60–65.

[70] F. F. Kabbinavar, H. I. Hurwitz, J. Yi, S. Sarkar and O. Rosen. 'Addition of bevacizumab to fluorouracil-based first-line treatment of metastatic colorectal cancer: pooled analysis of cohorts of older patients from two randomized clinical trials'. In: *Journal of Clinical Oncology* 27.2 (2009), pp. 199–205.

[71] B. J. Giantonio, P. J. Catalano, N. J. Meropol, P. J. O'Dwyer, E. P. Mitchell, S. R. Alberts, M. A. Schwartz and A. B. Benson III. 'Bevacizumab in combination with oxaliplatin, fluorouracil, and leucovorin (FOLFOX4) for previously treated metastatic colorectal cancer: results from the Eastern Cooperative Oncology Group Study E3200'. In: *Journal of clinical oncology* 25.12 (2007), pp. 1539–1544.

[72] D. Cunningham, I. Lang, E. Marcuello, V. Lorusso, J. Ocvirk, D. B. Shin, D. Jonker, S. Osborne, N. Andre, D. Waterkamp and M. Saunders. 'Bevacizumab plus capecitabine versus capecitabine alone in elderly patients with previously untreated metastatic colorectal cancer (AVEX): an open-label, randomised phase 3 trial'. In: *The lancet oncology* 14.11 (2013), pp. 1077–1085.

[73] R. Li, M. Liang, X. Liang, L. Yang, M. Su and K. P. Lai. 'Chemotherapeutic effectiveness of combining cetuximab for metastatic colorectal cancer treatment: A system review and meta-analysis'. In: *Frontiers in Oncology* 10.May (2020), pp. 1–10. ISSN: 2234943X.

[74] G. Fornasier, S. Francescon and P. Baldo. 'An update of efficacy and safety of cetuximab in metastatic colorectal cancer: a narrative review'. In: *Advances in therapy* 35.10 (2018), pp. 1497–1509.

[75] F. Di Nicolantonio, M. Martini, F. Molinari, A. Sartore Bianchi, S. Arena, P. Saletti, S. De Dosso, L. Mazzucchelli, M. Frattini, S. Siena and A. Bardelli. 'Wild-type BRAF is required for response to panitumumab or cetuximab in metastatic colorectal cancer'. In: (2008).

[76] M. Sorich, M. Wiese, A. Rowland, G. Kichenadasse, R. McKinnon and C. Karapetis. 'Extended RAS mutations and anti-EGFR monoclonal antibody survival benefit in metastatic colorectal cancer: a meta-analysis of randomized, controlled trials'. In: *Annals of Oncology* 26.1 (2015), pp. 13–21.

[77] F. Di Fiore, F. Blanchard, F. Charbonnier, F. Le Pessot, A. Lamy, M. Galais, L. Bastit, A. Killian, R. Sesboüé, J. Tuech, A. Queuniet, B. Paillot, J. Sabourin, F. Michot, P. Michel and T. Frebourg. 'Clinical relevance of KRAS mutation detection in metastatic colorectal cancer treated by Cetuximab plus chemotherapy'. In: *British journal of cancer* 96.8 (2007), pp. 1166–1169.

[78] A. Lievre, J.-B. Bachet, V. Boige, A. Cayre, D. Le Corre, E. Buc, M. Ychou, O. Bouché, B. Landi, C. Louvet, T. Andre and P. Laurent-Puig. 'KRAS mutations as an independent prognostic factor in patients with advanced colorectal cancer treated with cetuximab'. In: *Journal of clinical oncology* 26.3 (2008), pp. 374–379.

[79] V. Heinemann, F. Rivera, B. H. O'Neil, S. Stintzing, R. Koukakis, J.-H. Terwey and J.-Y. Douillard. 'A study-level meta-analysis of efficacy data from head-to-head first-line trials of epidermal growth factor receptor inhibitors versus bevacizumab in patients with RAS wild-type metastatic colorectal cancer'. In: *European journal of cancer* 67 (2016), pp. 11–20.

[80] B. Zheng, X. Wang, M. Wei, Q. Wang, J. Li, L. Bi, X. Deng and Z. Wang. 'First-line cetuximab versus bevacizumab for RAS and BRAF wild-type metastatic colorectal cancer: a systematic review and meta-analysis'. In: *BMC cancer* 19.1 (2019), pp. 1–12.

[81] V. Heinemann, L. F. von Weikersthal, T. Decker, A. Kiani, F. Kaiser, S.-E. Al-Batran, T. Heintges, C. Lerchenmüller, C. Kahl, G. Seipelt, S. Held and S. Stintzing. 'FOLFIRI plus cetuximab or bevacizumab for advanced colorectal cancer: final survival and per-protocol analysis of FIRE-3, a randomised clinical trial'. In: *British journal of cancer* 124.3 (2021), pp. 587–594.

[82] R. P. Marques, A. R. Godinho, P. Heudtlass, H. L. Pais, A. Quintela and A. P. Martins. 'Cetuximab versus bevacizumab in metastatic colorectal cancer: a comparative effectiveness study'. In: *Journal of Cancer Research and Clinical Oncology* 146.5 (2020), pp. 1321–1334.

[83] J. Tol, M. Koopman, A. Cats, C. J. Rodenburg, G. J. Creemers, J. G. Schrama, F. L. Erdkamp, A. H. Vos, C. J. van Groeningen, H. A. Sinnige, D. Richel, E. Voest and J. Punt. 'Chemotherapy, bevacizumab, and cetuximab in metastatic colorectal cancer'. In: *New England Journal of Medicine* 360.6 (2009), pp. 563–572.

[84] D. T. Le, P. Kavan, T. W. Kim, M. E. Burge, E. Van Cutsem, H. Hara, P. M. Boland, J.-L. Van Laethem, R. Geva, H. Taniguchi, L. Diaz and B. O'Neil. *KEYNOTE-164: Pembrolizumab for patients with advanced microsatellite instability high (MSI-H) colorectal cancer.* 2018.

[85] M. J. Overman, R. McDermott, J. L. Leach, S. Lonardi, H.-J. Lenz, M. A. Morse, J. Desai, A. Hill, M. Axelson, R. A. Moss, M. Goldberg and T. Andre. 'Nivolumab in patients with metastatic DNA mismatch repair-deficient or microsatellite instability-high colorectal cancer (CheckMate 142): an open-label, multicentre, phase 2 study'. In: *The lancet oncology* 18.9 (2017), pp. 1182–1191.

[86] M. J. Overman, S. Lonardi, K. Y. M. Wong, H.-J. Lenz, F. Gelsomino, M. Aglietta, M. A. Morse, E. Van Cutsem, R. McDermott, A. Hill, M. Sawyer and T. Andre. 'Durable clinical benefit with nivolumab plus ipilimumab in DNA mismatch repair-deficient/microsatellite instability-high metastatic colorectal cancer'. In: (2018).

[87] G. Kroemer, L. Galluzzi, O. Kepp and L. Zitvogel. 'Immunogenic cell death in cancer therapy'. In: *Annual review of immunology* 31 (2013), pp. 51–72.

[88] C. Pozzi, A. Cuomo, I. Spadoni, E. Magni, A. Silvola, A. Conte, S. Sigismund, P. S. Ravenda, T. Bonaldi, M. G. Zampino, C. Cancelliere and M. Rescigno. 'The EGFR-specific antibody cetuximab combined with chemotherapy triggers immunogenic cell death'. In: *Nature medicine* 22.6 (2016), pp. 624–631.

[89] S. Trivedi, R. M. Srivastava, F. Concha-Benavente, S. Ferrone, T. M. Garcia-Bates, J. Li and R. L. Ferris. 'Anti-EGFR targeted monoclonal antibody isotype influences antitumor cellular immunity in head and neck cancer patients'. In: *Clinical Cancer Research* 22.21 (2016), pp. 5229–5237.

[90] J. R. Groom and A. D. Luster. 'CXCR3 ligands: redundant, collaborative and antagonistic functions'. In: *Immunology and cell biology* 89.2 (2011), pp. 207–215.

[91] L. Holubec, J. Polivka, M. Safanda, M. Karas and V. Liska. 'The role of cetuximab in the induction of anticancer immune response in colorectal cancer treatment'. In: *Anticancer research* 36.9 (2016), pp. 4421–4426.

[92] S. C. Lee, R. M. Srivastava, A. López-Albaitero, S. Ferrone and R. L. Ferris. 'Natural killer (NK): dendritic cell (DC) cross talk induced by therapeutic monoclonal antibody triggers tumor antigen-specific T cell immunity'. In: *Immunologic research* 50.2 (2011), pp. 248–254.

[93] R. Bellucci, A. Martin, D. Bommarito, K. Wang, S. H. Hansen, G. J. Freeman and J. Ritz. 'Interferon-γ-induced activation of JAK1 and JAK2 suppresses tumor cell susceptibility to NK cells through upregulation of PD-L1 expression'. In: *Oncoimmunology* 4.6 (2015), e1008824.

[94] Y. Inoue, S. Hazama, N. Suzuki, Y. Tokumitsu, S. Kanekiyo, S. Tomochika, R. Tsunedomi, Y. Tokuhisa, M. Iida, K. Sakamoto, S. Takeda and H. Nagano. 'Cetuximab strongly enhances immune cell infiltration into liver metastatic sites in colorectal cancer'. In: *Cancer science* 108.3 (2017), pp. 455–460.

[95] H.-B. Jie, P. J. Schuler, S. C. Lee, R. M. Srivastava, A. Argiris, S. Ferrone, T. L. Whiteside and R. L. Ferris. 'CTLA-4+ regulatory T cells increased in cetuximab-treated head and neck cancer patients suppress NK cell cytotoxicity and correlate with poor prognosis'. In: *Cancer research* 75.11 (2015), pp. 2200–2210.

[96] H. Jie, N. Gildener-Leapman, J. Li, R. Srivastava, S. Gibson, T. Whiteside and R. Ferris. 'Intratumoral regulatory T cells upregulate immunosuppressive molecules in head and neck cancer patients'. In: *British journal of cancer* 109.10 (2013), pp. 2629–2635.

[97] J. L. Coombes, K. R. Siddiqui, C. V. Arancibia-Cárcamo, J. Hall, C.-M. Sun, Y. Belkaid and F. Powrie. 'A functionally specialized population of mucosal CD103+ DCs induces Foxp3+ regulatory T cells via a TGF-β–and retinoic acid–dependent mechanism'. In: *The Journal of experimental medicine* 204.8 (2007), pp. 1757–1764.

[98] F. Ghiringhelli, C. Ménard, M. Terme, C. Flament, J. Taieb, N. Chaput, P. E. Puig, S. Novault, B. Escudier, E. Vivier and L. Zitvogel. 'CD4+ CD25+ regulatory T cells inhibit natural killer cell functions in a transforming growth factor–β–dependent manner'. In: *The Journal of experimental medicine* 202.8 (2005), pp. 1075–1085.

[99] S. Ohki, M. Shibata, K. Gonda, T. Machida, T. Shimura, I. Nakamura, T. Ohtake, Y. Koyama, S. Suzuki, H. Ohto and S. Takenoshita. 'Circulating myeloid-derived suppressor cells are increased and correlate to immune suppression, inflammation and hypoproteinemia in patients with cancer'. In: *Oncology reports* 28.2 (2012), pp. 453–458.

[100] T. Oida, L. Xu, H. L. Weiner, A. Kitani and W. Strober. 'TGF-β-mediated suppression by CD4+ CD25+ T cells is facilitated by CTLA-4 signaling'. In: *The Journal of Immunology* 177.4 (2006), pp. 2331–2339.

[101] M. Terme, N. Chaput, B. Combadiere, A. Ma, T. Ohteki and L. Zitvogel. 'Regulatory T cells control dendritic cell/NK cell cross-talk in lymph nodes at the steady state by inhibiting CD4+ self-reactive T cells'. In: *The Journal of Immunology* 180.7 (2008), pp. 4679–4686.

[102] X. Chen, D. Fosco, D. E. Kline, L. Meng, S. Nishi, P. A. Savage and J. Kline. 'PD-1 regulates extrathymic regulatory T-cell differentiation'. In: *European journal of immunology* 44.9 (2014), pp. 2603–2616.

[103] K. Pogoda, M. Pyszniak, P. Rybojad and J. Tabarkiewicz. 'Monocytic myeloid-derived suppressor cells as a potent suppressor of tumor immunity in non-small cell lung cancer'. In: *Oncology Letters* 12.6 (2016), pp. 4785–4794.

[104] N. Eissler, Y. Mao, D. Brodin, P. Reuterswärd, H. Andersson Svahn, J. I. Johnsen, R. Kiessling and P. Kogner. 'Regulation of myeloid cells by activated T cells determines the efficacy of PD-1 blockade'. In: *Oncoimmunology* 5.12 (2016), e1232222.

[105] A. K. Singh, R. K. Arya, A. K. Trivedi, S. Sanyal, R. Baral, O. Dormond, D. M. Briscoe and D. Datta. 'Chemokine receptor trio: CXCR3, CXCR4 and CXCR7 crosstalk via CXCL11 and CXCL12'. In: *Cytokine & growth factor reviews* 24.1 (2013), pp. 41–49.

[106] Z. Andric, G. Gálffy, M. C. Dols, B. Szima, G. Stojanovic, M. Petrovic, E. F. Font, D. V. Baz, S. P. Aix, O. Juan-Vidal, Z. Szalai and F. Ciardiello. '103P First-line avelumab in combination with cetuximab and chemotherapy in patients with advanced squamous non-small cell lung cancer (NSCLC)'. In: *Journal of Thoracic Oncology* 16.4 (2021), S753–S754.

[107] S. Stintzing and V. Heinemann. 'FIRE-6 studie'. In: *Forum*. Vol. 34. 4. Springer. 2019, pp. 371–373.

[108] A. Madu, S. Ocheni, O. Ibegbulam, A. Chukwura and K. Madu. 'Comparison of absolute neutrophil to CD4 lymphocyte values as a marker of immunosuppression in cancer patients on cytotoxic chemotherapy'. In: *African Health Sciences* 15.2 (2015), pp. 581–589.

[109] E. C. T. Register. *Homepage*. Mar. 2022. URL: https://www.clinicaltrialsregister.eu.

[110] E. A. Eisenhauer, P. Therasse, J. Bogaerts, L. H. Schwartz, D. Sargent, R. Ford, J. Dancey, S. Arbuck, S. Gwyther, M. Mooney, L. Rubinstein, L. Shankar, L. Dodd, R. Kaplan, D. Lacombe and J. Verweij. 'New response evaluation criteria in solid tumours: Revised RECIST guideline (version 1.1)'. In: *European Journal of Cancer* 45.2 (2009), pp. 228–247. ISSN: 09598049.

[111] S. F. D. I. Lab. *RRID Portal*. Mar. 2022. URL: https://scicrunch.org/resources.

[112] J. H. Kerry S. Campbell. 'NK cell biology: An update and future directions'. In: *American Academy of Allergy, Asthma and Immunology* 132.3 (2013), pp. 536–544. ISSN: 1097-6825. arXiv: NIHMS150003.

[113] R. Kim. 'Cancer immunoediting: from immune surveillance to immune escape'. In: *Cancer Immunotherapy* (2007), pp. 9–27.

[114] H. Ghadially, L. Brown, C. Lloyd, L. Lewis, A. Lewis, J. Dillon, R. Sainson, J. Jovanovic, N. J. Tigue, D. Bannister, L. Bamber, V. Valge-Archer and R. W. Wilkinson. 'MHC class i chain-related protein A and B (MICA and MICB) are predominantly expressed intracellularly in tumour and normal tissue'. In: *British Journal of Cancer* 116.9 (2017), pp. 1208–1217. ISSN: 15321827.

[115] S. Xing and L. Ferrari de Andrade. 'NKG2D and MICA/B shedding: a 'tag game' between NK cells and malignant cells'. In: *Clinical and Translational Immunology* 9.12 (2020), pp. 1–10. ISSN: 20500068.

[116] A. Maniar, X. Zhang, W. Lin, B. R. Gastman, C. D. Pauza, S. E. Strome and A. I. Chapoval. 'Human $\gamma\delta$ T lymphocytes induce robust NK cell-mediated antitumor cytotoxicity through CD137 engagement'. In: *Blood* 116.10 (2010), pp. 1726–1733. ISSN: 15280020.

[117] L. Vidard, C. Dureuil, J. Baudhuin, L. Vescovi, L. Durand, V. Sierra and E. Parmantier. 'CD137 (4-1BB) Engagement Fine-Tunes Synergistic IL-15– and IL-21–Driven NK Cell Proliferation'. In: *The Journal of Immunology* 203.3 (2019), pp. 676–685. ISSN: 0022-1767.

[118] W. Li, Z. Zhu, W. Chen, Y. Feng and D. S. Dimitrov. 'Crystallizable fragment glycoengineering for therapeutic antibodies development'. In: *Frontiers in Immunology* 8.NOV (2017). ISSN: 16643224.

[119] B. K. Choi, Y. H. Kim, C. H. Kim, M. S. Kim, K. H. Kim, H. S. Oh, M. J. Lee, D. K. Lee, D. S. Vinay and B. S. Kwon. 'Peripheral 4-1BB Signaling Negatively Regulates NK Cell Development through IFN-γ'. In: *The Journal of Immunology* 185.3 (2010), pp. 1404–1411. ISSN: 0022-1767.

[120] S. sadat Navabi, M. Doroudchi, A. H. Tashnizi and M. Habibagahi. 'Natural Killer Cell Functional Activity After 4-1BB Costimulation'. In: *Inflammation* 38.3 (2015), pp. 1181–1190. ISSN: 15732576.

[121] Q. Wang, P. Zhang, Q. Zhang, X. Wang, J. Li, C. Ma, W. Sun and L. Zhang. 'Analysis of CD137 and CD137L expression in human primary tumor tissues'. In: *Croatian medical journal* 49.2 (2008), pp. 192–200.

[122] G. GmbH. *Homepage*. Mar. 2022. URL: https://www.glycotope.com.

[123] A. Tamm and R. E. Schmidt. 'The binding epitopes of human CD16 (Fc gamma RIII) monoclonal antibodies. Implications for ligand binding.' In: *Journal of immunology (Baltimore, Md. : 1950)* 157.4 (1996), pp. 1576–15781. ISSN: 0022-1767.

[124] S. Böttcher, M. Ritgen, M. Brüggemann, T. Raff, S. Lüschen, A. Humpe, M. Kneba and C. Pott. 'Flow cytometric assay for determination of FcγRIIIA-158 V/F polymorphism'. In: *Journal of Immunological Methods* 306.1-2 (2005), pp. 128–136. ISSN: 00221759.

[125] R Core Team. *R: A Language and Environment for Statistical Computing*. R Foundation for Statistical Computing. Vienna, Austria, 2020.

[126] RStudio Team. *RStudio: Integrated Development Environment for R*. RStudio, Inc. Boston, MA, 2019.

[127] T. Ara. *brunnermunzel: (Permuted) Brunner-Munzel Test*. R package version 1.4.1. 2020.

[128] M. Kuhn. *caret: Classification and Regression Training*. R package version 6.0-90. 2021.

[129] Z. Gu, R. Eils and M. Schlesner. 'Complex heatmaps reveal patterns and correlations in multidimensional genomic data'. In: *Bioinformatics* (2016).

[130] C. O. Wilke. *cowplot: Streamlined Plot Theme and Plot Annotations for 'ggplot2'*. R package version 1.1.1. 2020.

[131] H. Wickham, R. François, L. Henry and K. Müller. *dplyr: A Grammar of Data Manipulation*. R package version 1.0.8. 2022.

[132] K. Blighe, S. Rana and M. Lewis. *EnhancedVolcano: Publication-ready volcano plots with enhanced colouring and labeling*. R package version 1.12.0. 2021.

[133] J. Faraway. *faraway: Functions and Datasets for Books by Julian Faraway*. R package version 1.0.7. 2016.

[134] M. W. Beck. *ggord: Ordination Plots with ggplot2*. R package version 1.1.6. 2021.

[135] H. Wickham. *ggplot2: Elegant Graphics for Data Analysis*. Springer-Verlag New York, 2016. ISBN: 978-3-319-24277-4.

[136] C. Weihs, U. Ligges, K. Luebke and N. Raabe. 'klaR Analyzing German Business Cycles'. In: *Data Analysis and Decision Support*. Ed. by D. Baier, R. Decker and L. Schmidt-Thieme. Berlin: Springer-Verlag, 2005, pp. 335–343.

[137] D. Bates, M. Mächler, B. Bolker and S. Walker. 'Fitting Linear Mixed-Effects Models Using lme4'. In: *Journal of Statistical Software* 67.1 (2015), pp. 1–48.

[138] A. Kuznetsova, P. B. Brockhoff and R. H. B. Christensen. 'lmerTest Package: Tests in Linear Mixed Effects Models'. In: *Journal of Statistical Software* 82.13 (2017), pp. 1–26.

[139] J. Ooms. *magick: Advanced Graphics and Image-Processing in R*. R package version 2.7.3. 2021.

[140] S. M. Bache and H. Wickham. *magrittr: A Forward-Pipe Operator for R*. R package version 2.0.2. 2022.

[141] C. Strobl, A.-L. Boulesteix, T. Kneib, T. Augustin and A. Zeileis. 'Conditional Variable Importance for Random Forests'. In: *BMC Bioinformatics* 9.307 (2008).

[142] K. Müller and H. Wickham. *tibble: Simple Data Frames*. R package version 3.1.6. 2021.

[143] H. Wickham and M. Girlich. *tidyr: Tidy Messy Data*. R package version 1.2.0. 2022.

[144] H. Wickham, M. Averick, J. Bryan, W. Chang, L. D. McGowan, R. François, G. Grolemund, A. Hayes, L. Henry, J. Hester, M. Kuhn, T. L. Pedersen, E. Miller, S. M. Bache, K. Müller, J. Ooms, D. Robinson, D. P. Seidel, V. Spinu, K. Takahashi, D. Vaughan, C. Wilke, K. Woo and H. Yutani. 'Welcome to the tidyverse'. In: *Journal of Open Source Software* 4.43 (2019), p. 1686.

[145] J. H. Krijthe. *Rtsne: T-Distributed Stochastic Neighbor Embedding using Barnes-Hut Implementation*. R package version 0.15. 2015.

[146] M. Hervé. *RVAideMemoire: Testing and Plotting Procedures for Biostatistics*. R package version 0.9-81. 2021.

[147] B. Lab. *BioRender*. June 2022. URL: https://biorender.com.

[148] J. D. Mellor, M. P. Brown, H. R. Irving, J. R. Zalcberg and A. Dobrovic. 'A critical review of the role of Fc gamma receptor polymorphisms in the response to monoclonal antibodies in cancer'. In: *Journal of Hematology and Oncology* 6.1 (2013), pp. 1–10. ISSN: 17568722.

[149] L. Hosking, S. Lumsden, K. Lewis, A. Yeo, L. McCarthy, A. Bansal, J. Riley, I. Purvis and C.-F. Xu. 'Detection of genotyping errors by Hardy–Weinberg equilibrium testing'. In: *European Journal of Human Genetics* 12.5 (2004), pp. 395–399.

[150] T. Lehrnbecher, C. B. Foster, S. Zhu, S. F. Leitman, L. R. Goldin, K. Huppi and S. J. Chanock. 'Variant genotypes of the low-affinity Fcγ receptors in two control populations and a review of low-affinity Fcγ receptor polymorphisms in control and disease populations'. In: *Blood* 94.12 (1999), pp. 4220–4232. ISSN: 00064971.

[151] W.-L. van der Pol, M. D. Jansen, W. J. Sluiter, B. van de Sluis, F. G. J. Leppers-van de Straat, T. Kobayashi, R. G. J. Westendorp, T. W. J. Huizinga and J. G. J. van de Winkel. 'Evidence for non-random distribution of Fcγ receptor genotype combinations'. In: *Immunogenetics* 55.4 (July 2003), pp. 240–246. ISSN: 0093-7711.

[152] S. Sheather. *A modern approach to regression with R*. Springer Science & Business Media, 2009.

[153] Y. Dodge. *The concise encyclopedia of statistics*. Springer Science & Business Media, 2008.

[154] B. S. Everitt and A. Skrondal. 'The Cambridge dictionary of statistics'. In: (2010).

[155] K. Azuma, K. Ota, A. Kawahara, S. Hattori, E. Iwama, T. Harada, K. Matsumoto, K. Takayama, S. Takamori, M. Kage, T. Hoshino, Y. Nakanishi and I. Okamoto. 'Association of PD-L1 overexpression with activating EGFR mutations in surgically resected nonsmall-cell lung cancer'. In: *Annals of Oncology* 25.10 (2014), pp. 1935–1940. ISSN: 15698041.

[156] S. Peng, R. Wang, X. Zhang, Y. Ma, L. Zhong, K. Li, A. Nishiyama, S. Arai, S. Yano and W. Wang. 'EGFR-TKI resistance promotes immune escape in lung cancer via increased PD-L1 expression'. In: *Molecular Cancer* 18.1 (2019), pp. 1–14. ISSN: 14764598.

[157] A. J. Schoenfeld, H. Rizvi, C. Bandlamudi, J. L. Sauter, W. D. Travis, N. Rekhtman, A. J. Plodkowski, R. Perez-Johnston, P. Sawan, A. Beras, J. V. Egger, M. Ladanyi, K. C. Arbour, C. M. Rudin, G. J. Riely, B. S. Taylor, M. T. Donoghue and M. D. Hellmann. 'Clinical and molecular correlates of PD-L1 expression in patients with lung adenocarcinomas'. In: *Annals of Oncology* 31.5 (2020), pp. 599–608. ISSN: 15698041.

[158] J. A. Bowles and G. J. Weiner. 'CD16 polymorphisms and NK activation induced by monoclonal antibody-coated target cells'. In: *Journal of Immunological Methods* 304.1-2 (2005), pp. 88–99. ISSN: 00221759.

[159] N. Congy-Jolivet, A. Bolzec, D. Ternant, M. Ohresser, H. Watier and G. Thibault. 'FcγRIIIa expression is not increased on natural killer cells expressing the FcγRIIIa-158V allotype'. In: *Cancer Research* 68.4 (2008), pp. 976–980. ISSN: 00085472.

[160] S. G. Luke. 'Evaluating significance in linear mixed-effects models in R'. In: *Behavior Research Methods* 49.4 (2017), pp. 1494–1502. ISSN: 15543528.

[161] R. Bender and S. Lange. 'Adjusting for multiple testing - When and how?' In: *Journal of Clinical Epidemiology* 54.4 (2001), pp. 343–349. ISSN: 08954356.

[162] T. V. Perneger. 'What's wrong with Bonferroni adjustments'. In: *Bmj* 316.7139 (1998), pp. 1236–1238.

[163] P. Bauer. 'Multiple testing in clinical trials'. In: *Statistics in medicine* 10.6 (1991), pp. 871–890.

[164] D. A. Savitz and A. F. Olshan. 'Describing data requires no adjustment for multiple comparisons: a reply from Savitz and Olshan'. In: *American Journal of Epidemiology* 147.9 (1998), pp. 813–814.

[165] H. M. Dijstelbloem, C. G. Kallenberg and J. G. Van De Winkel. 'Inflammation in autoimmunity: Receptors for IgG revisited'. In: *Trends in Immunology* 22.9 (2001), pp. 510–516. ISSN: 14714906.

[166] J. C. Edberg, C. D. Langefeld, J. Wu, K. L. Moser, K. M. Kaufman, J. Kelly, V. Bansal, W. M. Brown, J. E. Salmon, S. S. Rich, J. B. Harley and R. P. Kimberly. 'Genetic linkage and association of Fcγ receptor IIIA (CD16A) on chromosome 1q23 with human systemic lupus erythematosus'. In: *Arthritis and Rheumatism* 46.8 (2002), pp. 2132–2140. ISSN: 00043591.

[167] K. Sullivan, A. Jawad, L. Piliero, N. Kim, X. Luan, D. Goldman and M. Petri. 'Analysis of polymorphisms affecting immune complex handling in systemic lupus erythematosus'. In: *Rheumatology* 42.3 (2003), pp. 446–452.

[168] M. D. Carcao, V. S. Blanchette, C. D. Wakefield, D. Stephens, J. Ellis, K. Matheson and G. A. Denomme. 'Fcγ receptor IIa and IIIa polymorphisms in childhood immune thrombocytopenic purpura'. In: *British journal of haematology* 120.1 (2003), pp. 135–141.

[169] B. Z. Alizadeh, G. Valdigem, M. J. Coenen, A. Zhernakova, B. Franke, A. Monsuur, P. L. Van riel, P. Barrera, T. R. Radstake, B. O. Roep, C. Wijmenga and B. P. Koeleman. 'Association analysis of functional variants of the FcgRIIa and FcgRIIIa genes with type 1 diabetes, celiac disease and rheumatoid arthritis'. In: *Human Molecular Genetics* 16.21 (2007), pp. 2552–2559. ISSN: 09646906.

[170] X. Li, A. W. Gibson and R. P. Kimberly. 'Human FcR polymorphism and disease'. In: *Fc Receptors* (2014), pp. 275–302.

[171] N. Sugita, K. Yamamoto, T. Kobayashi, W. L. Van Der Pol, T. Horigome, H. Yoshie, J. G. J. Van De Winkel and K. Hara. 'Relevance of FcγRIIIa-158V-F polymorphism to recurrence of adult periodontitis in Japanese patients'. In: *Clinical and Experimental Immunology* 117.2 (Dec. 2001), pp. 350–354. ISSN: 0009-9104.

[172] R. J. Pleass and J. M. Woof. 'Fc receptors and immunity to parasites'. In: *Trends in parasitology* 17.11 (2001), pp. 545–551.

[173] R. A. Clynes, T. L. Towers, L. G. Presta and J. V. Ravetch. 'Inhibitory Fc receptors modulate in vivo cytoxicity against tumor targets'. In: *Nature medicine* 6.4 (2000), pp. 443–446.

[174] S. Treon, M. Hansen, A. Branagan, C. Emmanouilides, E. Kimby, S. Frankel, N. Touroutoglou, D. Maloney, K. Anderson and E. Fox. 'Polymorphisms in FcγRIIIA (CD16) receptor expression are associated with clinical response to rituximab in Waldenstrom's macroglobulinemia'. In: *Journal of Clinical Oncology* 22.14_suppl (2004), pp. 6556–6556.

[175] E. Louis, Z. El Ghoul, S. Vermeire, S. Dall'Ozzo, P. Rutgeerts, G. Paintaud, J. Belaiche, M. De Vos, A. Van Gossum, J.-F. Colombel and H. Watier. 'Association between polymorphism in IgG Fc receptor IIIa coding gene and biological response to infliximab in Crohn's disease'. In: *Alimentary pharmacology & therapeutics* 19.5 (2004), pp. 511–519.

[176] W.-K. Weng, D. Czerwinski, J. Timmerman, F. J. Hsu and R. Levy. 'Clinical Outcome of Lymphoma Patients After Idiotype Vaccination Is Correlated With Humoral Immune Response and Immunoglobulin G Fc Receptor Genotype'. In: *Journal of Clinical Oncology* 22.23 (2004), pp. 4717–4724. ISSN: 0732-183X.

[177] M. Hirvinen, R. Heiskanen, M. Oksanen, S. Pesonen, I. Liikanen, T. Joensuu, A. Kanerva, V. Cerullo and A. Hemminki. 'Fc-gamma receptor polymorphisms as predictive and prognostic factors in patients receiving oncolytic adenovirus treatment'. In: *Journal of Translational Medicine* 11.1 (2013), pp. 1–12. ISSN: 14795876.

[178] E. Hatjiharissi, L. Xu, D. D. Santos, Z. R. Hunter, B. T. Ciccarelli, S. Verselis, M. Modica, Y. Cao, R. J. Manning, X. Leleu, E. A. Dimmock, A. Kortsaris, C. Mitsiades, K. C. Anderson, E. A. Fox and S. P. Treon. 'Increased natural killer cell expression of CD16, augmented binding and ADCC activity to rituximab among individuals expressing the FcγRIIIa-158 V/V and V/F polymorphism'. In: *Blood* 110.7 (2007), pp. 2561–2564. ISSN: 00064971.

[179] W. Oboshi, T. Watanabe, Y. Matsuyama, A. Kobara, N. Yukimasa, I. Ueno, K. Aki, T. Tada and E. Hosoi. 'The influence of NK cell-mediated ADCC: Structure and expression of the CD16 molecule differ among FcγRIIIa-V158F genotypes in healthy Japanese subjects'. In: *Human Immunology* 77.2 (2016), pp. 165–171. ISSN: 18791166.

[180] E. Hatjiharissi, D. D. Santos, L. Xu, S. Verselis, M. Modica, X. Leleu, Z. Hunter, A. W. Ho, R. Manning, C. Patterson, K. Anderson, E. Fox and S. Treon. *Individuals Expressing FcγRIIIA-158 V/V and V/F Show Increased NK Cell Surface Expression of FcgRIIIA (CD16), Rituximab Binding, and Demonstrate Higher Levels of ADCC Activity in Response to Rituximab.* 2005.

[181] K. Kimura, D. Kobayashi, S. Hatoyama, M. Yamamoto, R. Takayanagi and Y. Yamada. 'Effects of FCGRIII a-158V/F polymorphism on antibody-dependent cellular cytotoxicity activity of adalimumab'. In: *Apmis* 125.12 (2017), pp. 1102–1107.

[182] Y. Seo, Y. Ishii, H. Ochiai, K. Fukuda, S. Akimoto, T. Hayashida, K. Okabayashi, M. Tsuruta, H. Hasegawa and Y. Kitagawa. 'Cetuximab-mediated ADCC activity is correlated with the cell surface expression level of EGFR but not with the KRAS/BRAF mutational status in colorectal cancer'. In: *Oncology Reports* 31.5 (2014), pp. 2115–2122. ISSN: 17912431.

[183] Y. Kawaguchi, K. Kono, K. Mimura, H. Sugai, H. Akaike and H. Fujii. 'Cetuximab induce antibody-dependent cellular cytotoxicity against EGFR-expressing esophageal squamous cell carcinoma'. In: *International Journal of Cancer* 120.4 (2007), pp. 781–787. ISSN: 00207136.

[184] S. Q. Ashraf, A. M. Nicholls, J. L. Wilding, T. G. Ntouroupi, N. J. Mortensen and W. F. Bodmer. 'Direct and immune mediated antibody targeting of ERBB receptors in a colorectal cancer cell-line panel'. In: *Proceedings of the National Academy of Sciences of the United States of America* 109.51 (2012), pp. 21046–21051. ISSN: 00278424.

[185] P. Correale, M. Marra, C. Remondo, C. Migali, G. Misso, F. P. Arcuri, M. T. Del Vecchio, A. Carducci, L. Loiacono, P. Tassone, A. Abbruzzese, P. Tagliaferri and M. Caraglia. 'Cytotoxic drugs up-regulate epidermal growth factor receptor (EGFR) expression in colon cancer cells and enhance their susceptibility to EGFR-targeted antibody-dependent cell-mediated-cytotoxicity (ADCC)'. In: *European Journal of Cancer* 46.9 (2010), pp. 1703–1711. ISSN: 09598049.

[186] R. Rosa, F. Monteleone, N. Zambrano and R. Bianco. 'In Vitro and In Vivo Models for Analysis of Resistance to Anticancer Molecular Therapies'. In: *Current Medicinal Chemistry* 21.14 (2014), pp. 1595–1606. ISSN: 09298673.

[187] J. Kato, M. Futamura, M. Kanematsu, S. Gaowa, R. Mori, T. Tanahashi, N. Matsuhashi and K. Yoshida. 'Combination therapy with zoledronic acid and cetuximab effectively suppresses growth of colorectal cancer cells regardless of KRAS status'. In: *International journal of cancer* 138.6 (2016), pp. 1516–1527.

[188] R. J. Taylor, V. Saloura, A. Jain, O. Goloubeva, S. Wong, S. Kronsberg, M. Nagilla, L. Silpino, J. De Souza, T. Seiwert, E. Vokes, V. Villaflor and E. E. Cohen. 'Ex vivo antibody-dependent cellular cytotoxicity inducibility predicts efficacy of cetuximab'. In: *Cancer Immunology Research* 3.5 (2015), pp. 567–574. ISSN: 23266074.

[189] S. Khanna, A. Thomas, D. Abate-Daga, J. Zhang, B. Morrow, S. M. Steinberg, A. Orlandi, P. Ferroni, J. Schlom, F. Guadagni and R. Hassan. 'Malignant mesothelioma effusions are infiltrated by CD3+ T cells highly expressing PD-L1 and the PD-L1+ tumor cells within these effusions are susceptible to ADCC by the anti-PD-L1 antibody avelumab'. In: *Journal of Thoracic Oncology* 11.11 (2016), pp. 1993–2005. ISSN: 15561380.

[190] C. Jochems, J. W. Hodge, M. Fantini, K. Y. Tsang, A. J. Vandeveer, J. L. Gulley and J. Schlom. 'ADCC employing an NK cell line (haNK) expressing the high affinity CD16 allele with avelumab, an anti-PD-L1 antibody'. In: *International Journal of Cancer* 141.3 (2017), pp. 583–593. ISSN: 10970215.

[191] J. E. Park, S. E. Kim, B. Keam, H. R. Park, S. Kim, M. Kim, T. M. Kim, J. Doh, D. W. Kim and D. S. Heo. 'Anti-tumor effects of NK cells and anti-PD-L1 antibody with antibody-dependent cellular cytotoxicity in PD-L1-positive cancer cell lines'. In: *Journal for immunotherapy of cancer* 8.2 (2020), pp. 1–11. ISSN: 20511426.

[192] N. Chen, W. Fang, J. Zhan, S. Hong, Y. Tang, S. Kang, Y. Zhang, X. He, T. Zhou, T. Qin, Y. Huang, X. Yi and L. Zhang. 'Upregulation of PD-L1 by EGFR activation mediates the immune escape in EGFR-driven NSCLC: Implication for optional immune targeted therapy for NSCLC patients with EGFR mutation'. In: *Journal of Thoracic Oncology* 10.6 (2015), pp. 910–923. ISSN: 15561380.

[193] E. A. Akbay, S. Koyama, J. Carretero, A. Altabef, J. H. Tchaicha, C. L. Christensen, O. R. Mikse, A. D. Cherniack, E. M. Beauchamp, T. J. Pugh, M. D. Wilkerson, P. E. Fecci, M. Butaney, J. B. Reibel, M. Soucheray, T. J. Cohoon, P. A. Janne, M. Meyerson, D. Neil Hayes, G. I. Shapiro, T. Shimamura, L. M. Sholl, S. J. Rodig, G. J. Freeman, P. S. Hammerman, G. Dranoff and K. K. Wong. 'Activation of the PD-1 pathway contributes to immune escape in EGFR-driven lung tumors'. In: *Cancer Discovery* 3.12 (2013), pp. 1355–1363. ISSN: 21598274.

[194] Y. M. Lin, W. W. Sung, M. J. Hsieh, S. C. Tsai, H. W. Lai, S. M. Yang, K. H. Shen, M. K. Chen, H. Lee, K. T. Yeh and C. J. Chen. 'High PD-L1 expression correlates with metastasis and poor prognosis in oral squamous cell carcinoma'. In: *PLoS ONE* 10.11 (2015), pp. 1–11. ISSN: 19326203.

[195] C.-W. Li, S.-O. Lim, E. M. Chung, Y.-S. Kim, A. H. Park, J. Yao, J.-H. Cha, W. Xia, L.-C. Chan, T. Kim, S.-S. Chang, H.-H. Lee, C.-K. Chou, Y.-L. Liu, H.-C. Yeh, E. Perillo, A. Dunn, C.-W. kuo and M.-C. Hung. 'Eradication of triple-negative breast cancer cells by targeting glycosylated PD-L1'. In: *Cancer cell* 33.2 (2018), pp. 187–201.

[196] C.-W. Li, S.-O. Lim, W. Xia, H.-H. Lee, L.-C. Chan, C.-W. Kuo, K.-H. Khoo, S.-S. Chang, J.-H. Cha, T. Kim and M.-C. Hung. 'Glycosylation and stabilization of programmed death ligand-1 suppresses T-cell activity'. In: *Nature communications* 7.1 (2016), pp. 1–11.

[197] D. S. Vinay and B. S. Kwon. 'Role of 4-1BB in immune responses'. In: *Seminars in immunology*. Vol. 10. 6. Elsevier. 1998, pp. 481–489.

[198] D. Laderach, A. Wesa and A. Galy. '4-1BB-ligand is regulated on human dendritic cells and induces the production of IL-12'. In: *Cellular immunology* 226.1 (2003), pp. 37–44.

[199] T. Grimmig, M. Gasser, R. Moench, L. J. Zhu, K. Nawalaniec, S. Callies, M. Wagner, B. Polat, S. S. Mothi, Y. Luo, C. M. Ribas, O. Malafaia, L. L. Hsiao and A. M. Waaga-Gasser. 'Expression of Tumor-mediated CD137 ligand in human colon cancer indicates dual signaling effects'. In: *OncoImmunology* 8.12 (2019). ISSN: 2162402X.

[200] C. Cordon-Cardo, Z. Fuks, M. Drobnjak, C. Moreno, L. Eisenbach and M. Feldman. 'Expression of HLA-A, B, C antigens on primary and metastatic tumor cell populations of human carcinomas'. In: *Cancer research* 51.23 Part 1 (1991), pp. 6372–6380.

[201] P. Möller and G. Hämmerling. 'The role of surface HLA-A, B, C molecules in tumour immunity.' In: *Cancer surveys* 13 (1992), pp. 101–127.

[202] W. Wang, A. K. Erbe, J. A. Hank, Z. S. Morris and P. M. Sondel. 'NK cell-mediated antibody-dependent cellular cytotoxicity in cancer immunotherapy'. In: *Frontiers in Immunology* 6.JUL (2015). ISSN: 16643224.

[203] H.-G. Ljunggren and K. Kärre. 'In search of the 'missing self': MHC molecules and NK cell recognition'. In: *Encyclopedia of Genetics, Genomics, Proteomics and Informatics* 11.7 (2008), pp. 1225–1225.

[204] M. Draghi, N. Yawata, M. Gleimer, M. Yawata, N. M. Valiante and P. Parham. 'Single-cell analysis of the human NK cell response to missing self and its inhibition by HLA class I'. In: *Blood* 105.5 (2005), pp. 2028–2035. ISSN: 00064971.

[205] P. Parham. 'MHC class I molecules and KIRS in human history, health and survival'. In: *Nature Reviews Immunology* 5.3 (2005), pp. 201–214. ISSN: 14741733.

[206] M. Broussas, L. Broyer and L. Goetsch. 'Evaluation of antibody-dependent cell cytotoxicity using lactate dehydrogenase (LDH) measurement'. In: *Glycosylation Engineering of Biopharmaceuticals*. Springer, 2013, pp. 305–317.

[207] K. T. Brunner, J. Mauel, J. C. Cerottini and B. Chapuis. 'Quantitative assay of the lytic action of immune lymphoid cells on 51-Cr-labelled allogeneic target cells in vitro; inhibition by isoantibody and by drugs.' In: *Immunology* 14.2 (1968), pp. 181–96. ISSN: 0019-2805.

[208] V. R. Simhadri, M. Dimitrova, J. L. Mariano, O. Zenarruzabeitia, W. Zhong, T. Ozawa, A. Muraguchi, H. Kishi, M. C. Eichelberger and F. Borrego. 'A human anti-M2 antibody mediates antibody-dependent cell-mediated cytotoxicity (ADCC) and cytokine secretion by resting and cytokine-preactivated natural killer (NK) cells'. In: *PLoS One* 10.4 (2015), e0124677.

[209] E. Decaup, C. Rossi, P. Gravelle, C. Laurent, J. Bordenave, M. Tosolini, A. Tourette, E. Perrial, C. Dumontet, M. Poupot, C. Klein, A. Savina, J.-J. Fournie and C. Bezombes. 'A tridimensional model for NK cell-mediated ADCC of follicular lymphoma'. In: *Frontiers in Immunology* (2019), p. 1943.

[210] K. Godoy-Ramirez, K. Franck and H. Gaines. 'A novel method for the simultaneous assessment of natural killer cell conjugate formation and cytotoxicity at the single-cell level by multi-parameter flow cytometry'. In: *Journal of immunological methods* 239.1-2 (2000), pp. 35–44.

[211] M. Yamashita, S. Kitano, H. Aikawa, A. Kuchiba, M. Hayashi, N. Yamamoto, K. Tamura and A. Hamada. 'A novel method for evaluating antibody-dependent cell-mediated cytotoxicity by flowcytometry using cryopreserved human peripheral blood mononuclear cells'. In: *Scientific Reports* 6.August 2015 (2016), pp. 1–10. ISSN: 20452322.

[212] I. Jedema, N. M. Van Der Werff, R. M. Barge, R. Willemze and J. H. Falkenburg. 'New CFSE-based assay to determine susceptibility to lysis by cytotoxic T cells of leukemic precursor cells within a heterogeneous target cell population'. In: *Blood* 103.7 (2004), pp. 2677–2682. ISSN: 00064971.

[213] M. A. Gillissen, E. Yasuda, G. de Jong, S. E. Levie, D. Go, H. Spits, P. M. van Helden and M. D. Hazenberg. 'The modified FACS calcein AM retention assay: A high throughput flow cytometer based method to measure cytotoxicity'. In: *Journal of Immunological Methods* 434 (2016), pp. 16–23. ISSN: 18727905.

[214] J. Zhou, R. Zhong and E. D. Ball. *Regulation of Bcl-2 family proteins in antibody-dependent cellular cytotoxicity (ADCC) of small cell lung cancer cells mediated by a bispecific molecule OKT3xbombesin antagonist*. 2005.

[215] N. Hertoghs, K. V. Schwedhelm, K. D. Stuart, M. J. McElrath and S. C. De Rosa. 'OMIP-064: a 27-color flow cytometry panel to detect and characterize human NK cells and other innate lymphoid cell subsets, MAIT cells, and $\gamma\delta$ T cells'. In: *Cytometry Part A* 97.10 (2020), pp. 1019–1023.

[216] S. Vanikova, A. Koladiya and J. Musil. 'OMIP-080: 29-Color flow cytometry panel for comprehensive evaluation of NK and T cells reconstitution after hematopoietic stem cells transplantation'. In: *Cytometry Part A* 101.1 (2022), pp. 21–26.

[217] Y. D. Mahnke, M. H. Beddall and M. Roederer. 'OMIP-029: Human NK-cell phenotypization'. In: *Cytom Part A* 87 (2015), pp. 986–988.

[218] A. M. Trotta, A. Ottaiano, C. Romano, G. Nasti, A. Nappi, C. De Divitiis, M. Napolitano, S. Zanotta, R. Casaretti, C. D'Alterio, A. Avallone, D. Califano, R. V. Iaffaioli and S. Scala. 'Prospective evaluation of cetuximab-mediated antibody-dependent cell cytotoxicity in metastatic colorectal cancer patients predicts treatment efficacy'. In: *Cancer Immunology Research* 4.4 (2016), pp. 366–374. ISSN: 23266074.

[219] R. Fujii, J. Schlom and J. W. Hodge. 'A potential therapy for chordoma via antibody-dependent cell-mediated cytotoxicity employing NK or high-affinity NK cells in combination with cetuximab'. In: *Journal of neurosurgery* 128.5 (2017), pp. 1419–1427.

[220] J.-E. Park, S.-E. Kim, B. Keam, H.-R. Park, S. Kim, M. Kim, T. M. Kim, J. Doh, D.-W. Kim and D. S. Heo. 'Anti-tumor effects of NK cells and anti-PD-L1 antibody with antibody-dependent cellular cytotoxicity in PD-L1-positive cancer cell lines'. In: *Journal for immunotherapy of cancer* 8.2 (2020).

[221] A. Akhter, R. M. Faridi, G. Tripathi, P. Dharmani-Khan, D. Stewart, A. Mansoor and F. Khan. 'P027 FCGRIIIA gene variant influences differential rituximab mediated NK cell response against different B-cell lymphoma targets'. In: *Human Immunology* 78 (2017), p. 72.

[222] R. Moroi, K. Endo, Y. Kinouchi, H. Shiga, Y. Kakuta, M. Kuroha, Y. Kanazawa, Y. Shimodaira, T. Horiuchi, S. Takahashi and T. Shimosegawa. 'FCGR3A-158 polymorphism influences the biological response to infliximab in Crohn's disease through affecting the ADCC activity'. In: *Immunogenetics* 65.4 (2013), pp. 265–271.

[223] F. Bibeau, E. Lopez-Crapez, F. D. Fiore, S. Thezenas, M. Ychou, F. Blanchard, A. Lamy, F. Penault-Llorca, T. Frébourg, P. Michel, J. C. Sabourin and F. Boissière-Michot. 'Impact of fcγRIIa-fcγRIIIa polymorphisms and KRAS mutations on the clinical outcome of patients with metastatic colorectal cancer treated with cetuximab plus irinotecan'. In: *Journal of Clinical Oncology* 27.7 (2009), pp. 1122–1129. ISSN: 0732183X.

[224] J. Rodríguez, R. Zarate, E. Bandres, V. Boni, A. Hernández, J. J. Sola, B. Honorato, N. Bitarte and J. García-Foncillas. 'Fc gamma receptor polymorphisms as predictive markers of Cetuximab efficacy in epidermal growth factor receptor downstream-mutated metastatic colorectal cancer'. In: *European Journal of Cancer* 48.12 (2012), pp. 1774–1780. ISSN: 09598049.

[225] M. C. Etienne-Grimaldi, J. Bennouna, J. L. Formento, J. Y. Douillard, M. Francoual, I. Hennebelle, E. Chatelut, E. Francois, R. Faroux, C. El Hannani, J. H. Jacob and G. Milano. 'Multifactorial pharmacogenetic analysis in colorectal cancer patients receiving 5-fluorouracil-based therapy together with cetuximab-irinotecan'. In: *British Journal of Clinical Pharmacology* 73.5 (2012), pp. 776–785. ISSN: 03065251.

[226] A. Stein, D. Simnica, C. Schultheiß, R. Scholz, J. Tintelnot, E. Gökkurt, L. von Wenserski, E. Willscher, L. Paschold, M. Sauer, S. Lorenzen, J. Riera-Knorrenschild, R. Depenbusch, T. J. Ettrich, S. Dörfel, S.-E. Al-Batran, M. Karthaus, U. Pelzer, L. Waberer, A. Hinke, M. Bauer, C. Massa, B. Seliger, C. Wickenhauser, C. Bokemeyer, S. Hegewisch-Becker and M. Binder. 'PD-L1 targeting and subclonal immune escape mediated by PD-L1 mutations in metastatic colorectal cancer'. In: *Journal for ImmunoTherapy of Cancer* 9.7 (2021), e002844. ISSN: 20511426.

[227] L. Dahan, E. Norguet, M. C. Etienne-Grimaldi, J. L. Formento, M. Gasmi, I. Nanni, J. Gaudart, S. Garcia, L. Ouafik, J. F. Seitz and G. Milano. 'Pharmacogenetic profiling and cetuximab outcome in patients with advanced colorectal cancer'. In: *BMC Cancer* 11 (2011), pp. 1–11. ISSN: 14712407.

[228] J. Pander, H. Gelderblom, N. F. Antonini, J. Tol, J. H. Krieken, T. van der Straaten, C. J. Punt and H. J. Guchelaar. 'Correlation of FCGR3A and EGFR germline polymorphisms with the efficacy of cetuximab in KRAS wild-type metastatic colorectal cancer'. In: *European Journal of Cancer* 46.10 (2010), pp. 1829–1834. ISSN: 09598049.

[229] W. Zhang, M. Azuma, G. Lurje, M. A. Gordon, D. Yang, A. Pohl, Y. Ning, P. Bohanes, A. Gerger, T. Winder, E. Hollywood, K. Danenberg, L. Saltz and H.-J. Lenz. 'Molecular predictors of combination targeted therapies (cetuximab, bevacizumab) in irinotecan-refractory colorectal cancer (BOND-2 study)'. In: *Anticancer research* 30.10 (2010), pp. 4209–4217.

[230] W. Zhang, M. Gordon, A. M. Schultheis, D. Yang, F. Nagashima, M. Azuma, H. M. Chang, E. Borucka, G. Lurje, A. E. Sherrod, S. Iqbal, S. Groshen and H. J. Lenz. 'FCGR2A and FCGR3A polymorphisms associated with clinical outcome of epidermal growth factor receptor-expressing metastatic colorectal cancer patients treated with single-agent cetuximab'. In: *Journal of Clinical Oncology* 25.24 (2007), pp. 3712–3718. ISSN: 0732183X.

[231] F. Graziano, A. Ruzzo, F. Loupakis, E. Canestrari, D. Santini, V. Catalano, R. Bisonni, U. Torresi, I. Floriani, G. Schiavon, F. Andreoni, P. Maltese, E. Rulli, B. Humar, A. Falcone, L. Giustini, G. Tonini, A. Fontana, G. Masi and M. Magnani. 'Pharmacogenetic profiling for cetuximab plus irinotecan therapy in patients with refractory advanced colorectal cancer'. In: *Journal of Clinical Oncology* 26.9 (2008), pp. 1427–1434. ISSN: 0732183X.

[232] J. B. Kjersem, E. Skovlund, T. Ikdahl, T. Guren, C. Kersten, A. M. Dalsgaard, M. K. Yilmaz, T. Fokstuen, K. M. Tveit and E. H. Kure. 'FCGR2A and FCGR3A polymorphisms and clinical outcome in metastatic colorectal cancer patients treated with first-line 5-fluorouracil/folinic acid and oxaliplatin +/- cetuximab'. In: *BMC Cancer* 14.1 (2014), pp. 1–9. ISSN: 14712407.

[233] C. L. Nigro, V. Ricci, D. Vivenza, M. Monteverde, G. Strola, F. Lucio, F. Tonissi, E. Miraglio, C. Granetto, M. Fortunato and M. C. Merlano. 'Evaluation of antibody-dependent cell-mediated cytotoxicity activity and cetuximab response in KRAS wildtype metastatic colorectal cancer patients'. In: *World Journal of Gastrointestinal Oncology* 8.2 (2016), pp. 222–230. ISSN: 19485204.

[234] E. M. Bertino, E. L. McMichael, X. Mo, P. Trikha, M. Davis, B. Paul, M. Grever, W. E. Carson and G. A. Otterson. 'A phase I trial to evaluate antibody-dependent cellular cytotoxicity of cetuximab and lenalidomide in advanced colorectal and head and neck cancer'. In: *Molecular Cancer Therapeutics* 15.9 (2016), pp. 2244–2250. ISSN: 15388514.

[235] A. P. De Souza and C. Bonorino. 'Tumor immunosuppressive environment: effects on tumor-specific and nontumor antigen immune responses'. In: *Expert review of anticancer therapy* 9.9 (2009), pp. 1317–1332.

[236] W. H. Yeap, K. L. Wong, N. Shimasaki, E. C. Y. Teo, J. K. S. Quek, H. X. Yong, C. P. Diong, A. Bertoletti, Y. C. Linn and S. C. Wong. 'CD16 is indispensable for antibody-dependent cellular cytotoxicity by human monocytes'. In: *Scientific reports* 6.1 (2016), pp. 1–22.

[237] L. Lattanzio, N. Denaro, D. Vivenza, C. Varamo, G. Strola, M. Fortunato, E. Chamorey, A. Comino, M. Monteverde, C. Lo Nigro, G. Milano and M. Merlano. 'Elevated basal antibody-dependent cell-mediated cytotoxicity (ADCC) and high epidermal growth factor receptor (EGFR) expression predict favourable outcome in patients with locally advanced head and neck cancer treated with cetuximab and radiotherapy'. In: *Cancer Immunology, Immunotherapy* 66.5 (2017), pp. 573–579. ISSN: 14320851.

[238] R. Maréchal, J. De Schutter, N. Nagy, P. Demetter, A. Lemmers, J. Devière, I. Salmon, S. Tejpar and J.-L. Van Laethem. 'Putative contribution of CD56 positive cells in cetuximab treatment efficacy in first-line metastatic colorectal cancer patients'. In: *BMC cancer* 10.1 (2010), pp. 1–11.

[239] T. E. Reichert, L. Strauss, E. M. Wagner, W. Gooding and T. L. Whiteside. 'Signaling abnormalities, apoptosis, and reduced proliferation of circulating and tumor-infiltrating lymphocytes in patients with oral carcinoma'. In: *Clinical cancer research* 8.10 (2002), pp. 3137–3145.

[240] A. P. Krawczyk and D. M. Kowalski. 'Genetic and immune factors underlying the efficacy of cetuximab and panitumumab in the treatment of patients with metastatic colorectal cancer'. In: *Wspolczesna Onkologia* 18.1 (2014), pp. 413–422. ISSN: 14282526.

[241] R. Elgueta, M. J. Benson, V. C. De Vries, A. Wasiuk, Y. Guo and R. J. Noelle. 'Molecular mechanism and function of CD40/CD40L engagement in the immune system'. In: *Immunological reviews* 229.1 (2009), pp. 152–172.

[242] J. Q. Zhang, S. Zeng, G. A. Vitiello, A. M. Seifert, B. D. Medina, M. J. Beckman, J. K. Loo, J. Santamaria-Barria, J. H. Maltbaek, N. J. Param, J. Moral, J. Zhao, V. Balachandran, F. Rossi, C. Antonescu and R. DeMatteo. 'Macrophages and CD8+ T cells mediate the antitumor efficacy of combined CD40 ligation and imatinib therapy in gastrointestinal stromal tumors'. In: *Cancer immunology research* 6.4 (2018), pp. 434–447.

[243] R. J. Davis, R. L. Ferris and N. C. Schmitt. 'Costimulatory and coinhibitory immune checkpoint receptors in head and neck cancer: unleashing immune responses through therapeutic combinations'. In: *Cancers of the Head & Neck* 1.1 (2016), pp. 1–11. ISSN: 2059-7347.

[244] D. Sathawane, R. S. Kharat, S. Halder, S. Roy, R. Swami, R. Patel and B. Saha. 'Monocyte CD40 expression in head and neck squamous cell carcinoma (HNSCC)'. In: *Human Immunology* 74.1 (2013), pp. 1–5. ISSN: 01988859.

[245] M. Kinouchi, K. Miura, T. Mizoi, K. Ishida, W. Fujibuchi, H. Sasaki, S. Ohnuma, K. Saito, Y. Katayose, T. Naitoh, F. Motoi, K. Shiiba, S. Egawa, C. Shibata and M. Unno. 'Infiltration of CD40-positive tumor-associated macrophages indicates a favorable prognosis in colorectal cancer patients.' In: *Hepato-gastroenterology* 60.121 (2013), pp. 83–88.

[246] G. L. Beatty, E. G. Chiorean, M. P. Fishman, B. Saboury, U. R. Teitelbaum, W. Sun, R. D. Huhn, W. Song, D. Li, L. L. Sharp, D. Torigian, P. O'Dwyer and R. Vonderheide. 'CD40 agonists alter tumor stroma and show efficacy against pancreatic carcinoma in mice and humans'. In: *Science* 331.6024 (2011), pp. 1612–1616.

[247] C. J. Perry, A. R. Muñoz-Rojas, K. M. Meeth, L. N. Kellman, R. A. Amezquita, D. Thakral, V. Y. Du, J. X. Wang, W. Damsky, A. L. Kuhlmann, J. Sher, M. Bosenberg, K. Miller-Jensen and S. Kaech. 'Myeloid-targeted immunotherapies act in synergy to induce inflammation and antitumor immunity'. In: *Journal of Experimental Medicine* 215.3 (2018), pp. 877–893.

[248] R. H. Vonderheide. 'CD40 agonist antibodies in cancer immunotherapy'. In: *Annual review of medicine* 71 (2020), pp. 47–58.

[249] K. R. Wiehagen, N. M. Girgis, D. H. Yamada, A. A. Smith, S. R. Chan, I. S. Grewal, M. Quigley and R. I. Verona. 'Combination of CD40 agonism and CSF-1R blockade reconditions tumor-associated macrophages and drives potent antitumor immunity'. In: *Cancer immunology research* 5.12 (2017), pp. 1109–1121.

Statutory Declaration

"I, Stefan Kolling, by personally signing this document in lieu of an oath, hereby affirm that I prepared the submitted dissertation on the topic *The role of antibody-dependent cellular cytotoxicity for IgG1 monoclonal antibody therapy of metastatic colorectal cancer* (*Die Rolle von Antikörperabhängiger zellulärer Zytotoxizität für die Behandlung des metastatischen kolorektalen Karzinoms mit IgG1 monoklonalen Antikörpern* in German), independently and without the support of third parties, and that I used no other sources and aids than those stated.

All parts which are based on the publications or presentations of other authors, either in letter or in spirit, are specified as such in accordance with the citing guidelines. The sections on methodology (in particular regarding practical work, laboratory regulations, statistical processing) and results (in particular regarding figures, charts and tables) are exclusively my responsibility.

Furthermore, I declare that I have correctly marked all of the data, the analyses, and the conclusions generated from data obtained in collaboration with other persons, and that I have correctly marked my own contribution and the contributions of other persons (cf. declaration of contribution). I have correctly marked all texts or parts of texts that were generated in collaboration with other persons.

My contributions to any publications to this dissertation correspond to those stated in the below joint declaration made together with the supervisor. All publications created within the scope of the dissertation comply with the guidelines of the ICMJE (International Committee of Medical Journal Editors; www.icmje.org) on authorship. In addition, I declare that I shall comply with the regulations of Charité – Universitätsmedizin Berlin on ensuring good scientific practice.

I declare that I have not yet submitted this dissertation in identical or similar form to another Faculty.

The significance of this statutory declaration and the consequences of a false statutory declaration under criminal law (Sections 156, 161 of the German Criminal Code) are known to me."

Berlin, 16 July 2022

.....

(Stefan Kolling)

For reasons of personal data protection, my curriculum vitae will not be published in the electronic version of my work.

Mein Lebenslauf wird aus datenschutzrechtlichen Gründen in der elektronischen Version meiner Arbeit nicht veröffentlicht.

List of Publications

[1] Wittenbecher F, Lesch S, Kolling S, Blau IW, Vuong L, Borchert F, Movasshagi K, Tietze-Bürger C, Penack O, Ahn J, Bullinger L. Paired donor and recipient immunophenotyping in allogeneic hematopoietic stem cell transplantation: a cellular network approach. Frontiers in Immunology. 2022 May 23;13:874499.

[2] Schmiester M, Maier R, Riedel R, Durek P, Frentsch M, Kolling S, Mashreghi MF, Jenq R, Zhang L, Peterson CB, Bullinger L. Flow cytometry can reliably capture gut microbial composition in healthy adults as well as dysbiosis dynamics in patients with aggressive B-cell non-Hodgkin lymphoma. Gut Microbes. 2022 Dec 31;14(1):2081475.

[3] Kolling S, Ventre F, Geuna E, Milan M, Pisacane A, Boccaccio C, Sapino A, Montemurro F. "Metastatic cancer of unknown primary" or "primary metastatic cancer"?. Frontiers in Oncology. 2020 Jan 17;9:1546.

[4] Stella GM, Kolling S, Benvenuti S, Bortolotto C. Lung-seeking metastases. Cancers. 2019 Jul 19;11(7):1010.

[5] Stella GM, Corino A, Berzero G, Kolling S, Filippi AR, Benvenuti S. Brain metastases from lung cancer: Is MET an actionable target?. Cancers. 2019 Feb 26;11(3):271.

[6] Whelan B, Kolling S, Oborn BM, Keall P. Passive magnetic shielding in MRI-Linac systems. Physics in Medicine & Biology. 2018 Mar 26;63(7):075008.

[7] Kolling S, Oborn BM, Keall PJ, Horvat J. Magnetization curves of sintered heavy tungsten alloys for applications in MRI-guided radiotherapy. Medical Physics. 2014 Jun;41(6Part1):061707.

[8] Oborn BM, Kolling S, Metcalfe PE, Crozier S, Litzenberg DW, Keall PJ. Electron contamination modeling and reduction in a 1 T open bore inline MRI-linac system. Medical physics. 2014 May;41(5):051708.

[9] Kolling S, Oborn B, Keall P. Impact of the MLC on the MRI field distortion of a prototype MRI-linac. Medical physics. 2013 Dec;40(12):121705.

Acknowledgements

"Quäl dich, du Sau!"
"Please keep going."

Udo Bölts, Team Telekom

Similar to these gentle performance-enhancing words shouted at a young and promising cyclist during the heat of Le Tour de France in 1997, more than a few people have supported me throughout this research project.

Albeit using considerably more eloquent speech than Udo Bölts, my three supervisors Il-Kang Na, Marco Frentsch and Phillip Schiele kept me on track and made sure I was always going in the right direction. I could not have asked for better supervision and highly appreciate the vast amount of time they sacrificed to give advice on my experiments. In this regard, a special thank you to Phillip Schiele who I may or may have not woken up by calling him late at night whenever my experimental samples landed on the laboratory floor rather than in the flow cytometry device. Just as important was the daily dose of support from all of my eucalyptic colleagues at AG Na that came in various shapes and forms, such as unorthodox brainstorming sessions during lunch breaks, cheering me up with ice cream, sweets and bifi, taking care of my cell cultures when on holiday, tolerating the two or three jokes I played on them or keeping me on the verge of anaemia by constantly asking for a blood donation (this list is not exhaustive).

Despite this being my umpteenth thesis, my family still has not grown tired of giving me a helping hand (or even arm, some would argue) at innumerable occasions and I feel incredibly privileged to always have them on my side - rest assured this will not remain my last thesis, I will keep you on your toes. Luckily though, you get to share the work with my second family comprising a wonderful bunch of friends from all other the world. Each one of you has helped me in their very own way to get through the rough and frustrating patches that are inherent in any research project, while at the same time doing an excellent job at pretending not to be bored by my neverending in-detail accounts of "what went wrong this time". I am glad you did not let them ruin our competitive table tennis matches, hikes, bike trips or other Covid lockdown activities, but instead offered the perfect dose of unwinding distraction to have me go back to the laboratory - as enthusiastic and motivated as a narcoleptic could possibly be - the Monday after.

Lucia, you are without a doubt a "thesis first responder" expert by now. Congratulations on having just completed a thesis hat-trick with me. Admittedly, this time has certainly been the most challenging to date with more than a thousand kilometres of distance between the two of us for most of the time. Although this made the delivery of your infamous food care packages more difficult, you nonetheless managed to find creative ways to be there for me. With you by my side, I feel ready to write my next thesis on the International Space Station!

Thanks everyone and
stay *hara hachi bun me*,

Stefan

CHARITÉ

CharitéCentrum für Human- und Gesundheitswissenschaften

Charité | Campus Charité Mitte | 10117 Berlin

Institut für Biometrie und klinische Epidemiologie (iBikE)

Direktor: Prof. Dr. Frank Konietschke

Postanschrift:
Charitéplatz 1 | 10117 Berlin
Besucheranschrift:
Reinhardtstr. 58 | 10117 Berlin

Tel. +49 (0)30 450 562171
frank.konietschke@charite.de
https://biometrie.charite.de/

Name, Vorname: Kolling, Stefan

Emailadresse: stefan.kolling@charite.de
Matrikelnummer: 229893
PromotionsbetreuerIn: Professor Il-Kang Na

Promotionsinstitution / Klinik: BCRT/BIH (CVK)

Bescheinigung

Hiermit bescheinige ich, dass Herr Stefan Kolling innerhalb der Service Unit Biometrie des Instituts für Biometrie und klinische Epidemiologie (iBikE) bei mir eine statistische Beratung zu einem Promotionsvorhaben wahrgenommen hat. Folgende Beratungstermine wurden wahrgenommen:

- Termin 1: 24.03.2021
- Termin 2: 08.06.2022

Folgende wesentliche Ratschläge hinsichtlich einer sinnvollen Auswertung und Interpretation der Daten wurden während der Beratung erteilt:

- Auswertung der Daten mittels deskriptiver Analysen sowie Kaplan-Meier/Log-Rank-Test und Mixed Models
- Die Fallzahl pro Gruppe ist für eine sinnvolle Interpretation/Auswertung von Kaplan-Meier-Kurven und Log-Rank-Test evtl. zu klein

Diese Bescheinigung garantiert nicht die richtige Umsetzung der in der Beratung gemachten Vorschläge, die korrekte Durchführung der empfohlenen statistischen Verfahren und die richtige Darstellung und Interpretation der Ergebnisse. Die Verantwortung hierfür obliegt allein dem Promovierenden. Das Institut für Biometrie und klinische Epidemiologie übernimmt hierfür keine Haftung.

Datum: 08.06.2022 Name des Beraters: Prof. Dr. Frank Konietschke/Stephen Schüürhuis